Relocation of Eastern Tennessee Earthquakes Using hypoDD

by

Meredith M. Dunn

**Thesis submitted to the Faculty of the
Virginia Polytechnic Institute and State University in partial fulfillment of the requirements for the degree of**

**Masters of Science in Geophysics
in the
Department of Geosciences**

**Martin C. Chapman, Chair
John A. Hole
J. Arthur Snoke**

**August 2, 2004
Blacksburg, Virginia**

(Keywords: Earthquakes, Eastern Tennessee Seismic Zone, Hypocenter Relocation)

Relocation of Eastern Tennessee Earthquakes Using hypoDD

by

Meredith M. Dunn

(Abstract)

The double difference earthquake location algorithm, implemented in the program HYPODD, was used to relocate a data set of approximately 1000 earthquakes in the eastern Tennessee seismic zone (ETSZ), using a recently developed velocity model. The double difference algorithm is used to calculate accurate relative hypocenter locations by removing the effects of un-modeled velocity structure. The study examines the earthquake hypocenter relocations in an effort to resolve fault orientations and thereby gain insights into the tectonics of the seismic zone. The analysis involves visual comparison of three-dimensional perspective plots of the hypocenter relocations oriented according to focal mechanism nodal planes derived from events within several, dense clusters of earthquakes.

The northwestern boundary of the seismic zone corresponds to the steep magnetic gradient of the New York-Alabama lineament. The double-difference relocations reinforced previous interpretations of a vertical boundary between seismic and relatively aseismic crust at that location. Areas at the northeastern and southwestern ends of the ETSZ exhibit northwest trending hypocenter alignments, which are perpendicular to the overall northeastern trend of the seismic zone. These alignments agree with focal mechanism nodal plane orientations and are interpreted as seismogenic faults. In the central, most seismically active portion of the ETSZ, relocations appear to indicate a diffuse zone of hypocenters that are west-striking and north-dipping. The orientation of this zone of earthquake hypocenters is consistent with an existing seismic reflection profile that images mid to upper crustal reflectors with apparent dips of approximately 35 degrees to the north.

The interpreted fault planes are all consistent with an east-northeast oriented, sub-horizontal maximum regional compressive stress, consistent with findings in previous studies.

ACKNOWLEDGMENTS

I would like to express my deepest gratitude to my advisor, Dr. Martin Chapman. He suggested the topic of this thesis, provided unlimited instruction and guidance in my studies, and provided me with the research assistantship that made it possible. I thank him for his wisdom, patience, and continued support in my academic endeavors. I also thank Dr. J.A. Snoke for his painstaking instruction in the classroom and his contributions to the writing of the manuscript. Thanks to Dr. John Hole for his review and comments on the manuscript.

Thanks go to the faculty and staff of Virginia Polytechnic Institute and State University who have provided me the necessary atmosphere, instruction, and resources to undertake this project. Also, a very special thanks to my fellow geophysics graduate students, from whom I have learned so much and without whom I would not have been able to complete this project or the necessary class work.

My sincerest gratitude goes to my family. My father and mother, Scott and Amy, have seen me through all situations in my life to help me reach this place. Thanks to my siblings, Marsha, Michael, and Mark for supporting me and helping me have fun along the way. They continue to be an inspiration to my life.

The financial support for my graduate studies was provided through grant award number 01HQAG0016 through the United States Geological Survey.

Table of Contents

Introduction…… 1

Chapter 1: Geologic and Tectonic History of the Study Area…… 4

Previous Studies of the Eastern Tennessee Seismic Zone……... 7

Summary…….. 12

Chapter 2: Description and Analysis Approach……..... 14

Double-Difference Algorithm……...……...……... 15

HypoDD……..... …. 19

Example of hypoDD from Hayward Fault, California……..... 25

Chapter 3: Testing HypoDD with a Synthetic Data Set……. ... 28

Chapter 4: HypoDD applied to the Eastern Tennessee Seismic Zone……... 34

MAXSEP 20 km……... 35

MAXSEP 10 km…….. 37

Cluster 1, MAXSEP 10 km……...… 37

Cluster 2, MAXSEP 10 km……...…… 41

Cluster 3, MAXSEP 10 km……...…… 43

Cluster 4,5, and 6, MAXSEP 10 km..... 48

MAXSEP 5 km……...… 49

Cluster 1, MAXSEP 5 km……...…… 50

Cluster 2, MAXSEP 5 km……..……. 52

Cluster 3, MAXSEP 5 km……..……. 56

Combined Subset of Clusters 1 and 2, MAXSEP 5 km……..……..…….. 58

Sensitivity Testing of hypoDD…… 62

Conclusions…….…..….. **64**

References……..…. **68**

Appendix 1.…… **71**

Appendix 2.……**73**

Appendix 3.……..……**74**

List of Illustrations

Figure 1 The Eastern Tennessee Seismic Zone……..……3

Figure 1.1 Magnetic Intensity and Bouguer Gravity Anomalies of NY-AL lineament..7

Figure 1.2 Focal Mechanisms for eastern Tennessee seismic zone…….....12

Figure 2.1 Illustration of hypoDD parameters……22

Figure 2.2 Example of hypoDD from Northern Hayward Fault……..…26

Figure 3.1 HYPOELLIPSE locations of synthetic data using error-free arrival times...28

Figure 3.2 HYPOELLIPSE locations of synthetic data using systematic errors……30

Figure 3.3 HYPODD relocations of synthetic data using systematic errors……...…31

Figure 3.4 HYPOELLIPSE locations of synthetic data containing systematic and random errors……32

Figure 3.5 HYPODD relocations of synthetic data containing systematic and random errors…….33

Figure 4.1 MAXSEP 20 km…….....36

Figure 4.2 Cluster Locations, MAXSEP 10 km.…….……...…….38

Figure 4.3 Cluster 1,MAXSEP 10 km-Comparison of Epicenters…….……...….39

Figure 4.4 Cluster 1, MAXSEP 10 km-Comparison of Hypocenters…….……40

Figure 4.5 Cluster 2, MAXSEP 10 km……...……44

Figure 4.6 Cluster 3, MAXSEP 10 km-Comparison of Epicenters……...….45

Figure 4.7 Cluster 3, MAXSEP 10 km-Comparison of Hypocenters…….....47

Figure 4.8 Cluster 4, MAXSEP 10 km…….……...……48

Figure 4.9 Cluster Locations, MAXSEP 5 km……..…….50

Figure 4.10 Cluster 1, MAXSEP 5 km……..……..53

Figure 4.11 Cluster 2, MAXSEP 5 km……...…….55

Figure 4.12 Cluster 3, MAXSEP 5 km……..……..57

Figure 4.13 Subset of Clusters 1 and 2, MAXSEP 5 km…….59

Figure 4.14 ARAL1 Reflection Profile……...…….61

Figure 4.15 Interpreted Orientations of Possible Seismogenic Features…….…….67

List of Tables

Table 4.1 Cluster Breakdown, MAXSEP 10 km……...……41

Table 4.2 Focal Mechanisms Solutions……...……..43

Table 4.3 Cluster Breakdown, MAXSEP 5 km……..49

INTRODUCTION

The Eastern Tennessee Seismic Zone, shown in figure 1, is one of most densely concentrated areas of seismic activity east of the Rocky Mountains and is second only to the New Madrid seismic zone in seismic strain energy release (Powell et al, 1994). The seismic zone is approximately 300 km long and 50 km wide area located in eastern Tennessee, western North Carolina, northwestern Georgia and northeastern Alabama (Powell et al., 1994). The largest historical earthquake was moment magnitude 4.6. This recent shock occurred April 29, 2003 near Forth Payne, AL. The depth of seismicity in the area is estimated to be approximately five to twenty-six kilometers, starting at the base of the Paleozoic section and extending down to mid-crustal depths (Vlahovic et al., 1998). The thickness of the crust in the seismic zone is in the range 43-52 km (Chapman and Bollinger, 1985).

The ETSZ is located mainly in the Valley and Ridge Province of the Appalachians (figure 1). The Valley and Ridge Province consists primarily of Paleozoic sedimentary rocks overlying Precambrain crystalline basement. The sedimentary section is composed mainly of interbedded sandstones, shales, and dolomites that have been caught up in the many folds and thrust faults in the area. Focal depths indicate that the ETSZ earthquakes occur mainly in the Precambrian basement rock, beneath the Paleozoic thrust sheets (Bollinger et al, 1991).

Unlike many active plate margin areas such as California, the earthquakes that occur in Eastern Tennessee cannot be attributed to mapped surface faults. Eastern Tennessee is in the interior of the North American plate. Understanding the causes of intra-plate earthquakes is a difficult problem because the seismogenic faults may be minor features. Also, strain rates are low in intra-plate regions and therefore major earthquakes are infrequent. As a result, the primary data set for understanding intra-plate seismicity is derived primarily from regional

network monitoring of small magnitude earthquakes. In the case of ETSZ, the seismicity occurs in the Precambrian basement and may be totally unrelated to the surface geology. Knowledge of the locations and orientations of brittle faults in the Precambrian Basement rocks of the ETSZ is fundamental for understanding the nature of the seismicity. The faults may exist as a result of the long and complex tectonic history of the Southern Appalachians. Modern seismicity may be occurring on ancient faults that are being reactivated in the current stress field.

The purpose of my study is to examine the fault orientation in the Eastern Tennessee Seismic Zone. I approach the problem by using an earthquake location algorithm developed by Felix Waldhauser and William Ellsworth (2000). The program that implements the algorithm is named HYPODD (Waldhauser, 2001).

HYPODD is based on a double difference approach that greatly reduces the errors in relative earthquake locations introduced by un-modeled velocity variations. The algorithm produces more reliable relative hypocenter locations than does the standard individual event location approach (e.g., Hypoellipse, Lahr, 1980). A number of conditions must be fulfilled in order for the potential advantages of the double difference algorithm to be realized. These conditions, along with the theory underlying the double difference algorithm will be reviewed below in chapter #2

Accurate relative hypocenter locations and earthquake focal mechanisms are most important for understanding the tectonic framework of a seismically active area. Hypocenter clusters in the seismic zone provide the only available data set from which the orientations of potential seismogenic faults can be inferred. Therefore, the relocation of earthquake hypocenters in the Eastern Tennessee Seismic Zone (ETSZ) is the basic objective of my study. Focal mechanisms greatly aid in the interpretation of the results obtained from the relocation effort.

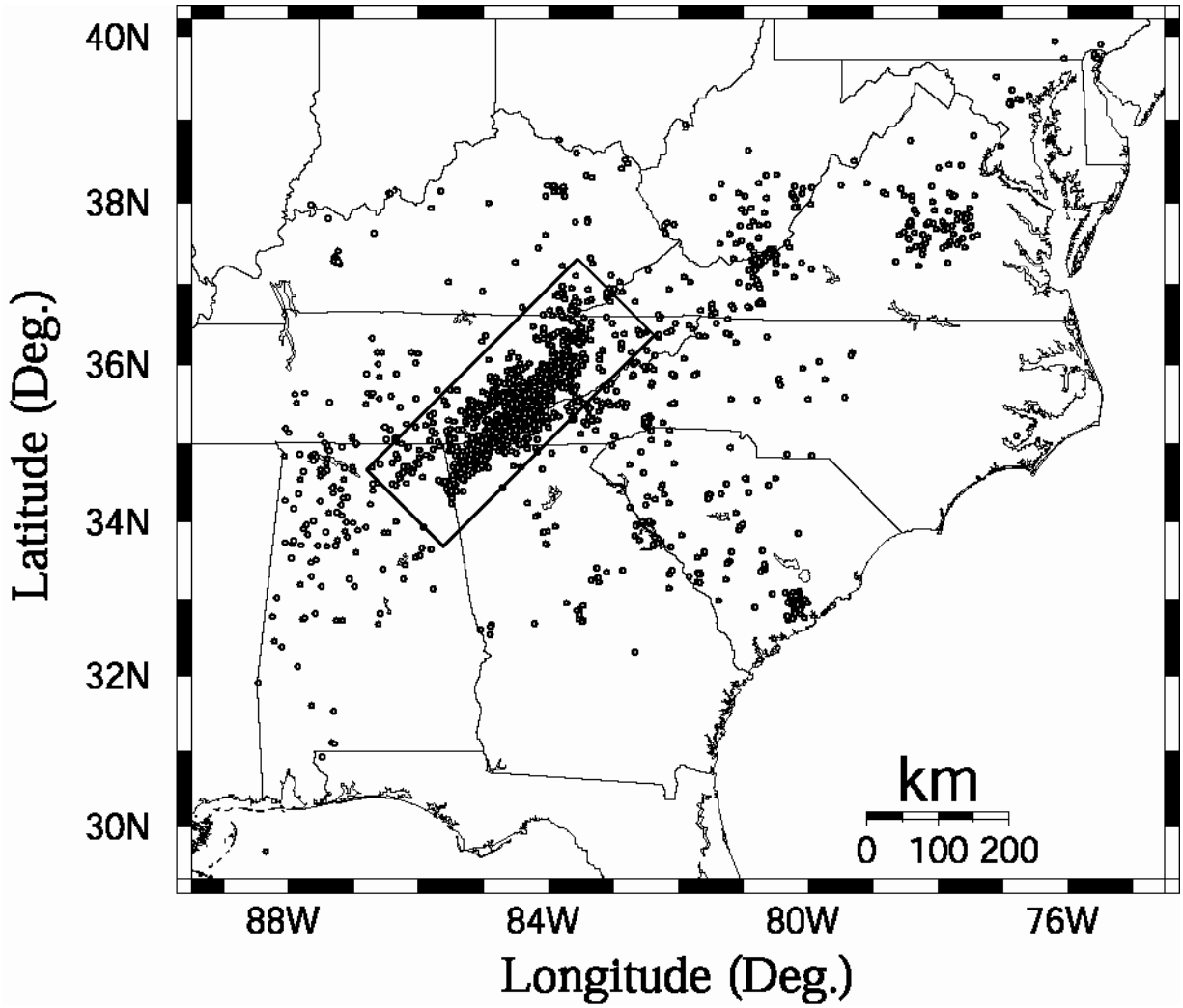

Figure 1 Epicenters of instrumentally located earthquakes with magnitude greater than 0.0 for the period 1977-2002 are shown as dots. The general area of the study area is indicated by the rectangle.

Chapter 1: Geologic and Tectonic History of the Study Area

The geologic history of the study area is complex. Seismicity occurs within Precambrian basement rocks that are covered by younger Paleozoic thrust sheets. The tectonic history of the basement is most relevant to this study. The modern seismicity indicates that basement faults are being reactivated by a modern stress field that may or may not be aligned with the ancient stress field that originally created the basement tectonic fabric.

The first major tectonic event to impact the Southern Appalachian region was the Grenville Orogeny approximately 1.3 to 1.1 billion years ago. Seismicity is occurring in Grenville basement rocks. The Grenville orogeny was the culmination of the formation of the supercontinent Rodinia. Between 600 and 800 million years ago, Rodinia fragmented and subsequently re-formed as a new supercontinent, Pannotia. At the beginning of the Paleozoic, Pannotia broke up yielding Laurentia (North America and Greenland) Gondwana (South America, Africa, Antarctica, India, and Australia), Siberia and Baltica and creating the Iapetus Ocean. As the Iapetus Ocean grew, a passive plate margin was formed along the eastern edge of Laurentia, or proto- North America (Marshak, 2001).

The next major collisional orogenic event to affect the eastern margin of Laurentia was the Taconic Orogeny, in the middle Ordovician, marking the collision of Laurentia with a volcanic island arc. The collision deformed and metamorphosed strata of the former passive margin basin and created a mountain range (Marshak, 2001). In the Devonian (380 million years ago) another continent-island arc collision occurred, resulting in the Acadian Orogeny (Wheeler, 1995).

The final closing of the Iapetus Ocean occurred 250 to 300 million years ago, in the Permian. This was a major continent-continent collision believed to be between the proto-North American continent and the South American continent (Wheeler, 1995). The result of this continent-continent collision was the formation of the supercontinent Pangea. The deformation associated with the formation of Pangea is known in eastern North America as the Alleghanian Orogeny and is the major episode of deformation in the southern Appalachian region (Cook et al., 1979).

Pangea began to break apart in the Late Triassic. At the end of the Jurassic, rifting had created the early Atlantic Ocean (Marshak, 2001). Eastern North America was in an extensional stress field regime and rift basins developed along the Appalachian margin. The modern day stress field has been in place since the Cretaceous, approximately 70 million years ago. This is a compressive stress field, produced from an initial continental resistance to plate motion and from ridge-push along the East Coast (Zoback & Zoback, 1991).

The eastern margin of North America was tectonically active during the Paleozoic and early Mesozoic (Marshak, 2001). Since the Cretaceous, the area has been a passive margin. There is no obvious explanation for many of the aspects of the seismicity of eastern North America in the context of plate tectonics. Generally, it is accepted that the seismicity is due to reactivation of existing faults (Wheeler, 1995 and references therein); however, the question remains as to the location and type of the faults and when the faults were originally formed. For example, one explanation for seismicity in the Valley and Ridge and Blue Ridge regions proposed by Wheeler (1995) holds that the earthquakes occur as compressional reactivation of normal faults formed originally during the rifting of Pannotia and opening of the Iapetus Ocean. Other authors have proposed possible relationships between a variety of geological and

geophysical features and seismicity in the study area. The earthquakes in the ETSZ spatially occur over a broad area, which is usually indicative of a major fault system.

The seismicity in Eastern Tennessee is occurring on a primarily northeast trend in basement rock of Proterozoic age. Focal mechanisms in the area exhibit primarily strike-slip motion on nodal planes that dip steeply, and are consistent with an east-northeast maximum compressive stress direction (Chapman et al., 1997, Powell et al., 1994). The stress regime in eastern Tennessee is similar to that inferred for eastern North America as a whole (Zoback and Zoback,1991).

A major potential field anomaly exists in the eastern Tennessee seismic zone (King and Zietz, 1978). The feature is known as the New York-Alabama lineament. It is characterized by a steep gradient in the total magnetic intensity, which trends northeasterly from central Alabama through eastern Tennessee. King and Zietz (1978) originally proposed that the feature was continuous to the northeast, extending as far as New York. They speculated that the feature represents a major strike-slip fault in the basement (King and Zietz, 1978). The feature is best defined in eastern Tennessee and is spatially correlated with the present-day seismicity (Johnston et al 1985; Powell et al 1994, Chapman et al 1997, Vlahovic et al. 1998). Figure 1.1 shows the New York - Alabama lineament and the seismicity in the eastern Tennessee study area.

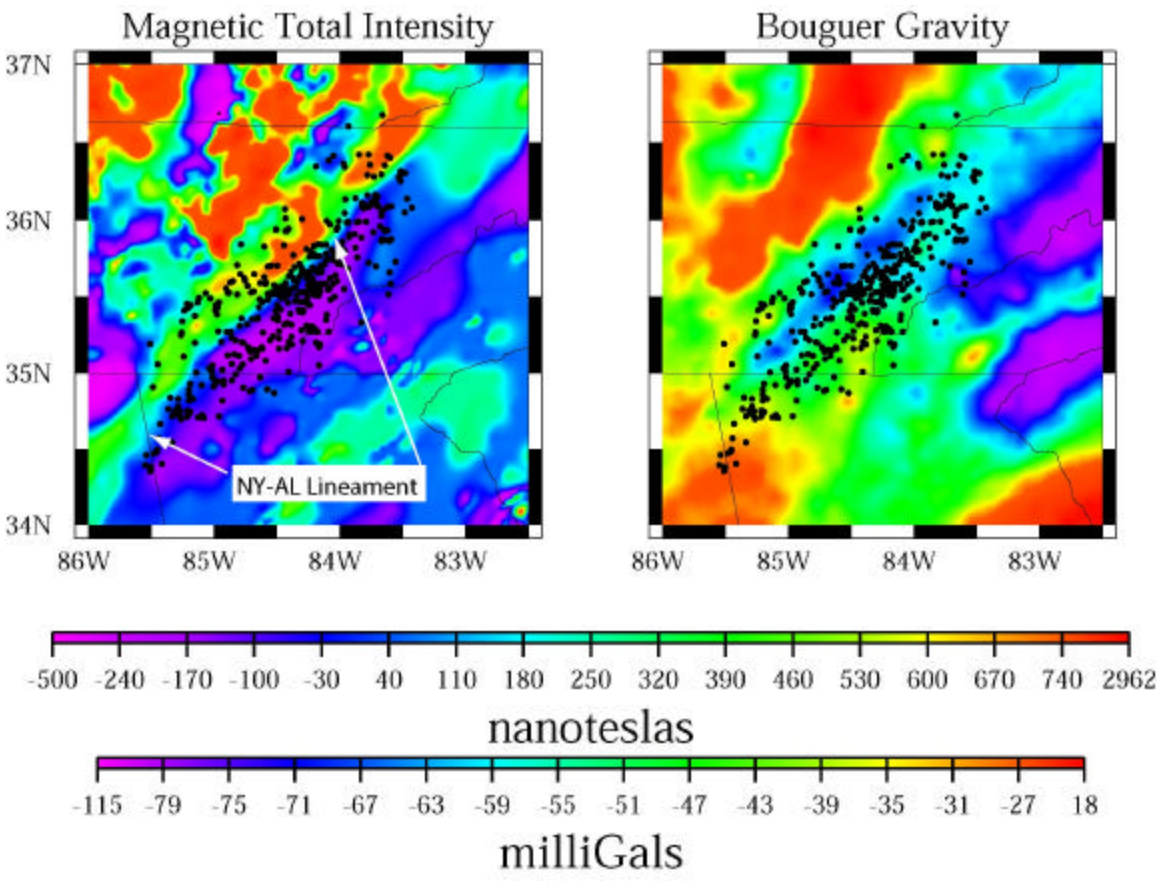

Figure 1.1: Total magnetic intensity (left) and Bouguer gravity anomaly (right). The New York - Alabama lineament (King and Zietz, 1978) is indicated. Earthquake epicenters (1977-1995) are indicated by black dots (modified from Vlahovic et al. 1998).

Previous Studies of the Eastern Tennessee Seismic Zone

Johnston et al. (1985) made the first attempt to link the seismicity in the ETSZ to the ideas of King and Zietz (1978) using data obtained from the first few years of instrumental monitoring in the region. One of the purposes of this study was to examine the seismicity of eastern Tennessee with regard to particular geological structures or geophysical anomalies. Johnston et al (1985) found that a majority of the earthquakes recorded were located in the Valley and Ridge province. This observation differs from the historical seismicity pattern, which was dispersed into western North Carolina (Johnston et al., 1985). The focal mechanisms that were produced from these data were considered to be well constrained and demonstrated strike-

slip faulting on north-south or east-west planes (Johnston et al., 1985). Johnston et al. cited four focal mechanisms, and the following year Teague et al. (1986) added ten more focal mechanisms. These additional focal mechanisms agreed with the earlier observations of Johnston et al. regarding possible fault plane orientation and slip direction. The studies of Johnston et al (1985) and Teague et al. (1986) indicated that the seismicity in eastern Tennessee occurs primarily in the basement, and hence may be largely unrelated to surface geology.

Johnston et al. (1985) observed very few hypocenters occurring to the northwest of the New York-Alabama lineament. Most earthquakes were located to the southeast of the lineament, suggesting that the magnetic lineament is the western boundary of the ETSZ (Johnston et al., 1985). Another magnetic lineament, the Clingman/Ocoee lineament, which is less obvious than the NY-AL lineament, appeared to mark an eastern bound of the seismicity (Johnston et al., 1985). Johnston et al. proposed that the two lineaments are not seismogenic, but are the bounds of a crustal block, referred to by Johnston as the Ocoee Block, that is producing the earthquakes (1985). Johnston et al. (1985) suggest that there is a vertical lithologic difference associated with the NY-AL lineament that corresponds with the western edge of the zone of seismicity.

The earthquake focal mechanisms and stress orientations in Eastern Tennessee were studied by Davison (1988). He inverted eleven focal mechanisms in eastern Tennessee to derive an estimate of the stress tensor. Davison found that the P-axes for a majority of the events trended northeast-southwest. The estimated maximum horizontal stress direction in eastern Tennessee was N50°E, in agreement with the previous studies of Johnston et al. (1985) and Teague et al. (1986). Davison's (1988) results are in good agreement with Zoback and Zoback (1988, 1991) indicating pervasive northeast trending maximum horizontal compressive stress.

Powell et al. (1994) developed a seismotectonic model based on the observed trend of seismicity in the ETSZ. The hypothesis that was ultimately proposed is that the ETSZ is

narrowing into a through-going strike-slip fault, trending along the western boundary of the Ocoee block, which coincides with the NY-AL lineament (Powell et al., 1994). The observation of an expanded pattern of seismicity in historical times versus a narrow belt of instrumentally located shocks suggested that seismicity in the Valley and Ridge of Tennessee is condensing (Powell et al., 1994). Powell et al. ruled out the possibility that the apparent narrowing of the recent seismicity was due to increased detection capability due to the seismic network. This was tested by comparing the locations of recent shocks derived from felt reports with those of pre-instrument shocks.

Powell et al. (1994) proposed that seismicity is occurring in the Ocoee block on North and east striking faults that are most favorably oriented in the modern stress field. Orientations of the nodal planes within the block are different from the northeast-southwest trend of the seismic zone because the overall trend of the seismic zone is controlled by the subsurface orientation of the Ocoee block (Powell et al., 1994). However, Powell et al. propose that the modern northerly and easterly trending slip is coalescing into a northeast trending, major strike-slip zone. Powell et al. proposed that faults within the Ocoee block may date from rifting associated with the formation of the Iapetus Ocean and may have been modified by Paleozoic compression and Mesozoic extension.

Kaufmann and Long (1996) looked further into the probable causes of Eastern Tennessee seismicity. They preformed an inversion of earthquake travel time residuals to better understand the velocity structure of the area. Two solutions were obtained. In one case, the velocity anomalies were constrained by Bouguer gravity anomalies. In the other case, the velocity anomalies were unconstrained. The results of the inversion led Kaufmann and Long to conclude that earthquake hypocenters in the ETSZ were associated with low velocity zones at mid-crustal depths. The area of the densest seismic activity, the central ETSZ, exhibited average to low

velocities (Kaufmann and Long 1996). Previous studies (Long and Zelt, 1991) proposed that this central area of seismicity in the eastern Tennessee seismic zone corresponds to a zone of weakness. Kaufmann and Long (1996) propose that this zone of weakness is due to increased fluid content in the crust, caused by increases in porosity and fracture density. In contrast to Johnston et al (1985), Kaufmann and Long (1996) view the New York Alabama lineament as unrelated to the seismicity in eastern Tennessee.

Hopkins (1995) reprocessed several petroleum industry reflection profiles in eastern Tennessee in a study that examined the New York - Alabama lineament and its possible relationship to the Grenville Front. Hopkins interpreted the source of the magnetic anomaly as a wedge-shaped block beneath Paleozoic sedimentary rocks in the Cumberland Plateau, which lies to the west of the ETSZ. The base of the wedge-shaped body imaged on the reflection profiles dips at 30 degrees to the northwest. The wedge pinches out to zero thickness beneath the location of the steep gradient in the magnetic field. The interpretation of Hopkins, if valid, challenges earlier conjecture by King and Zietz (1978), Johnston et al. (1985) and Powell et al (1994) concerning the nature of the anomaly and its relationship to seismicity. Those authors assumed that the source of the lineament is some sort of vertical lithologic contrast. Regardless of interpretation, the data set assembled by Hopkins (1995) shows that seismicity at latitude 35.5 degrees north in the most active part of the seismic zone is occurring in rocks that are strongly reflective. Average apparent dip on the reflection profile in this area is 35 degrees to the north.

Recently, Vlahovic et al. (1998) performed a joint hypocenter-velocity inversion for the eastern Tennessee seismic zone in an effort to resolve features in the basement below the Appalachian thrust sheets. This is the most recently developed velocity model for the region, and is based on a data set of 492 earthquakes occurring prior to 1995. The study resolved a strong low-velocity zone trending northeast, parallel to the seismicity. The southeastern margin

of the low velocity zone coincides with the NY-AL lineament. Areas of high velocity were resolved to the southeast and northwest (Vlahovic et al., 1998). The hypocenter locations occur mostly in a vertically bounded region approximately 30 km wide with depths of 4 to 22 km. The northwestern vertical boundary coincides with the NY-AL lineament. The earthquakes tend to occur in regions of average velocity or small velocity anomalies (Vlahovic et al., 1998).

In marked contrast to the interpretation of Kaufmann and Long (1996), Vlahovic et al. (1998) proposed that earthquakes concentrate along the steepest velocity gradients. The lack of correlation between seismicity and the regions of lowest velocity suggest that elevated pore pressure in fluid saturated rocks is not the dominant controlling mechanism for earthquake generation. Vlahovic et al. (1998) conclude that the earthquakes may occur on ancient faults separating rocks of different compositions.

Chapman et al. (1997) examined the spatial distribution of epicenters and focal mechanisms of earthquake in the data set used by Vlahovic et al (1998). A majority of the earthquakes exhibited strike-slip faulting (figure 1.2). The focal mechanism nodal planes trend predominately either north-south or east west: however, several mechanisms exhibit nodal planes oriented northeast and northwest. The study showed statistically significant epicenter alignments in the north-south, east-west and northeast-southwest directions, generally consistent with the focal mechanism solutions. Chapman et al., (1997) speculate that the seismic zone is comprised of reactivated left-stepping, en echelon, northeast striking basement faults, with intervening east-west trending faults.

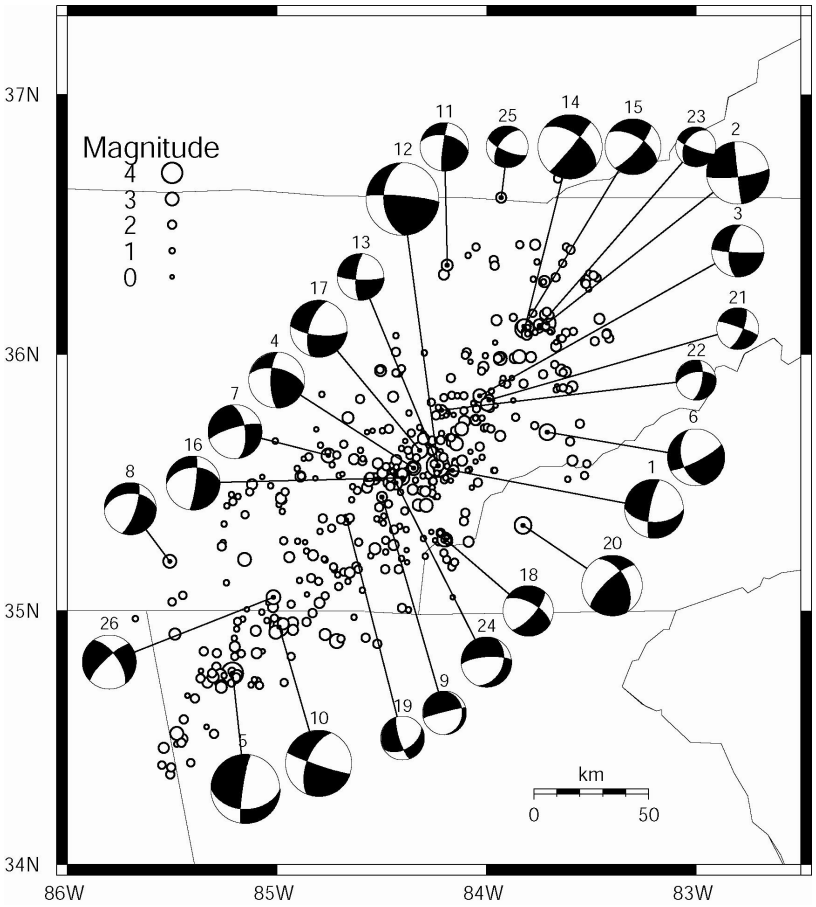

Figure 1.2: Focal mechanisms for the eastern Tennessee seismic zone. (from Chapman et al. 1997).

Summary

The eastern Tennessee seismic zone is characterized by a consistent regional stress regime, with primarily strike-slip faulting. The maximum compressive stress is sub-horizontal and trends east-northeast (Johnston et al., 1985, Teague et al., 1986, Davison, 1988, Chapman et al., 1997).

The seismicity correlates spatially with the New York - Alabama lineament, a major potential field anomaly (King and Zietz, 1978, Johnston et al., 1985, Powell et al., 1994, Hopkins, 1995, Vlahovic et al., 1998). According to the results of Vlahovic et al (1998), the NY-AL lineament is parallel to a low velocity region bounded high velocity regions at mid-crustal

depths. They find that earthquakes tend to occur not in regions of extremely high or low velocities, but in transitional zones between the two. Kaufmann and Long (1996) propose a different explanation, where the seismicity is associated with a low velocity zone. The results of Chapman et al. (1997) support the explanation of Vlahovic et al. (1998) and propose that the velocity transitions, discussed in represent a system of northeast trending en echelon basement faults.

Work discussed in the following chapters will attempt to test these hypotheses.

Chapter 2: Description of Data and Analysis Approach

The data set for this study is a compilation of 993 earthquakes recorded in east Tennessee, Alabama, Georgia, and North Carolina. The arrival time data were taken from the Southeastern United States Seismic Network Bulletins, from 1984 through 2002. This is the most comprehensive list of instrumentally recorded earthquakes to be considered to date for the Eastern Tennessee Seismic Zone. The ETSZ has been monitored by the Tennessee Valley Authority, the University of Memphis, the Georgia Institute of Technology, and the University of Tennessee at Knoxville since the early 1980's.

The earthquakes were recorded using a network of approximately 120 vertical component, 1Hz seismographs. It is important to note that not all of these stations were continuously operational from 1984 through 2002. Some stations have been de-activated and others have become operational during this period. The magnitudes of the earthquakes range from 0.0 to 4.6. The magnitude scale used is $mb_{(Lg)}$, which is equivalent to the short period teleseismic mb scale (Nuttli, 1973). Earthquakes were initially located individually using the program Hypoellipse (Lahr, 1980). In the interest of consistency, each earthquake was located again with hypoellipse, using only the Vlahovic et al. (1998) velocity model, unless otherwise specifically stated.

Although the eastern Tennessee seismic zone is the most seismically active area in the southeast, the data set for this study is small in comparison to that available for areas such as California. In active regions, such as the San Francisco Bay region, major faults are illuminated by recent seismicity. In comparison, far fewer earthquakes have been recorded in eastern Tennessee, and the seismic station density is much less. Thus, relating the observed seismicity to tectonic structures is more difficult in the ETSZ than in the San Francisco Bay area. To make

progress in the ETSZ, one must identify and examine small areas with the most frequent earthquake activity. Within such areas it may be possible to derive accurate locations of one earthquake relative to another. The basis of this study is the possibility that sufficiently accurate relative event locations in a few small clusters will illuminate seismogenic faults. The accuracy of individually located hypocenters is not sufficient for these purposes.

The program HYPODD (Waldhauser, 2001) will be used to identify and group clusters of earthquakes. The program then derives relative relocations within these clusters. It has been shown that these relative locations can greatly improve the image of seismogenic features in situations where adequate data are available (Waldhauser and Ellsworth, 2000).

Double-Difference Algorithm

HYPODD determines relative locations within clusters using the double-difference algorithm, developed by Waldhauser and Ellsworth (2000). Earthquakes are initially located individually with single event programs such as Hypoellipse. These programs require an a-priori velocity model of the crustal volume containing the hypocenters. The resulting event locations contain errors due to un-modeled velocity structure. The double-difference algorithm can improve relative location accuracy by removing effects due to un-modeled velocity structure.

For success, the algorithm requires that the difference between two events be small compared to the distance between the hypocenters of the earthquakes and a station. In that case, the travel time difference between the two events at a single station is approximately independent of un-modeled velocity heterogeneity along the ray paths between paired events at each station. The double difference algorithm attempts to minimize residual travel time differences, double differences, for a pair of earthquakes at a single station. The resulting solution will be largely free of systematic travel time errors due to velocity heterogeneity, but will retain any random errors that were present in the original locations. For example, error due to arrival time reading

inaccuracies will remain in the HYPODD solutions. For that reason all attempts must be made to reduce arrival time reading errors between event pairs.

Following Waldhauser and Ellsworth (2000), the first step in double-difference relocation is to determine the arrival time from a point (the hypocenter) to a seismic station.

$$T_k^i = t^i + \int_i^k u\,ds \qquad (1)$$

The arrival time is represented by T, and is determined for one earthquake, i, to a seismic station, k, expressed as a path integral along the ray. The origin time of event i is expressed by t^i, u is the slowness field, and ds is the element of path length.

The relationship between the travel time and the location of the event is nonlinear; it is linearized through a Taylor expansion.

$$\frac{\partial t_k^i}{\partial \mathbf{m}} \Delta \mathbf{m}^i = r_k^i \qquad (2)$$

where,

$$r_k^i = \left(t^{obs} - t^{cal}\right)_k^i \qquad (3)$$

Equation (2) relates the travel time residuals, r, for one event, i, linearly to the perturbation vector $\Delta\mathbf{m}^i$; which is the change in the hypocentral parameters: x,y,z, and the travel time, t. The travel time residuals are defined as the difference between the calculated travel time (t^{cal}) and the observed travel time (t^{obs}).

These equations are relevant for only one earthquake. For the double difference relocation to be successful there must be a relationship between two events.

$$\frac{\partial t_k^{ij}}{\partial \mathbf{m}} \Delta \mathbf{m}^{ij} = dr_k^{ij} \qquad (4)$$

Equation (4) relates the relative hypocentral parameters of two earthquakes, i and j. The change in relative hypocentral parameters is denoted by $\Delta\mathbf{m}^{ij}$, where $\Delta\mathbf{m}^{ij}=(\Delta dx^{ij}, \Delta dy^{ij}, \Delta dz^{ij}, \Delta dt^{ij})$. The partial derivatives of time, t, with respect to $\mathbf{m}^{ij}$ are the components of the slowness vector, which is a ray connecting the source and receiver.

The DOUBLE DIFFERENCE travel times of two events, assuming a constant slowness vector, is:

$$dr_k^{ij} = \left(t_k^i - t_k^j\right)^{obs} - \left(t_k^i - t_k^j\right)^{cal} \qquad (5)$$

The residual travel times of two events, i and j, for any phase, k (P or S), are determined by calculating the difference in observed and calculated travel times for the two earthquakes. Subsequently, the difference is taken between the observed and calculated travel times of the two events.

If the slowness is not constant, then:

$$dr_k^{ij} = \frac{\partial t_k^i}{\partial x}\Delta x^i + \frac{\partial t_k^i}{\partial y}\Delta y^i + \frac{\partial t_k^i}{\partial z}\Delta z^i + \Delta t^i - \frac{\partial t_k^j}{\partial x}\Delta x^j - \frac{\partial t_k^j}{\partial y}\Delta y^j - \frac{\partial t_k^j}{\partial z}\Delta z^j - \Delta t^j \qquad (6)$$

The hypocentral parameters are represented by x,y,z, and t, which is the origin time. The residual travel times are determined from the differences in the change in all four parameters for each of the two earthquakes involved in the event-pair. The equation can be simplified:

$$dr_k^{ij} = \frac{\partial t_k^i}{\partial \mathbf{m}}\Delta\mathbf{m}^i - \frac{\partial t_k^j}{\partial \mathbf{m}}\Delta\mathbf{m}^j \qquad (7)$$

All of the same parameters apply from equation (4); **m** represents the hypocentral parameters, location and origin time, these are the parameters being solved for.

Equation (7) can be combined into a system of linear equations.

$$\mathbf{WGm} = \mathbf{Wd} \qquad (8)$$

The matrix **G** contains the partial derivatives, matrix size is Mx4N, where M is the number of double difference observations and N is the number of events. The double differences are contained in the data vector, **d**, and **m** is now the change in location and origin time. Each equation will be weighted using the diagonal weighting matrix, **W** (Waldhauser and Ellsworth, 2000). **W** is comprised of the *a priori* weights based on the quality of arrival time picks…1 (full weight)… 0 (zero weight). P and S wave arrival times are weighted equally.

The approach used by Waldhauser and Ellsworth (2000) is to find the weighted least squares solution through the use of a system of normal equations, represented by:

$$\hat{\mathbf{m}} = \left(\mathbf{G}^T \mathbf{W}^{-1} \mathbf{G}\right)^{-1} \mathbf{G}^T \mathbf{W}^{-1} \mathbf{d} \qquad (9)$$

Where, $\hat{m}$ is used to denote least squares estimate of **m**.

Two methods will be used to minimize the travel time residuals, Singular Value Decomposition (SVD) and Conjugate Gradient Least Squares (LSQR). SVD is only applicable to small, well-constrained clusters, as it cannot handle large amounts of data.

$$\hat{\mathbf{m}} = \mathbf{V} \Lambda^{-1} \mathbf{U}^T \mathbf{d} \qquad (10)$$

The **U** and **V** are two matrices with the orthonormal singular vectors of the matrix **G**, from the equations above. The L is a diagonal matrix containing the singular values of the **G** matrix. As in the first equations, **d** still represents the data and $\hat{\boldsymbol{m}}$ is still the unknown parameters, origin time and location.

When relocating large clusters or many clusters simultaneously, SVD is no longer a viable option. LSQR (Paige and Saunders, 1982) solves for a solution to the damped least squares problem.

$$\left\| \mathbf{W} \begin{bmatrix} \mathbf{G} \\ l\mathbf{I} \end{bmatrix} \mathbf{m} - \mathbf{W} \begin{bmatrix} \mathbf{d} \\ \mathbf{0} \end{bmatrix} \right\|_2 = 0 \qquad (11)$$

When using LSQR, m still represents the location and origin time to be estimated and, **I** is the identity matrix.

One of the problems faced in minimizing the travel time residuals is the sparseness of the **G** matrix, since only two events are being linked together. If one event is poorly linked to another, the **G** matrix can become ill conditioned, leaving the solution un-stable when using LSQR. This problem can be dealt with by only allowing well-linked events into the solution process; however, this becomes a problem when moderately sized clusters or data sets are being used. LSQR deals with ill-conditioned systems by allowing damping of the solution; ? is the damping factor in equation (11).

A well-constrained solution to the least squares problem is essential for reliable earthquake relocations. An assessment of constraints and reliability involves sensitivity testing of the parameters that control HYPODD, such as MAXSEP, WDCT, and DIST. This is especially true when using a data of less than 1000 earthquakes, as well-linked events are difficult to establish and poorly linked events must be taken into account in order to reach any solution. This is the situation with the data set for this study.

HypoDD

In order for HYPODD to be effective, random errors must be minimized as much as possible. In principle, cross correlations of digital waveforms can be used to reduce uncertainty of travel time differences between earthquake pairs. Unfortunately, this is possible only for a very few events in the eastern Tennessee seismic zone. The bulk of the travel time data are determined from analog recordings. A major concern with analog data are reading errors in the determination of arrival times; HYPODD cannot reduce these types of errors.

P and S wave arrivals can be used by HYPODD, either jointly or independently. In the instance of a large data set it may be more computationally viable to perform separate relocations

using the P or S phases; however for this study, both phases are used jointly during each relocation. The basic procedure behind the HYPODD relocation is to identify events that can make an event pair, and identify the station or stations that each pair can be linked to in order to make travel time corrections to that station; ultimately a group of event pairs are linked together in clusters and the least squares solution for each cluster is found to achieve relative locations. HYPODD is useful for relocation of small magnitude earthquakes; it is often used in areas with very few large recorded earthquakes or with aftershocks of major earthquakes.

There are essentially three steps involved when relocating earthquakes with HYPODD: 1.) the forming of event pairs and links to neighbors, 2.) the formation of clusters, and 3.) double-difference relocation. The initial step is done using the program ph2dt. Ph2dt establishes links for each event-pair to neighboring event pairs that will ultimately determine clustering during the next step of relocation. An event-pair are two hypocenters that fall within a pre-defined distance of one another, and recorded at common stations. When ph2dt is run an event-pair is linked to a certain number of neighbors to form a continuous chain of event-pairs that will define a cluster. A neighbor is an event-pair that falls within a certain radius of another event-pair, the **MAXSEP**, and meets the minimum number of phase pair links, **MINLNK**, established by the program input. The **MINLNK** is the minimum number of phases that two pairs must record at a single station in order to be considered neighbors. The minimum number of phase links is typically at least eight, to allow at least one observation for the eight degrees of freedom. In the instance that the minimum number of links is not present, a weakly linked neighbor will be identified and may be used in relocation. These are considered the two most important criteria in establishing a neighbor.

There are several other parameters that are used to further screen event-pairs for possible neighbors. The **MAXDIST** is the maximum distance that can exist between an event pair and a

station; however, this parameter is typically used very liberally as there is a similar input for HYPODD which can be used to better constrain a cluster. For very large data sets it is possible for the large number of event pairs to exceed the limits of the computer storage and practical limits of execution time. Ph2dt gives several options to limit the possible neighbors and phases that will be used when running HYPODD. The most significant of these is the **MAXNGH**, the maximum number of neighbors that each pair is allowed to have. An event-pair's neighbors are listed from closest to farthest until the **MAXNGH** is reached. Also, the maximum number of links per pair can be specified under **MAXOBS**. Limits imposed by small values of these last two parameters are rarely utilized on data sets of a few thousand or less, such as in this study; they are only necessary for data sets consisting of several thousand or more events.

Five files are created in a ph2dt run: dt.ct, dt.cc, event.sel, event.dat, and ph2dt.log. The **ph2dt.log** file keeps a record of the most recent ph2dt run and pertinent information such as weakly linked and strongly linked events; also, it records any stations not present in the station list. The **dt.ct** file stores catalog data, and absolute travel time for pairs of selected earthquakes. The **dt.cc** file collects differential travel times for waveform cross-correlated earthquakes, if used. All of the events that were made available for the ph2dt program are recorded in event.dat and the selected events are recorded in event.sel. The files that HYPODD will use are the **dt.ct**, **dt.cc**, and **event.sel**; again since no cross-correlation data were used in this study, the file **dt.cc** was not created or used.

After analysis using ph2dt, strongly linked event-pairs have been identified and recorded, and can serve as input to HYPODD for the double-difference relocations. HYPODD first groups the event-pairs into clusters. A cluster can be as small as two earthquakes (one event-pair) or as large as the computer can computationally handle. A cluster is a continuous chain of event-pairs that are strongly linked and meet user defined criteria set forth in the HYPODD input, by the

values of **WDCT** or **DIST**. It is possible and likely that two clusters may be extremely close to each other and still be two separate clusters rather than one larger cluster. Depending on the input parameters, HYPODD may form a few large clusters with many events in them or several small clusters with a smaller number in each one; this is determined by the pre-specified values, such as **MAXSEP** or **WDCT**. HYPODD can relocate all of the clusters or a selected sub-set of clusters.

Figure 2.1 is a diagram illustrating some important parameters involved in linking event pairs and forming clusters.

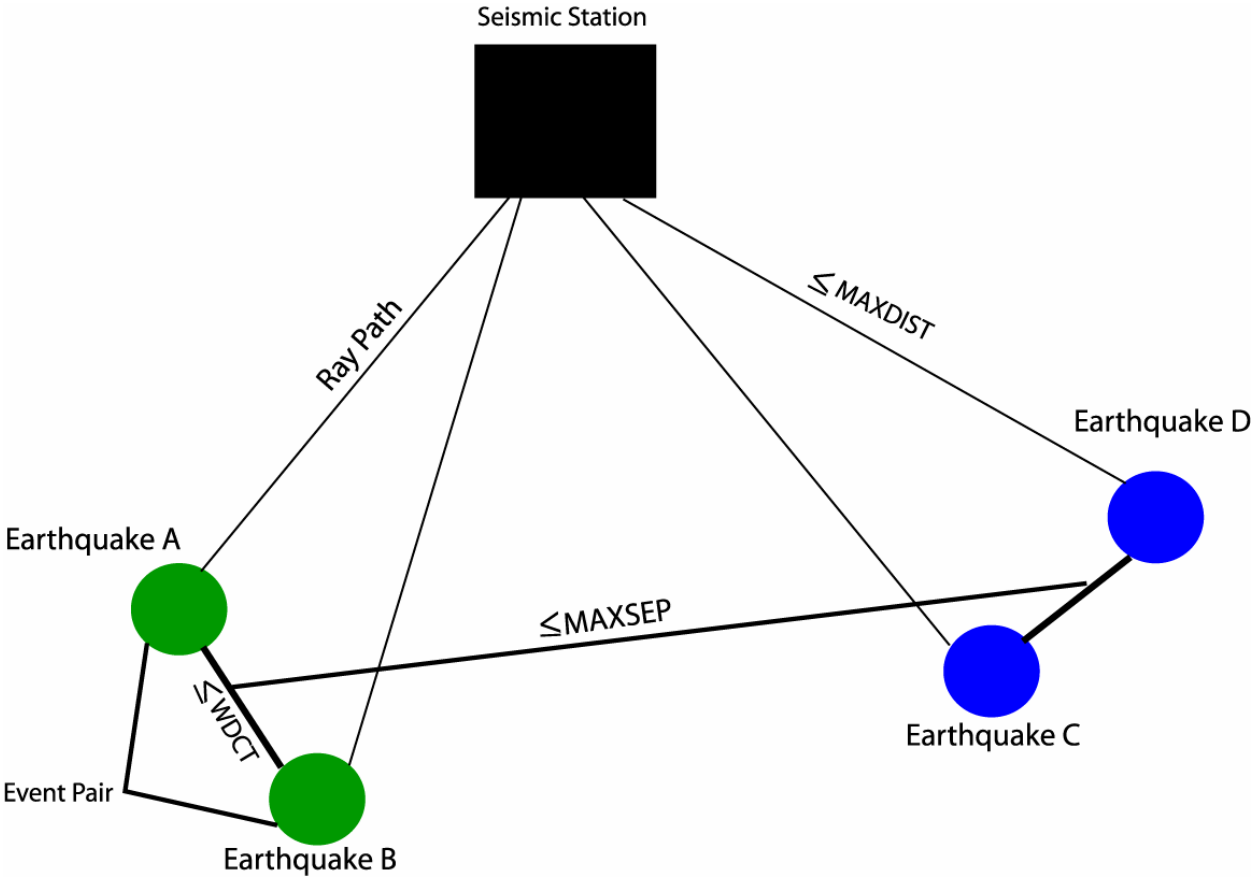

Figure 2.1: Diagram illustrating some important HYPODD parameters.

There are several input parameters that may be used to filter and strengthen the relocation solution. The type of data, whether catalog or waveforms of cross-correlation data as well as which phases (P or S, or both) are specified. One of the parameters used to define how large a cluster will be and how many events will be included is the maximum distance between the cluster centroid and possible stations, **DIST**. The larger the **DIST**, the more station pair-wise corrections can be made. The clustering is actually defined by the values of **OBSCC** and **OBSCT**, which define the minimum number of cross-correlation or catalog links, respectively, that must be present to form a continuous chain needed to identify a cluster. Typically this number is at least eight to account for the degrees of freedom, however, in the instance of smaller clusters this number may be increased to sixteen or more. HYPODD gives two options for the type of inversion to be used, singular value decomposition (SVD) or conjugate gradient least squares (LSQR); the inversion must be identified each time HYPODD is run.

The relocation process proceeds by iterative reduction of double difference residuals. The number of iterations is specified, considering the size of the data set and the size of the clusters. Weights are determined for P and S waves and assigned to a certain number of iterations. There can be any combination of the number of user specified iterations and weighting. Also included in the iteration process are the parameters **WDCT** and **WDCC**, which are the maximum event separation, in kilometers, for the catalog and cross-correlated data, respectively. These parameters are similar to **MAXSEP** in the ph2dt program, however, **MAXSEP** is the maximum distance between neighboring event-pairs and **WDCT** is the maximum distance between two hypocenters to form event-pairs. Considering the similarities between these two parameters in conjunction with the station and hypocenter spacing in eastern Tennessee, in order to maintain consistency, **MAXSEP** and **WDCT** were always set equal to each other in this study. Damping is used only when LSQR is the option chosen for inversion.

Damping is chosen for the different sets of iterations specified, between one and 100. The screen output from HYPODD gives a condition number for each iteration and the damping should be adapted based on this number. Waldhauser (2001) suggests that a condition number of 40-50 is desirable when using LSQR.

The damping chosen for each HYPODD run depends on the number of clusters being relocated and their size. For large clusters, or several clusters, the damping must be assigned liberally. A major problem in relocating a large number of clusters simultaneously is that the damping will usually be high; if the damping is too high, the relocated earthquake hypocenters may not move. The best approach is to relocate each major cluster individually, varying the damping for each, according to the condition number. For example, a cluster with 40 hypocenters might need a damping of 15 or 20, while, a cluster of 20 hypocenters may only need a damping of 10 or less. Wolfe (2002) examined the trade-off involved in relocations and damping. Wolfe found that the double-difference algorithm could successfully handle effects of un-modeled velocity structure in earthquakes spaced close together. However, at greater distances the need for a greater dmping value causes the relocations to be less well resolved.

The final input into HYPODD is a one-dimensional velocity model. This velocity model can have a maximum of twelve layers. The Vp/Vs ratio is input and fixed throughout the model. (The use of a fixed Vp/Vs ratio is a limitation of HYPODD). The P wave velocity and layer thickness are assigned for each layer. In this study the Vp/Vs ratio is held fixed at 1.73, the P wave travel times are held constant and the S wave travel times are varied by this ratio. The P and S wave arrival times are weighted the same in the HYPODD input. However, the original weights used in HYPOELLIPSE are preserved, therefore, the weighting of both P and S waves varies. It is also important to note that the HYPOELLIPSE single-event locations calculated for the data set did not use a constant Vp/Vs ratio, this value was varied in each layer.

The output from the HYPODD program is six files: hypoDD.loc, hypoDD.reloc, hypoDD.sta, hypoDD.res, hypoDD.src, and hypoDD.log. The **hypoDD.loc** file contains the individual locations before the relocations are preformed. The **hypoDD.reloc** file reports the relocations in the same format as the initial locations for comparison in matlab or other visual software. The **hypoDD.sta** file outputs station travel time residuals, and the **hypoDD.res** file outputs double difference residuals. The hypocenter-station take-off angles are contained in **hypoDD.src**, and **hypoDD.log** contains a summary of input and control parameters.

Another program that is included in the package with HYPODD and ph2dt is a plotting tool for matlab, eqplot.m that is a two- dimensional program to look at epicenter location and relocations and two possible cross-sections at specified points. This study utilizes this program for initial inspection of relocations before inputting the locations and relocations into a 3-D visualization package, Origin. Several tests to examine the sensitivity of the relocations to the choices of parameter values are necessary to assess solution stability.

Example of hypoDD from Hayward Fault, California

Waldhauser and Ellsworth (2000) applied the double difference algorithm to the northern Hayward Fault in California. The data set consisted of 346 earthquakes, ranging in magnitude from 0.7 to 4.0, recorded between 1984 and 1998. A maximum event separation, WDCT, of 10 km was used, as well as a 200 km maximum distance between the cluster centroid and stations, DIST; cross-correlation data were used. Two major clusters were formed and relocated. The initial, single event locations exhibited a diffuse zone of seismicity trending to the northwest, shown in figure 2.2. The HYPODD relocations, when performed on only the catalog data show a much more linear northwest striking zone of earthquakes, aligned with the map fault trace, an obvious improvement. When both the catalog and cross-correlation data are used in the relocation, the linear features are improved in the area of dense seismicity. The sub-surface

relocations of the two clusters show a tightening of the two clusters when only the catalog data were used. When both types of data were used, small linear features become apparent. There is an unmistakable overall improvement in the locations of the hypocenters and the major structure of the fault is more apparent.

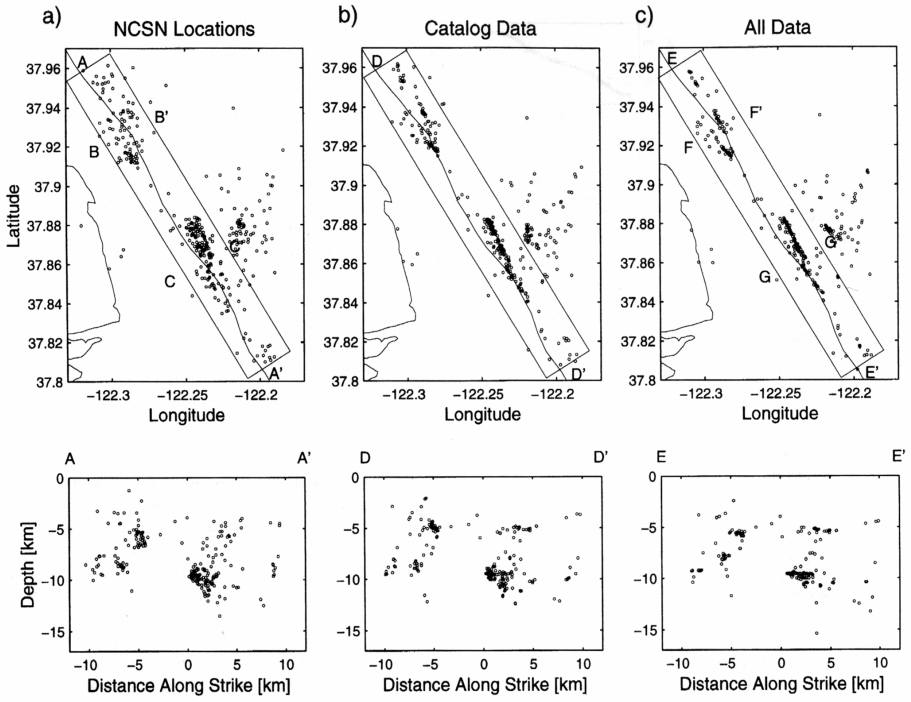

Figure 2.2: Locations and relocations of earthquakes along Northern Hayward Fault, CA. (a.) individual locations (b.) double difference locations of catalog data (c.) combined catalog and cross correlation relocations. (from Waldhauser and Ellsworth, 2000).

There are several differences in this study when compared to Waldhauser and Ellsworth's study of the Northern Hayward Fault. The location of the Hayward fault was known prior to the relocations: one of the goals in this study is to resolve possible fault locations and orientations in eastern Tennessee. It is unlikely that one major fault exists in the eastern Tennessee seismic zone. The solutions of Waldhauser and Ellsworth using the combination of the catalog and cross-correlation digital waveform data revealed more linear features, especially in the sub-

surface: however, this third step cannot as yet be performed in eastern Tennessee, due to the lack of sufficient digital data.

The analysis procedure described above will be applied to the ETSZ. Hopefully the diffuse pattern of hypocenters will condense into something that can be interpreted geologically.

Chapter 3: Testing HypoDD with a Synthetic Data Set

A simple synthetic data set was created for testing HYPODD. The synthetic data set consists of five earthquake hypocenters, separated by 1 km. The five earthquakes are contained in a hypothetical seismic network consisting of nine stations. The earthquakes will be located three separate times using HYPOELLIPSE (Lahr, 1980), once using no errors, once with only systematic errors added, and once with both systematic and random errors added. The two runs containing the errors and will then be relocated using HYPODD (Waldhauser, 2001). The results will be examined to assess the effect that systematic and random errors have on HYPODD relocations. All locations are based on a simple half-space velocity model that considers a constant Vp/Vs ratio, 1.72.

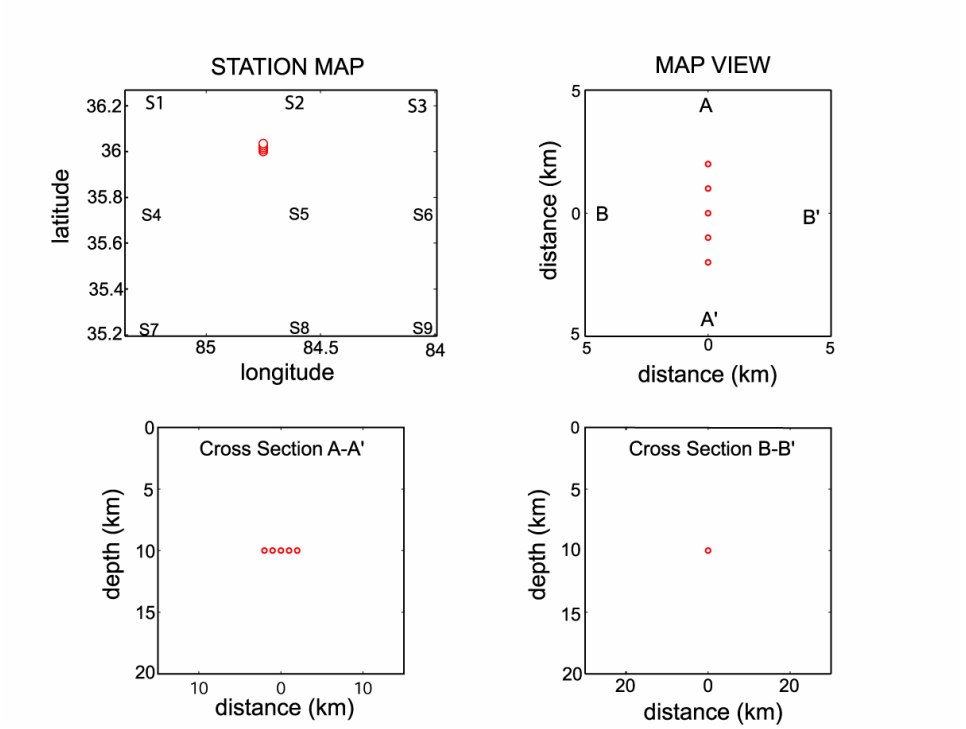

Figure 3.1:HYPOELLIPSE locations of five simulated earthquakes using error-free arrival times. Upper left: station map, with stations indicated as S1 through S9, epicenters shown as empty circles. Upper Right: detailed map view of epicenters and locations of profiles A-A' and B-B'. Lower Left: hypocenters projected onto profile A-A'. Lower Right: hypocenters projected onto profile B-B'.

Figure 3.1 shows the location of the five earthquakes with no errors. The five earthquakes occur along a linear north-south trend, shown in map view at the top right. The top left of figure 3.1 shows the hypothetical seismic network, the locations of the nine seismic stations (S1 through S9), and their relation to the cluster of five earthquakes. The sub-surface will be examined using two cross sections, A-A' and B-B'. The hypocenters associated with zero error are in a line at 10 kilometers depth, as shown on the north-south oriented profile A-A'. The hypocenters appear as one point at 10 kilometers on the east-west oriented profile B-B'.

The purpose of HYPODD is to identify and correct for systematic travel time errors, thus improving the locations of earthquake hypocenters. The ability of the program to achieve this was tested by adding systematic error to the theoretical travel times of the error-free events, shown in figure 3.1. The arrival times at stations S1 and S5 were made systematically early by subtracting 0.7 seconds and the arrival times at stations S2 and S4 were made late by adding 0.7 seconds. The effects of these systematic errors on the single-event HYPOELLIPSE locations are illustrated in figure 3.2. The epicenters were not significantly affected by the addition of the systematic error. However, the focal depths did show significant changes; the linear trend along cross section A-A' (bottom left of figure 3.2) has now been distorted. The cross section B-B' (bottom right of figure 3.2) is no longer a point, since the depths of the five earthquakes have been affected by the errors.

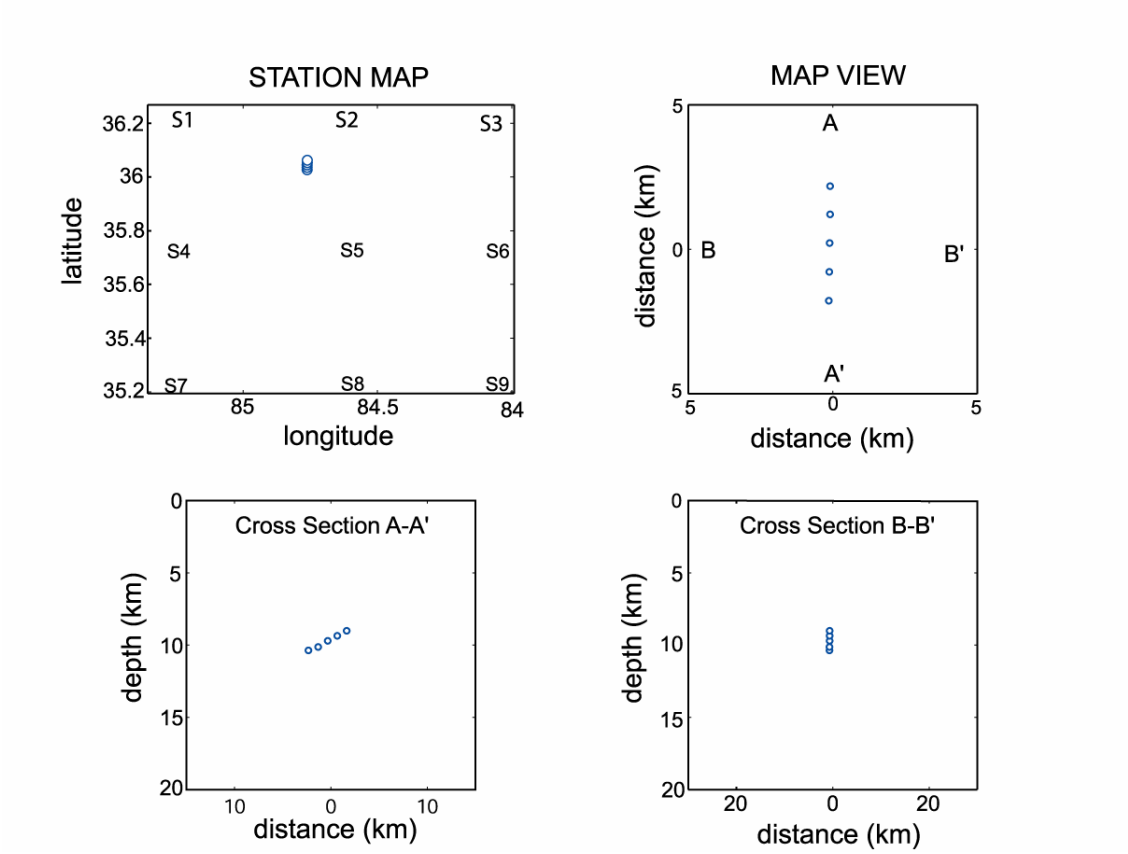

Figure 3.2: HYPOELLIPSE locations of data set containing systematic travel time errors

The HYPODD relocations using the data with the systematic errors recovered the hypocenters of the error-free locations (shown in figure 3.3). The map view shows the linear north-south trend of seismicity. The HYPOELLIPSE locations showed distortion primarily in the sub-surface when systematic errors were added. The sub-surface cross sections show that HYPODD did recover the 10 kilometer depth of all of the hypocenters. Cross section A-A' again exhibits the perfect linear trend at 10 kilometers; and cross section B-B' exhibits the point associated with the error-free data. This result, involving 5 hypocenters with systematic errors at four of nine stations, demonstrates that the double-difference algorithm can recover absolute hypocenter locations in the presence of a systematic travel time error. This is conditional on the existence of sufficient travel time data.

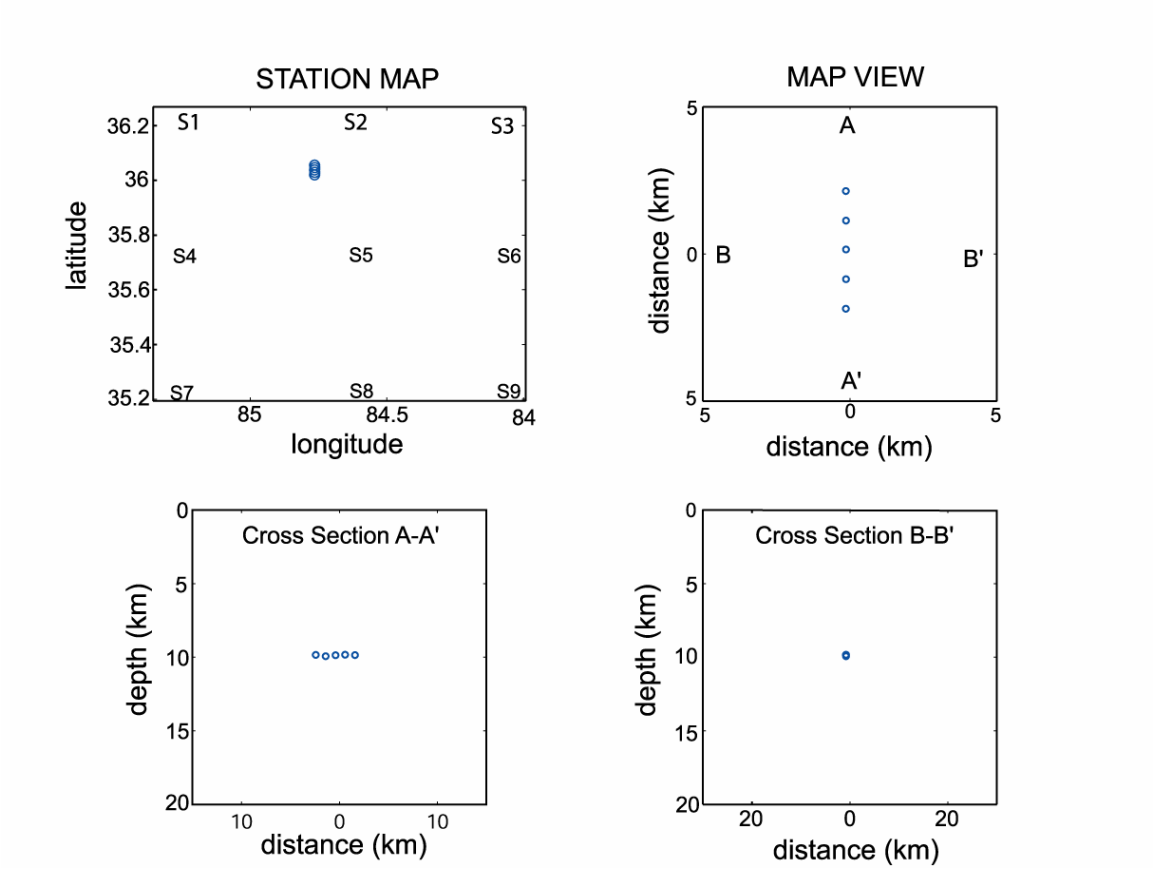

Figure 3.3: HYPODD relocations of synthetic data set with systematic errors only

In order to test HYPODD on a yet more realistic data set, random errors were added to the same systematic errors. The random errors were drawn from a random distribution with 0 mean and a standard deviation of 0.7 seconds. The single event HYPOELLIPSE locations are shown in figure 3.4. In map view, the north-south lineation is now more diffuse. Both cross sections, A-A' and B-B', show major changes in the focal depths.

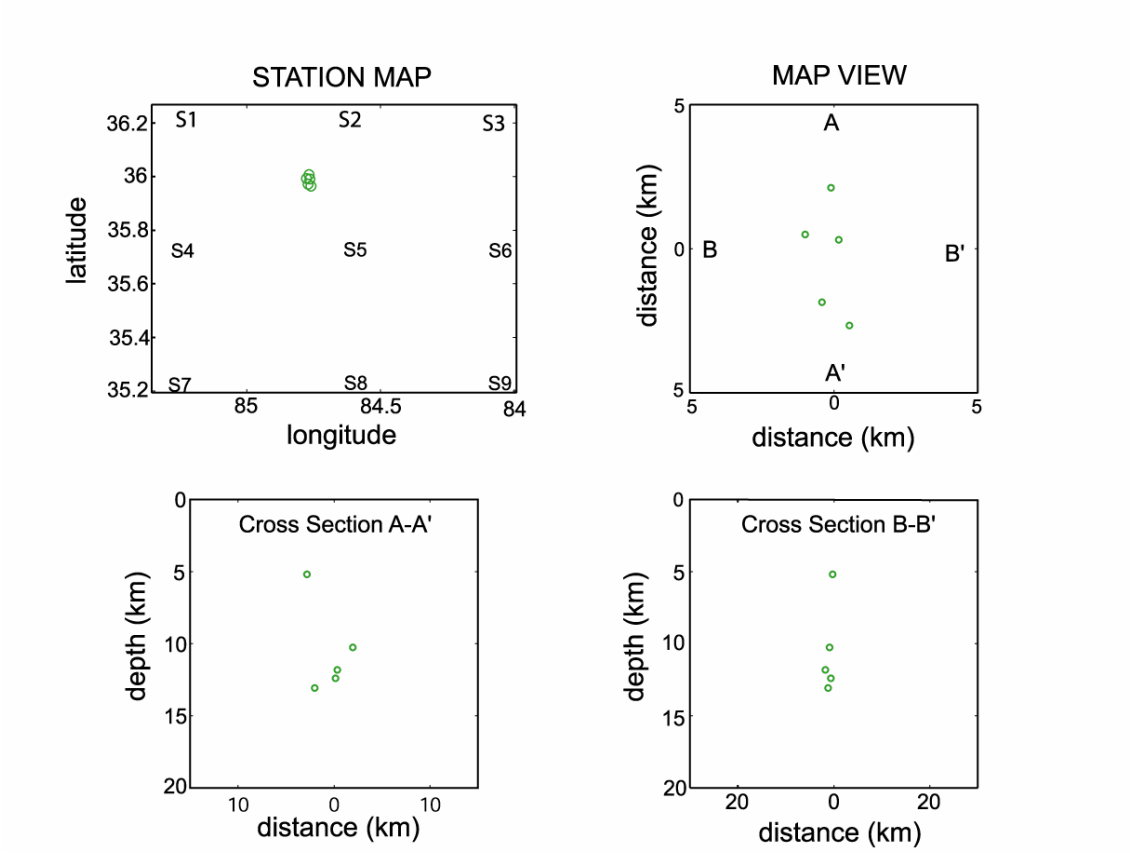

Figure 3.4: HYPOELLIPSE locations of synthetic data set containing systematic and random arrival time errors

The HYPODD relocations in figure 3.5 show improvement over the HYPOELLIPSE locations, in figure 3.4. The error-free hypocenters were not completely recovered because of the addition of random error. HYPODD did not relocate all five of the earthquakes; it failed to link one earthquake with the remaining four events in the cluster. The map view (figure 3.5) shows that the four relocations of the remaining earthquakes have become more linear than the HYPOELLIPSE locations, figure 3.4. In the sub-surface, along cross section A-A', the relocated hypocenters clustered back around the 10 kilometer depth of the error-free locations and three of the four hypocenters are at almost equal depth. Cross Section B-B' resembles the results of the error-free data set more closely. Three of the four earthquakes are clustered around the 10

kilometer depth, resembling the results with the error-free data set. The one hypocenter that did not cluster at 10 kilometers was pulled closer to the 10 kilometer depth by HYPODD.

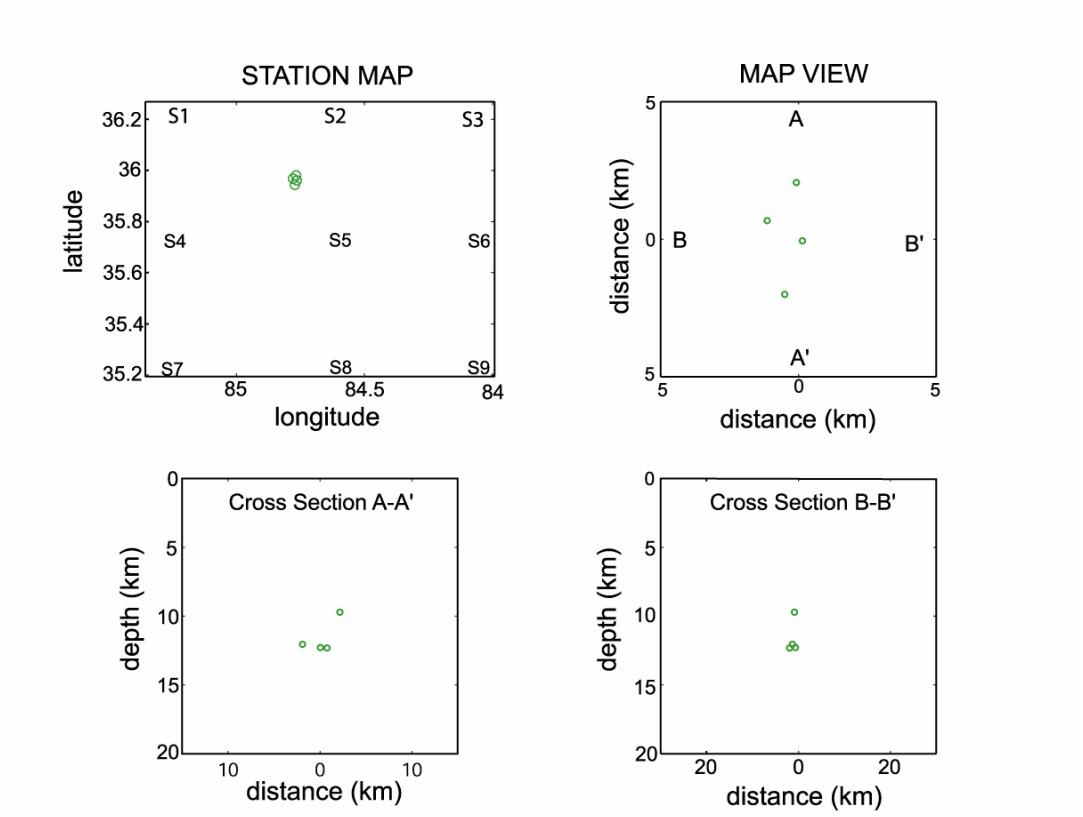

Figure 3.5: HYPODD relocations of data set containing both systematic and random arrival time errors.

The relocations using systematic error at the nine stations demonstrate that HYPODD is capable of correcting systematic errors. The solutions of the HYPODD relocation of the synthetic data set containing systematic and random errors did not yield the theoretical error-free solution, and demonstrates that HYPODD cannot correct for random arrival time errors. The results in the latter case give an indication as to how clusters of earthquakes will behave in reality.

Chapter 4: HypoDD applied to the Eastern Tennessee Seismic Zone

The complete data set contains 993 earthquakes that were located using Hypoellipse (Lahr, 1980) and the one dimensional velocity model of Vlahovic et al. (1998). A series of runs were based on three different values of MAXSEP: 5, 10 and 20 km. The MAXSEP of five kilometers carries the most stringent criteria to form event-pairs, neighbors, and clusters.

Larger maximum event separations (e.g., MAXSEP=20) result in the inclusion of a large number of earthquakes in each cluster. Unfortunately, the relative locations of these events are not substantially improved over the results obtained from HYPOELLIPSE. HYPODD is effective when the distance between event pairs is small, compared to the earthquake-station distance. This condition is not adequately met by the 20 km MAXSEP. Given the relatively small number of stations and large inter-station distances, solutions using MAXSEP equal to 20 km required high damping, with the result that most relocations were not significantly changed from original single event locations. Following the suggestion of Waldhauser and Ellsworth (2000), a MAXSEP of 10 km was applied. Again, relatively large damping values were required, and the largest cluster contained 280 relocated events. This suggested that optimal results could be obtained using smaller MAXSEP. Small values of MAXSEP reduce the number of events in the seismic zone that are relocated, but those events feature strong links. This in turn produces improved relative event locations. The results obtained using a maximum event separation of five kilometers will form the basis for most of the conclusions drawn in this study.

Below, I demonstrate examples of results obtained with MAXSEP values of 20 km and 10 km, and focus attention on the best event clusters resulting from relocations using a maximum event separation of 5 km.

MAXSEP 20 km

The maximum event separation of twenty kilometers resulted in 628 HYPOELLIPSE locations for input into HYPODD. HYPODD formed three clusters. The first cluster contained most of the hypocenters, 624 events. Of those, 576 earthquakes were used in the relocation. The remaining four earthquakes were broken into two small clusters, each containing two events, which were not relocated successfully.

In order to achieve a marginal condition number for the solution, a high value of damping was required. If large values of damping are required to achieve condition numbers in the range 1 to 80, instabilility of the system of double-difference equations is indicated. Waldhauser (2001) recommends using damping values in the range 0 to 80 in conjunction with condition numbers in the range 40 to 80. Solution stability is usually characterized by achieving a condition number of 40 or less with small damping values. In the case of MAXSEP 20 km, the solution is essentially unstable, and the high damping value results in insignificant changes in the relocations. The resulting cluster is extremely large and does not represent a useful improvement of the original locations.

Figure 4.1 shows a plot of the epicenters from the HYPODD relocations for cluster 1, MAXSEP 20 km. The locations are approximately the same as the original HYPOELLIPSE locations.

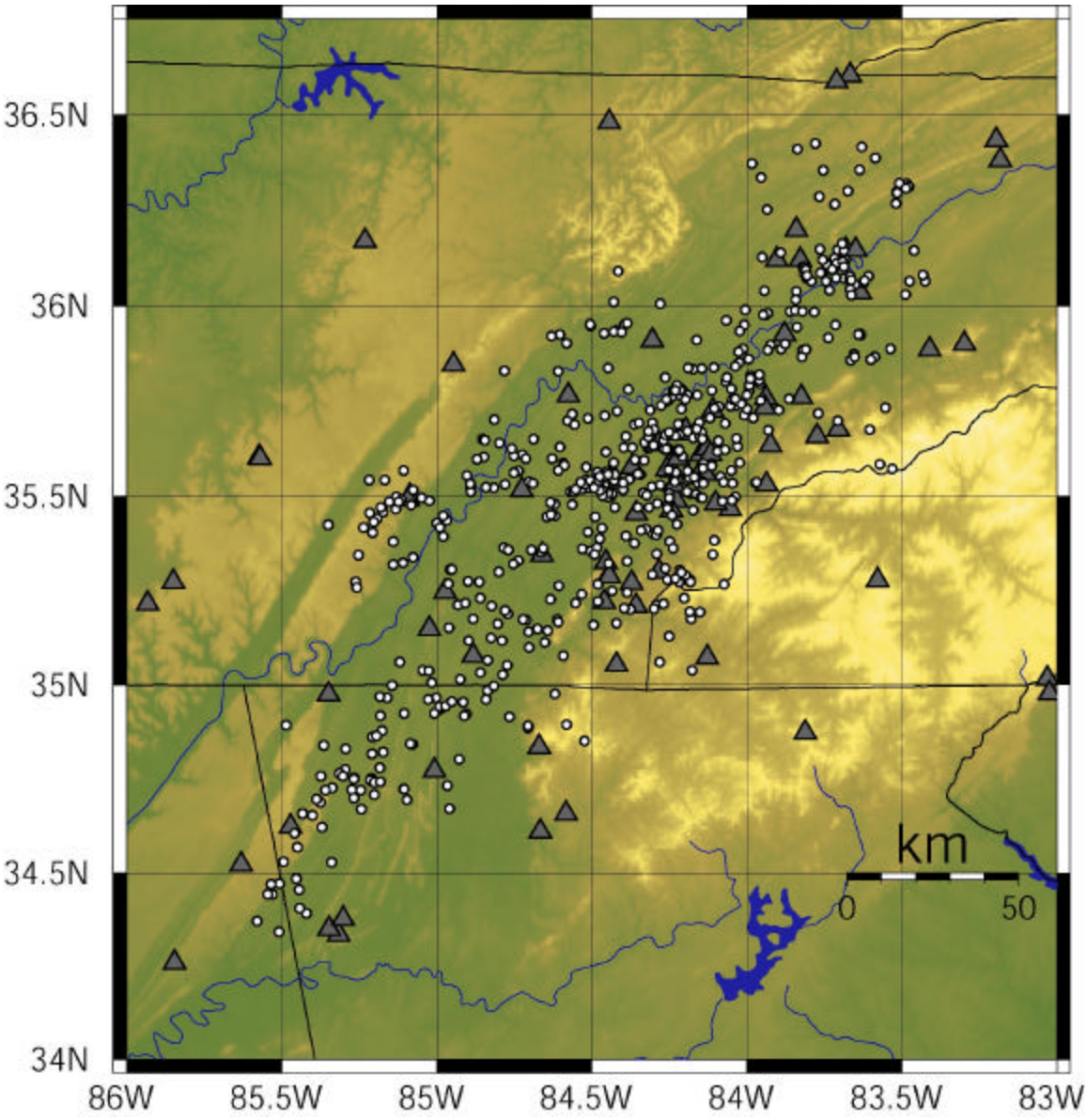

Figure 4.1 Epicenters of earthquakes relocated by HYPODD using MAXSEP set to 20 km. Filled triangles represent seismic stations. Topography is indicated by color shading, e.g., Smoky Mountains (yellow) and Tennessee Valley (dark green).

MAXSEP 10 km

The HYPODD relocations using MAXSEP 10 km formed thirty clusters, ranging in size from almost 300 hypocenters to just two events. Most of the clusters contained very few events. In most cases clusters containing only two events were not successfully relocated. In total, 536 HYPOELLIPSE locations formed the input data set and 507 events were relocated.

HYPODD does not relocate all events that meet the MAXSEP criteria imposed on the data set. Events are deleted if they are not linked as a result of user-specified criteria that define the weighting scheme used for each iteration (see Chapter 2). Also, during the interation procedure, some events are relocated near or above the Earth's surface. The occurrence of airquakes in small clusters can result in the entire cluster not being relocated. This problem can be addressed by increasing damping (which prevents large fluctuation of focal depth) or by improving spatial control (adding data from more stations near the event cluster). HYPODD removes airquakes and then relocates the remaining events in a given cluster.

Cluster 1, MAXSEP 10:

For MAXSEP 10 km, eleven clusters formed that contained five or more events. The largest cluster, cluster 1, contained 298 single-event locations. In cluster 1, 280 events were relocated with a final damping value of 45 and corresponding condition number of 45. Two other clusters have 40 or more relocated events. The remaining clusters have many fewer events and lack earthquakes with focal mechanism solutions. Table 4.1 lists cluster number, the geographic coordinates of the cluster-corner points, the number of HYPOELLIPSE single event locations, and the damping and condition number of final iteration. Figure 4.2 plots the events in the six largest clusters.

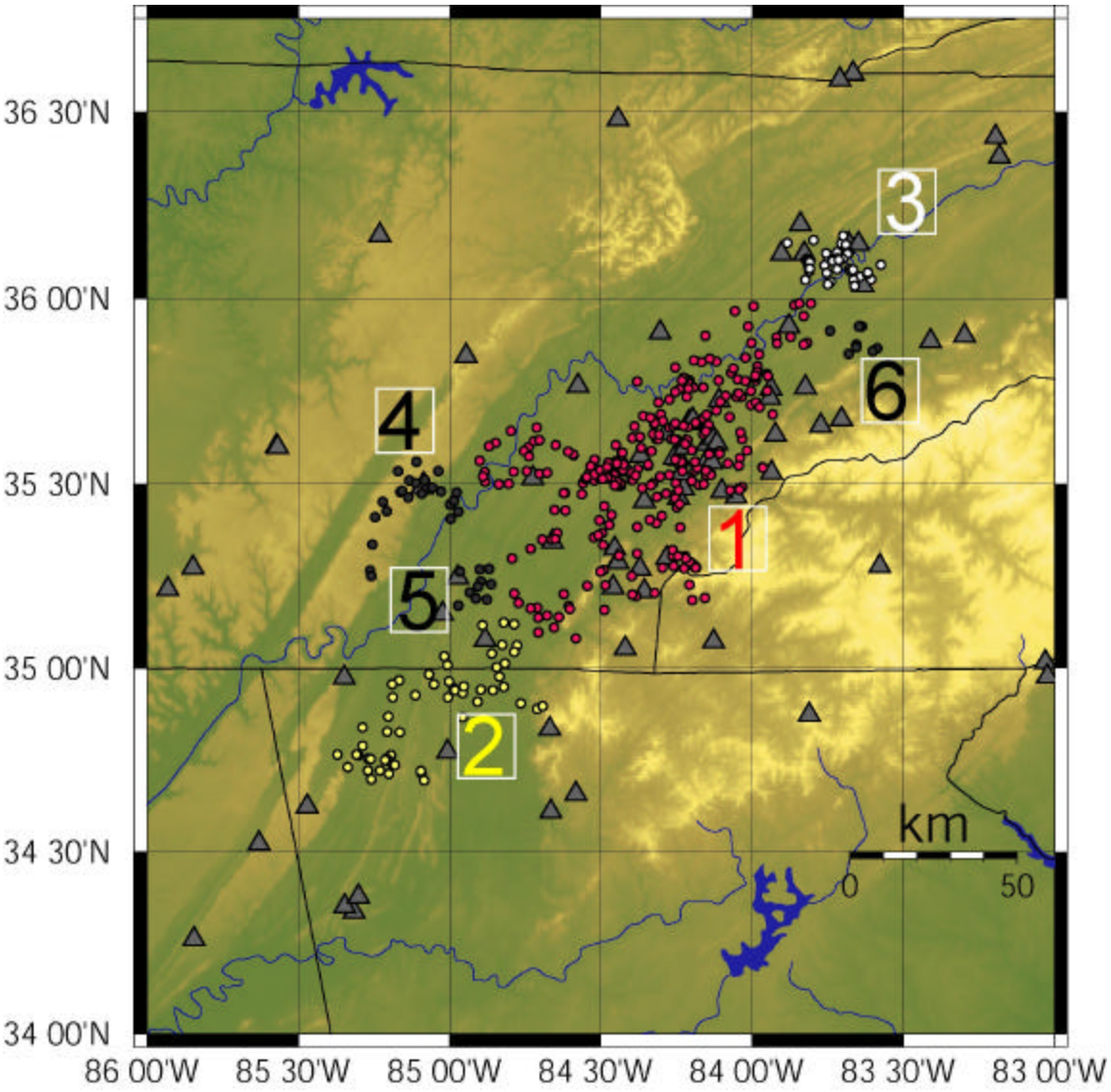

Figure 4.2 Locations of the six largest clusters, MAXSEP 10 km. Each epicenter cluster is indicated by numbers, 1(red), 2(yellow), 3(white), 4, 5, and 6 (black). Station locations are represented by triangles. Topography is indicated by color shading, e.g., Smoky Mountains (yellow) and Tennessee Valley (dark green).

The earthquakes comprising cluster 1 represent the most dense concentration of seismicity in the eastern Tennessee Seismic Zone, and for that reason cluster 1 can be expected to offer the best opportunity for the double difference algorithm to improve the locations.

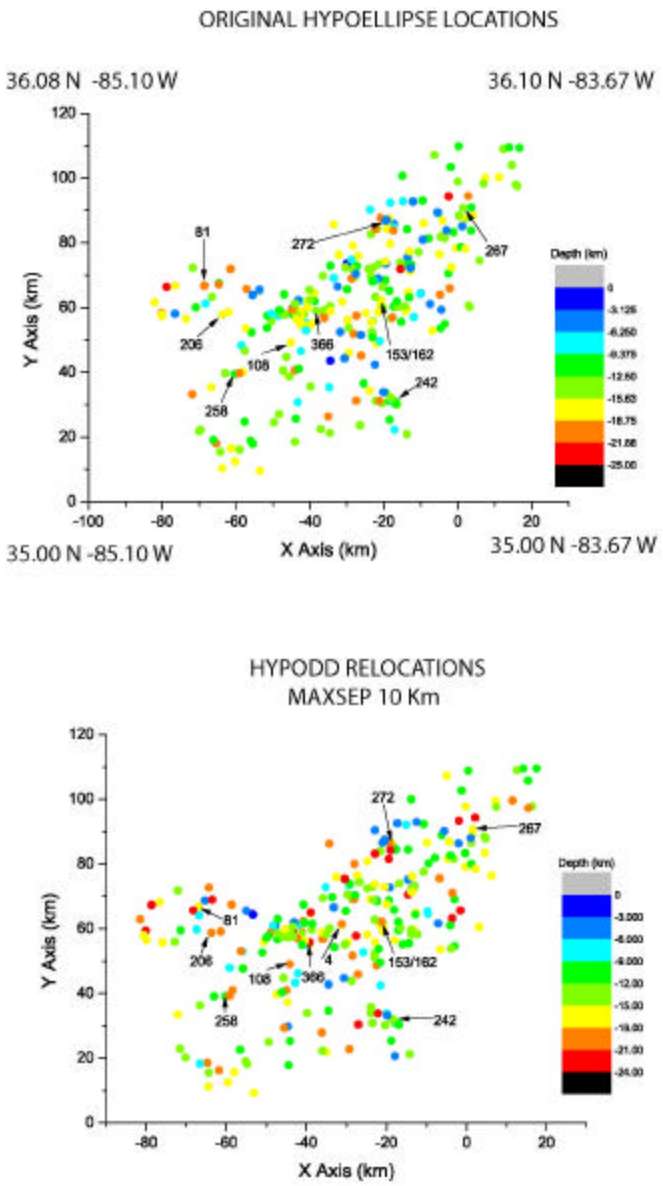

Figure 4.3. Comparison of HYPOELLIPSE original epicenters with those relocated in Cluster 1 using MAXSEP 10 km. The latitude and longitude of the corner points of the cluster are indicated on the top plot. Numbers correspond to focal mechanisms, listed in Table 4.2.

Figure 4.3 (above) compares the original HYPOELLIPSE epicenter locations for cluster 1 to the relocations derived using MAXSEP 10 km. Figure 4.4 (below) shows a perspective plot of the original hypocenters in cluster 1 and those relocated with HYPODD, using MAXSEP 10.

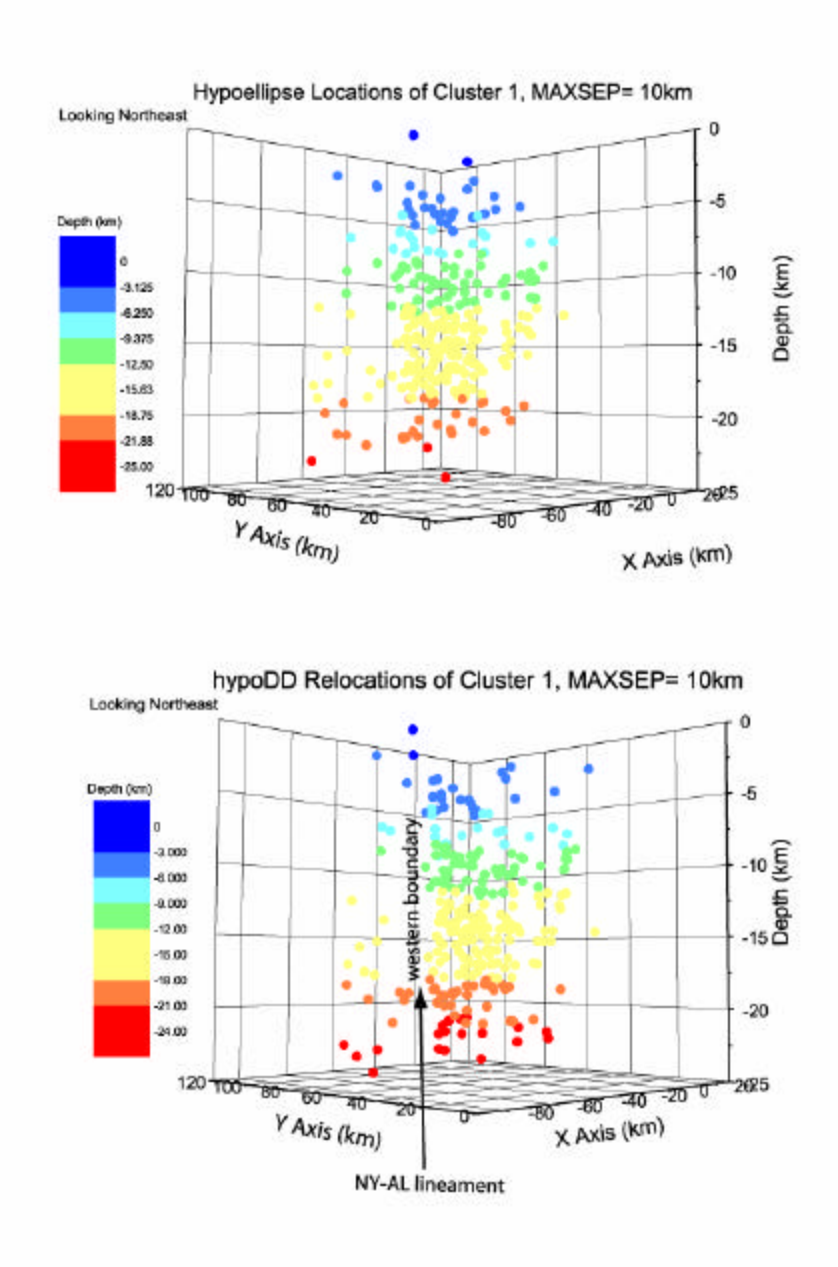

Figure 4.4. Top: Original HYPOELLIPSE hypocenters, cluster 1. Bottom: HYPODD relocations, MAXSEP 10 km, the corresponding latitude and longitude of the corner points of cluster 1 are shown.

There are no obvious major linear or planar structures revealed by the relocations in cluster 1. However, very significant changes in the hypocenter locations have occurred. Figure 4.4 shows two main characteristics: several of the deepest events have been relocated to greater depths, and

there is an obvious "tightening" of the relocated hypocenters. In figure 4.4 the northwestern margin of cluster 1 has been sharply defined by the relocations as a vertical boundary between seismogenic crust and relatively aseismic crust.

The mean change in the hypocenter locations for cluster 1 is 2.1 km, the mean absolute value of the change in depth is 1.7 km, and the mean horizontal shift is 1.0 km. The mean change in focal depth is only 0.2 km with the relocations on average being slightly deeper. However, particular events were shifted considerably. The maximum change in depth was 11.5 km and the maximum change in a horizontal direction was 3.6 km. The ten and ninety percentile changes in the hypocenter relocations were 0.7 km and 3.98 km respectively.

Table 4.1
Breakdown of Clusters Analyzed using MAXSEP 10 km

Cluster Number	Number of Events	Damping Value	Condition Number (last iteration)	Geographic Coordinates Of Corner Points °N	°W
1	298	45	45	36.08 36.10 35.00 35.00	85.10 83.67 85.10 83.67
2	63	25	30	35.35 35.35 34.64 34.64	85.47 84.60 85.47 84.60
3	27	15	36	36.40 36.40 35.99 35.99	84.00 83.50 84.00 83.50
4	11	15	15	35.63 35.63 35.22 35.22	84.94 85.21 84.94 85.21

Cluster 2, MAXSEP 10:

The relocated hypocenters for cluster 2 are shown in figure 4.5, below. Cluster 2 consists of 56 relocated earthquakes. Two focal mechanisms (Chapman et al., 1997) are available from

among events in this cluster and are shown in figure 4.5. My strategy is to use the focal mechanisms as a guide for examining the three dimensional spatial characteristics of the HYPODD relocations. Therefore, I have created a series of three dimensional plots aligned with the strike directions of the focal mechanism nodal planes. Table 4.2 identifies and outlines the location, strike, dip, and rake of the focal mechanisms examine with each cluster. The focal mechanisms available for cluster 2 indicate northerly and easterly striking nodal planes. When viewed in perspective, looking to the west, the relocated hypocenters suggest at least two possible northerly dipping planes. This interpretation is equivocal: however, it is consistent with focal mechanism #116. When the hypocenter view is oriented in a northerly direction, the pattern of hypocenters does not suggest planar features. Based upon the available information, I interpret the available information as suggesting that the seismogenic structures in cluster 2 may strike to the west and dip to the north.

The mean change in the hypocenter locations is 2.4 km. The mean change in a horizontal direction was 1.0 km and the mean change in the depth was 2.0 km. The range of hypocenter depths is approximately from 1 to 24 km. A majority of the events after relocation are at depths less than 10 km (figure 4.5).

Table 4.2
Focal Mechanisms Solutions

Event ID	Cluster No.	MAXSEP (km)	Yr/Mo/Da	Time	Lat. (°N)	Long. (°W)	Depth (km)	m_{bLg}	S_1*	D_1*	R_1*	S_2†	D_2†	R_2†
5	3	10	84/02/14	20:54	36.11	83.71	4.65	3.6	83	80	-2	173	88	-170
26	2	5	84/08/30	16:26	35.55	84.35	17.16	3.2	284	56	23	180	71	143
30	2	10	84/10/09	11:54	34.77	85.17	9.29	4.0	90	41	-11	189	82	-130
116	2	10	86/07/11	14:26	35.95	84.99	11.76	3.8	109	85	-30	202	61	-174
153	1	5	87/03/27	7:29	35.56	84.23	17.57	4.2	275	83	45	178	46	170
162	1	5	87/04/09	1:31	35.56	84.23	18.48	2.7	92	80	-18	185	73	-170
181	3	10	87/07/11	0:04	36.11	83.81	24.51	3.7	307	55	-4	40	87	-145
183	3	10	87/07/11	2:48	36.11	83.81	23.81	3.2	302	59	-16	41	76	-148
242	3	5	88/01/09	0:16	35.28	84.19	11.74	2.9	300	62	-22	40	71	-150
273	3	10	88/04/23	0:08	36.12	83.75	16.47	2.3	111	79	-49	214	42	-162
366	2	5	89/09/07	5:18	35.50	84.44	21.07	2.9	266	73	-58	22	36	-149

*S_1,D_1, and R_1: strike, dip, and rake of nodal plane 1 (degrees)
†S_2,D_2, and R_2:strike, dip, and rake of nodal plane 2 (degrees)
(Solutions for nodal plane orientations taken from Chapman et al., 1997)

Cluster 3, MAXSEP 10 km:

Cluster 3 is located near the northeastern tip of the seismic zone and contained 40 relocated hypocenters. Four focal mechanism solutions were derived by Chapman et al. (1997) for events in cluster 3. Figure 4.6, below, shows the epicenters and associated focal mechanisms. Three of the four focal mechanisms exhibit northeasterly and northwesterly trending nodal planes. The fourth solution indicated faulting on either northerly or easterly trending nodal planes.

Figure 4.6 shows that HYPODD was effective in tightening the distribution of epicenters in cluster 3. In particular, the subset of events in the vicinity of events #181 and #183, which exhibit northeasterly and northwesterly trending nodal planes, have been resolved into a short northwesterly trending alignment. This suggests that faulting occurred on the northwesterly trending nodal plane in the case of these events

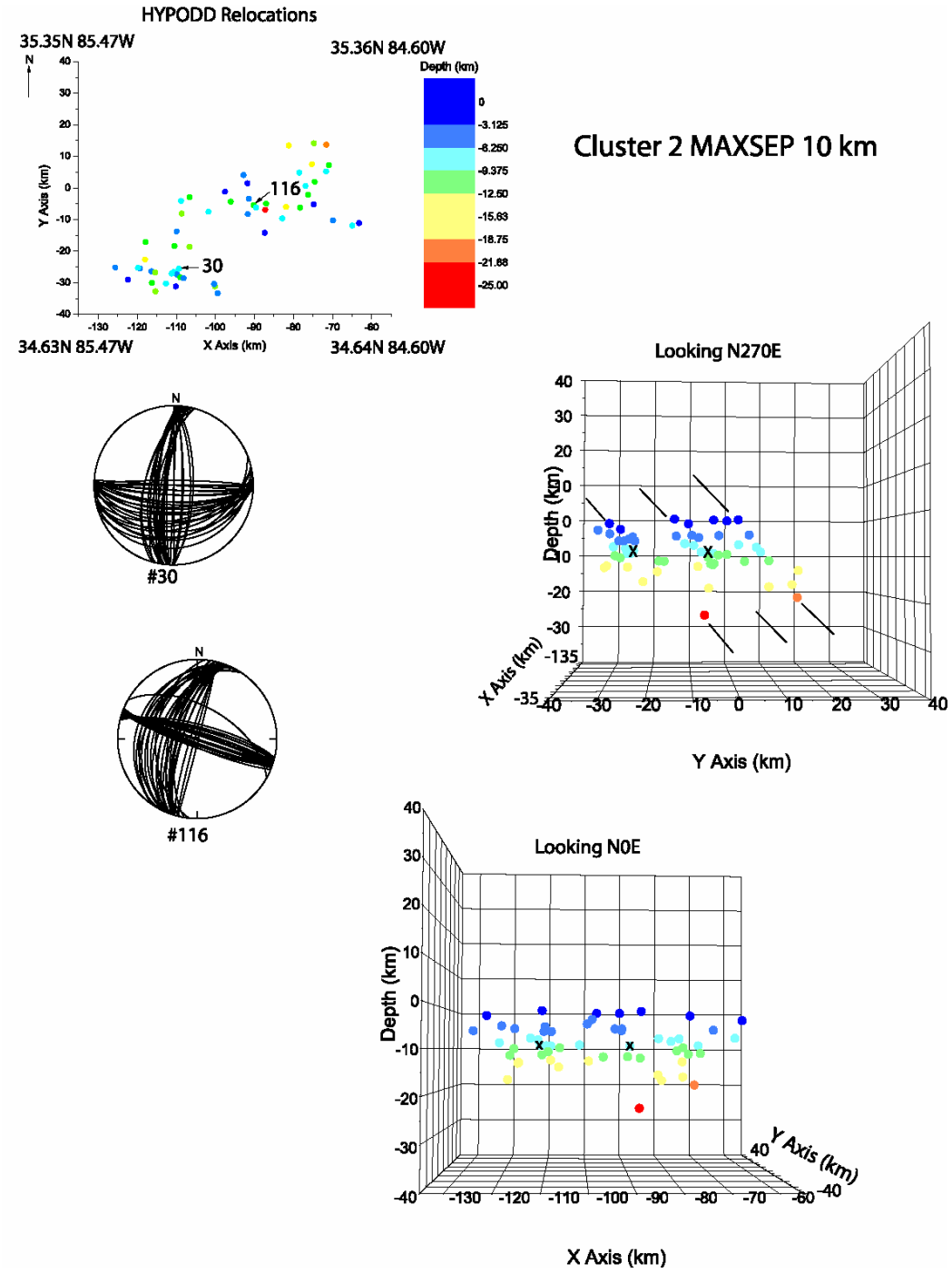

Figure 4.5. HYPODD Relocations of Cluster 2, MAXSEP 10 km. Upper Left: Map view of cluster 2 epicenters (latitude and longitude coordinates of the corner points of cluster 2 are shown). Upper Right: three dimensional perspective view, looking to the west. Lower Right: three dimensional perspective, looking to the north. In the map view the numbers associated with arrows indicate events with focal mechanisms. The individual focal mechanisms are illustrated with an X in the three-dimensional plots. . See APPENDIX 3 for listing of relocated hypocenters.

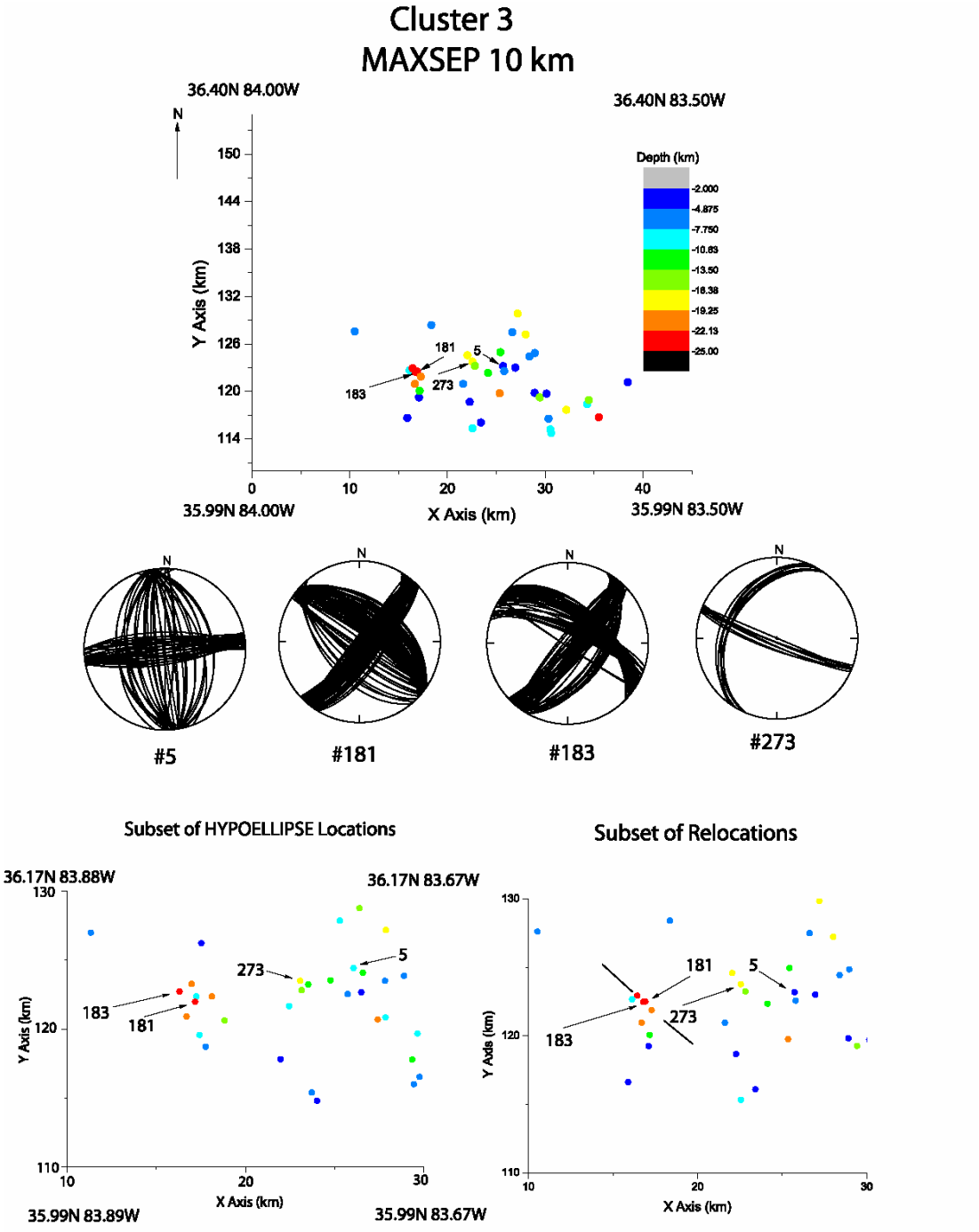

Figure 4.6. HYPODD Relocations of Cluster 3. Top: Map view of cluster 3 epicenter relocations. Lower Left: Map view of sub-set of HYPOELLIPSE locations (corresponding latitude and longitude of corner points of the cluster are indicated). Lower Right: Map view of subset of HYPODD epicenter relocations. Also Shown: focal mechanisms for four events in cluster 3 (from Chapman et al., 1997). In the map view the numbers associated with arrows indicate events with focal mechanisms. The individual focal mechanisms are illustrated with an X in the three-dimensional plots. See APPENDIX 3 for listing of relocated hypocenters.

Figure 4.7 (below) shows several three dimensional perspective views of cluster 3. Because of the various focal mechanism orientations, two sets of perspective view are examined. Event #5 exhibits north-south and east-west trending nodal planes. The views at the top of figure 4.7 do not distinguish between nodal planes for event #5. The hypocenters at shallow depth in cluster 3 do not align in agreement with focal mechanism #5. The two views at the bottom of figure 4.7 are aligned parallel to the nodal planes of events #181, #183, and #273. The events local to event #273 do not form a planar feature, and the subsurface perspective views at the bottom of figure 4.7 do not distinguish between northeast or northwesterly trending planes. The difficulty in interpretation is due to the fact that all events near #181 and #183 occur at similar focal depths.

In the case of cluster 3 the three dimensional interpretation of HYPODD relocations does not resolve obvious planar seismogenic structures. However, it appears that a short alignment of epicenters, with northwest trend, exists in association with events #181 and #183. This, along with the focal mechanisms, favors an interpretation of a northwest trending fault plane for those events.

The relocated hypocenters in cluster 3 occur at depths ranging from approximately 4 to 25 km. In contrast to cluster 2, several earthquakes, particularly events #181 and #183, occur at mid-crustal depths (25 km). The mean change for the relocated hypocenters is 2.3 km. The mean horizontal change is 1.2 km and the mean change in depth is 1.8 km. The maximum epicenter location change in cluster 3 is 9.2 km.

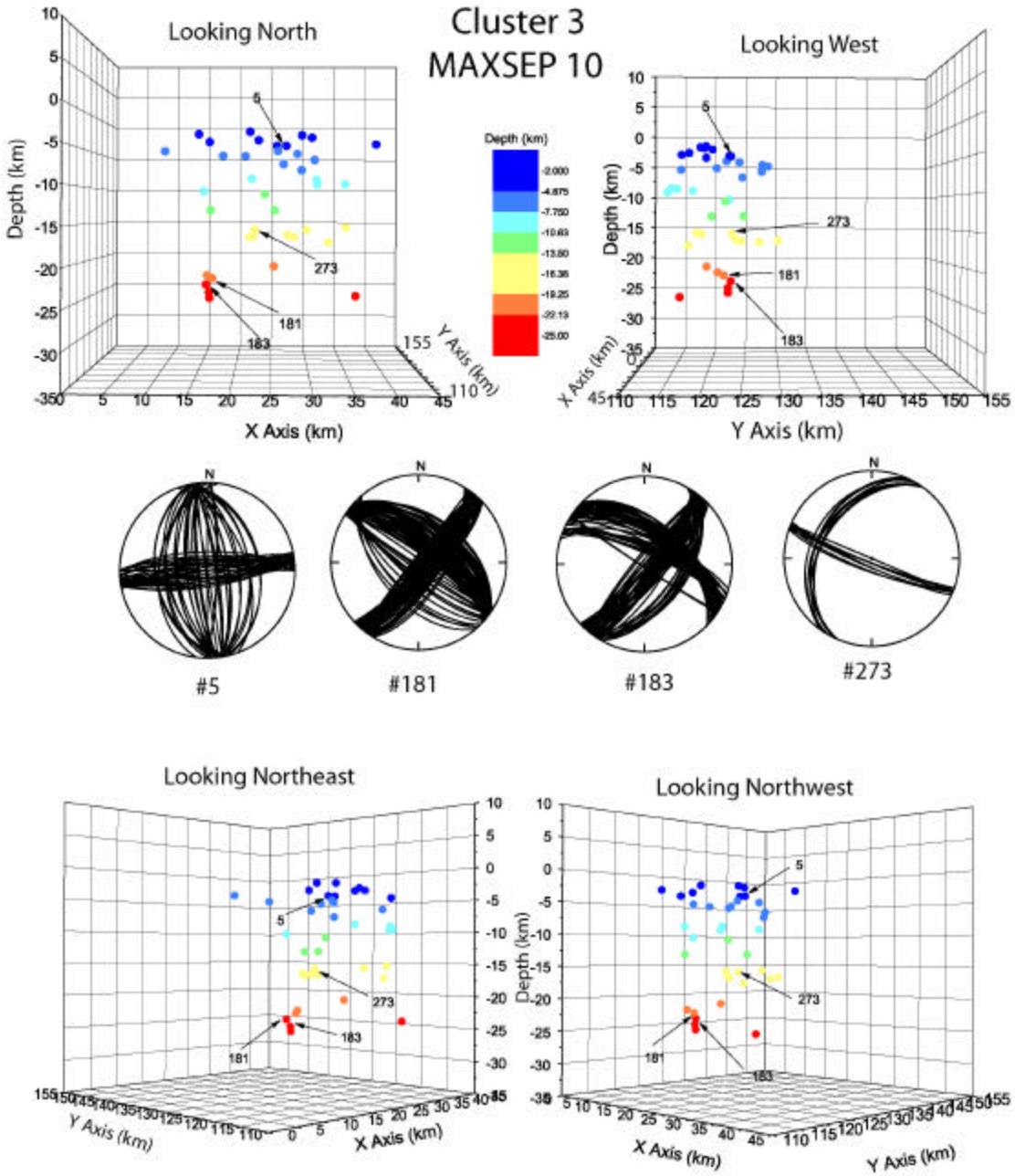

Figure 4.7. Hypocenter relocations of cluster 3. Top Left: three dimensional perspective oriented north. Top Right: Perspective view oriented west. Bottom Left: Perspective oriented northeast. Bottom Right: Perspective oriented northwest. Also Shown: focal mechanisms for four events in cluster 3 (from Chapman et al., 1997). In the map view the numbers associated with arrows indicate events with focal mechanisms. The individual focal mechanisms are illustrated with an X in the three-dimensional plots. See APPENDIX 3 for listing of relocated hypocenters.

Clusters 4, 5, and 6, MAXSEP 10 km:

Clusters 5 and 6 do not contain enough events for meaningful geologic interpretation. Cluster 4 is interesting because it lies to the west of the NY-AL lineament. Unfortunately, there are no focal mechanism solutions for this cluster. Figure 4.8 shows the HYPOELLIPSE single event locations and HYPODD relocations of the hypocenters. The relocations produced somewhat greater focal depths in this cluster. It is interesting to note that most of the events, more than 50 percent, occurred between 15 and 25 km, whereas, at least 50% of the events in clusters 1,2, and 3 are shallow events (depths less than 15 km).

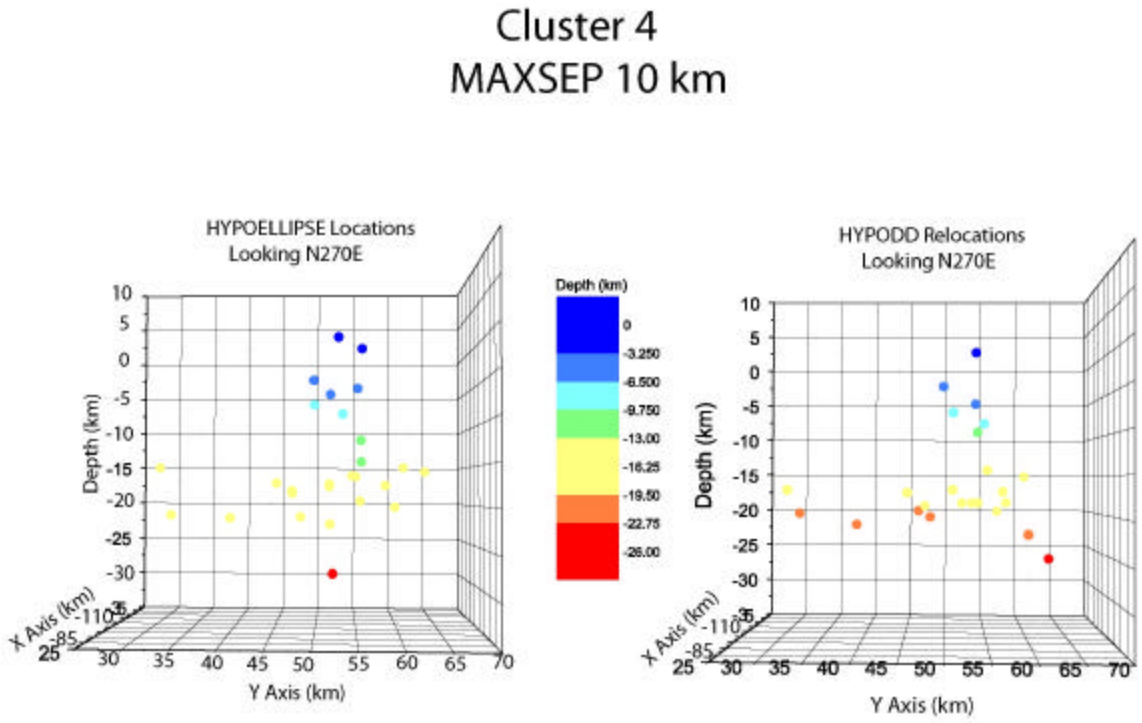

Figure 4.8. Comparison of HYPOELLIPSE single event locations and HYPODD relocations of cluster 4. Left: three dimensional plot of HYPOELLIPSE locations looking to the west. Right: HYPODD relocations.

MAXSEP 5 km

The value of MAXSEP 5 places the most stringent selection criterion upon the formation of event pair links and clusters. The earthquakes that pass the selection process are those that reside in the most active parts of the seismic zone. Hence, these events are assumed to occur on the more important seismogenic features.

There were 292 individual locations which satisfied the stringent criteria of MAXSEP 5 km. In the next step of the process, HYPODD formed 80 clusters. Eleven clusters contained five or more hypocenters. None of the clusters in this run were large; therefore, each cluster could be relocated using small damping values (10 or less in all cases). Three clusters contained 10 or more relocated hypocenters, these are shown in figure 4.9 below. The events in figure 4.9 were contained in cluster 1, using MAXSEP 10 km, figure 4.4. Table 4.3 lists the geographic coordinated of the corner points, the number of HYPOELLIPSE single-event locations, the damping value, and the condition number for each of the clusters examined with a MAXSEP 5 km.

Table 4.3
Breakdown of Clusters Analyzed using MAXSEP 5 km

Cluster Number	Number of Events	Damping Value	Condition Number (last iteration)	Geographic Coordinated of Corner Points °N	°W
1	35	10	32	35.72 35.72 35.45 35.45	84.33 83.98 84.33 83.98
2	34	10	26	35.72 35.72 35.45 35.45	84.61 84.28 84.61 84.28
3	14	10	27	35.35 35.36 35.18 35.18	84.33 84.11 84.33 84.11

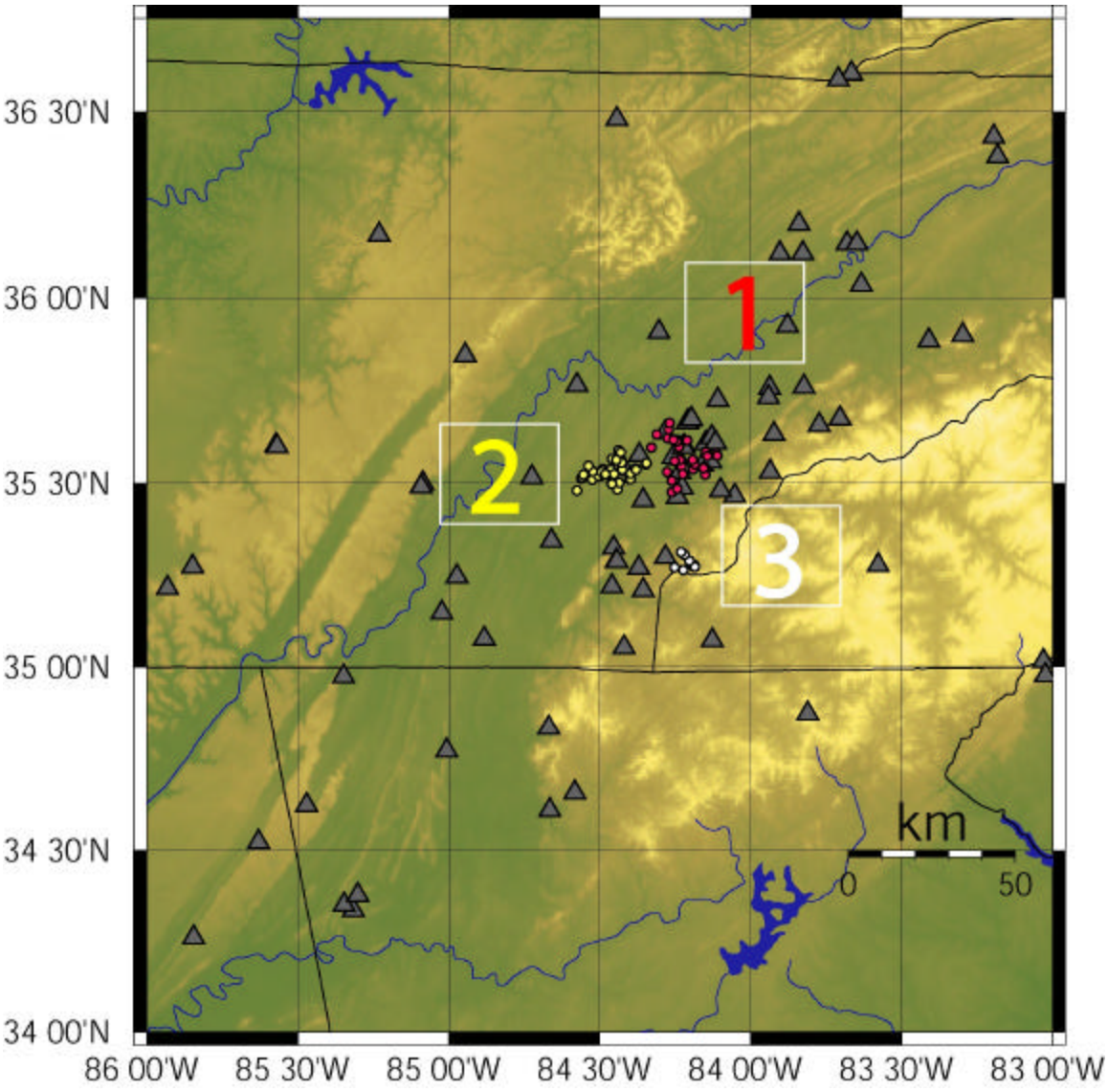

Figure 4.9. Locations of three largest clusters, MAXSEP 5 km. Each epicenter cluster is indicated by numbers, 1(red), 2(yellow), 3(white). Station locations are represented by triangles. Topography is indicated by color shading, e.g., Smoky Mountains (light) and Tennessee Valley (dark green).

Cluster 1, MAXSEP 5 km:

Figure 4.10 below shows the HYPOELLIPSE locations and HYPODD relocations of cluster 1. There were 32 events relocated in cluster 1, with focal depths ranging from 5 to 19 km. The mean change in the relocations for cluster 1 is 1.5 km: the mean horizontal change is

0.7 km, and the mean change in depth is 1.2 km. The maximum horizontal change is 5.3 km and the maximum change in depth is 4.9 km. These changes represent approximately half of the values encountered when relocating the events in clusters described above using MAXSEP 10 km. Note that because of the selection criteria (MAXSEP 5 km), these events sample the most active parts of the ETSZ.

Two focal mechanisms were calculated for cluster 1 by Chapman et al. (1997). These mechanisms exhibit strike-slip faulting, with north-south and east-west trending nodal planes. Event #153 was the magnitude 4.2, Vonore, TN earthquake; which is the third largest earthquake to have been instrumentally recorded in the seismic zone and the largest earthquake included in this data set. The Vonore earthquake produced an aftershock sequence that was monitored by a temporary local network (Nava et al., 1989). Nava et al. inferred unilateral rupture on a north-south nodal plane, based on location of the main shock and a sub-set of nearby aftershocks recorded using the temporary network. Nine aftershock epicenters were located within 3.5 km of the main shock and 6 of those aftershocks formed a north-south trending alignment with the main shock. However, as noted by Chapman et al. (1997), 12 additional "aftershocks" occurred at distances up to 50 km from the main shock and lie generally on an east-west alignment with the epicenter of the main shock. Event #162 was the largest of the local aftershocks and the only one recorded well by the permanent network, therefore, it is the only aftershock considered in this data set.

The three dimensional plots of cluster 1, figure 4.10, are oriented along the two nodal plane strike directions for events #153 and #162. Both the map view for the epicenters and the perspective view looking to the north support the conclusion of Nava et al. (1989), that faulting occurred on the north trending nodal plane. In Figure 4.10 there is an east-west trend of epicenters at Y coordinate value 63, extending from X coordinates -23 km to -12 km. In

perspective view to the west, the hypocenters local to events #153 and #162 suggest a northerly dipping planar feature. The dip of the westerly trending nodal plane of #153 is 83 degrees. The dip of event #162 is steep, but not well constrained. On the basis of the data in cluster 1, the HYPODD relocations fail to distinguish between the two possible fault orientations.

Cluster 2, MAXSEP 5 km:

Cluster 2 is located directly to the west of cluster 1 (figure 4.9). HYPODD relocated 34 events in this cluster. Figure 4.11 shows the HYPOELLIPSE locations and HYPODD relocations of cluster 2. The relocated focal depths in this cluster range from 8 to 22 km. The mean change in location in cluster 2 was 2.2 km. The mean horizontal change was 1.4 km and the mean change in depth was also 1.4 km. The maximum horizontal change in this cluster was 13.8 km and the maximum change in depth was 3.9 km. The mean changes for cluster 2 are approximately twice as large as cluster 1.

Two focal mechanisms were calculated for cluster 2 (Chapman et al., 1997). Event #366 shows a west trending, steeply dipping nodal plane; and a northerly trending, shallow dipping nodal plane. Event #26, on the western edge of the cluster, also has north-south and east-west trending nodal planes, with a steep dip on the northerly plane and a 56 degree dip on the east-west nodal plane.

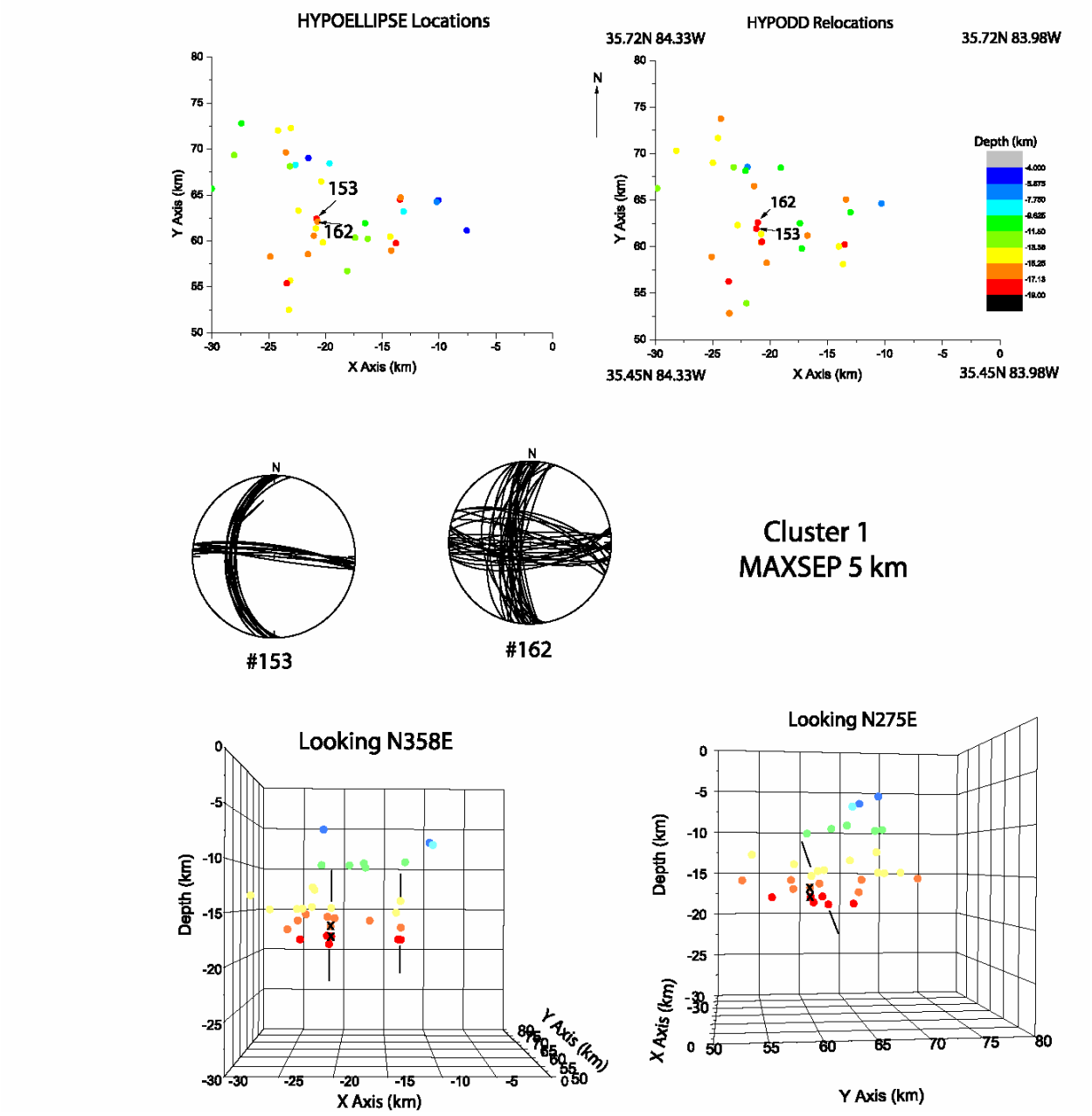

Figure 4.10. Hypocenter relocations of cluster 1 MAXSEP 5 km. Top Left: map view of HYPODD relocations (corresponding latitude and longitude of corner points of cluster 1 are shown). Top Right: HYPOELLIPSE single event locations. Bottom Left: three-dimensional perspective view oriented north. Bottom Right: Perspective oriented west. Also shown: focal mechanisms for two events in cluster 1 (from Chapman et al., 1997). In the map view the numbers associated with arrows indicate events with focal mechanisms. The individual focal mechanisms are illustrated with an X in the three-dimensional plots. See APPENDIX 3 for listing of relocated hypocenters.

Event #26 was magnitude 3.2 and event #366 was magnitude 2.9. Generally, the cluster trends east-west, which is parallel to one nodal plane of both focal mechanisms. This is significant, because the cluster represents, based on the selection criteria, one of the most seismically active areas in the seismic zone. Events on the western end of the cluster tend to be more shallow than the events occurring on the eastern edge.

The three-dimensional perspectives are oriented along the two nodal planes of the focal mechanisms. The perspective oriented to the north suggests a diffuse planar feature with shallow dip to the east. The perspective oriented to the west suggests a diffuse planar feature dipping more steeply to the north. Of the two possibilities suggested by the available data, I interpret the more likely case to be that represented by the west striking, north dipping feature. My reason for this interpretation is that both focal mechanisms suggest a steeply dipping, west striking, nodal plane. Whereas, focal mechanism #26 does not support a shallow dipping north striking fault plane.

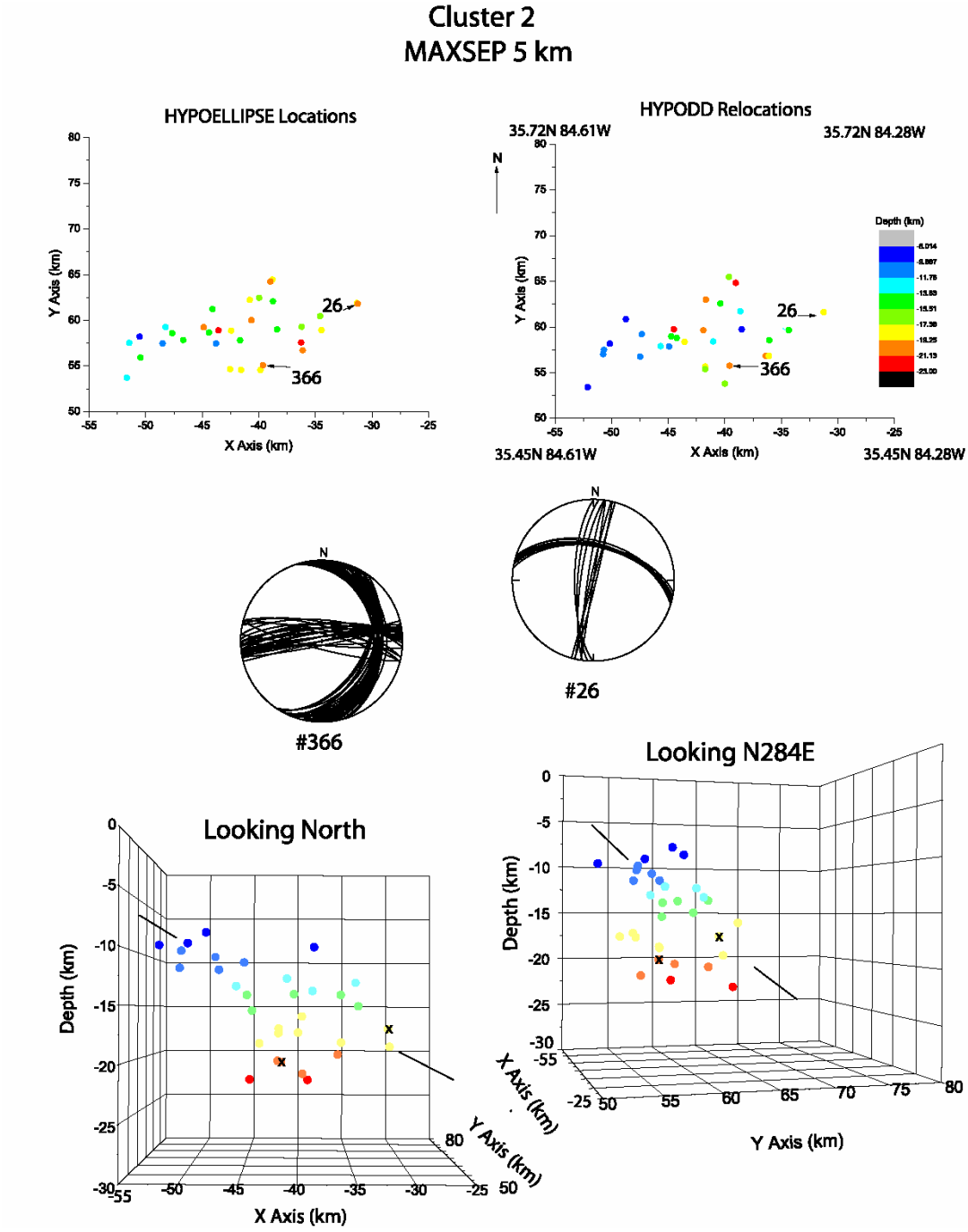

Figure 4.11. Hypocenter relocations of cluster 2 MAXSEP 5 km. Top Left: map view of HYPODD relocations (corresponding latitude and longitude of corner points of cluster 2 are shown). Top Right: HYPOELLIPSE single event locations. Bottom Left: three-dimensional perspective view oriented north. Bottom Right: Perspective oriented west. Also shown: focal mechanisms for two events in cluster 2 (from Chapman et al., 1997). In the map view the numbers associated with arrows indicate events with focal mechanisms. The individual focal mechanisms are illustrated with an X in the three-dimensional plots. See APPENDIX 3 for listing of relocated hypocenters.

Cluster 3, MAXSEP 5 km:

Cluster 3 is located on the Tennessee-North Carolina border, figure 4.9. The cluster consists of 14 HYPOELLIPSE single event locations, all of which were relocated by HYPODD.

Figure 4.12 shows the HYPOELLIPSE locations and the HYPODD relocations of cluster 3. The hypocenters in this cluster range in depth from 7 to 17 km. The mean change in the relocated hypocenters for cluster 3 is 2.3 km. The mean horizontal change is 0.6 km and the mean change in depth is 1.3 km. The maximum horizontal change for cluster 3 is 1.1 km and the maximum change is depth is 4.6 km. The HYPODD relocations of cluster 3 resolved a linear trend of epicenters.

There was one focal mechanism calculated for cluster 3 (Chapman et al., 1997). This event was a magnitude 2.9 earthquake. Event #242 is not a well constrained focal mechanism. However, the northwest trending nodal plane agrees perfectly with the linear trend of epicenters resolved by HYPODD. On the basis of this excellent correspondence, I conclude that the fault corresponds to the steeply dipping northwest trending plane.

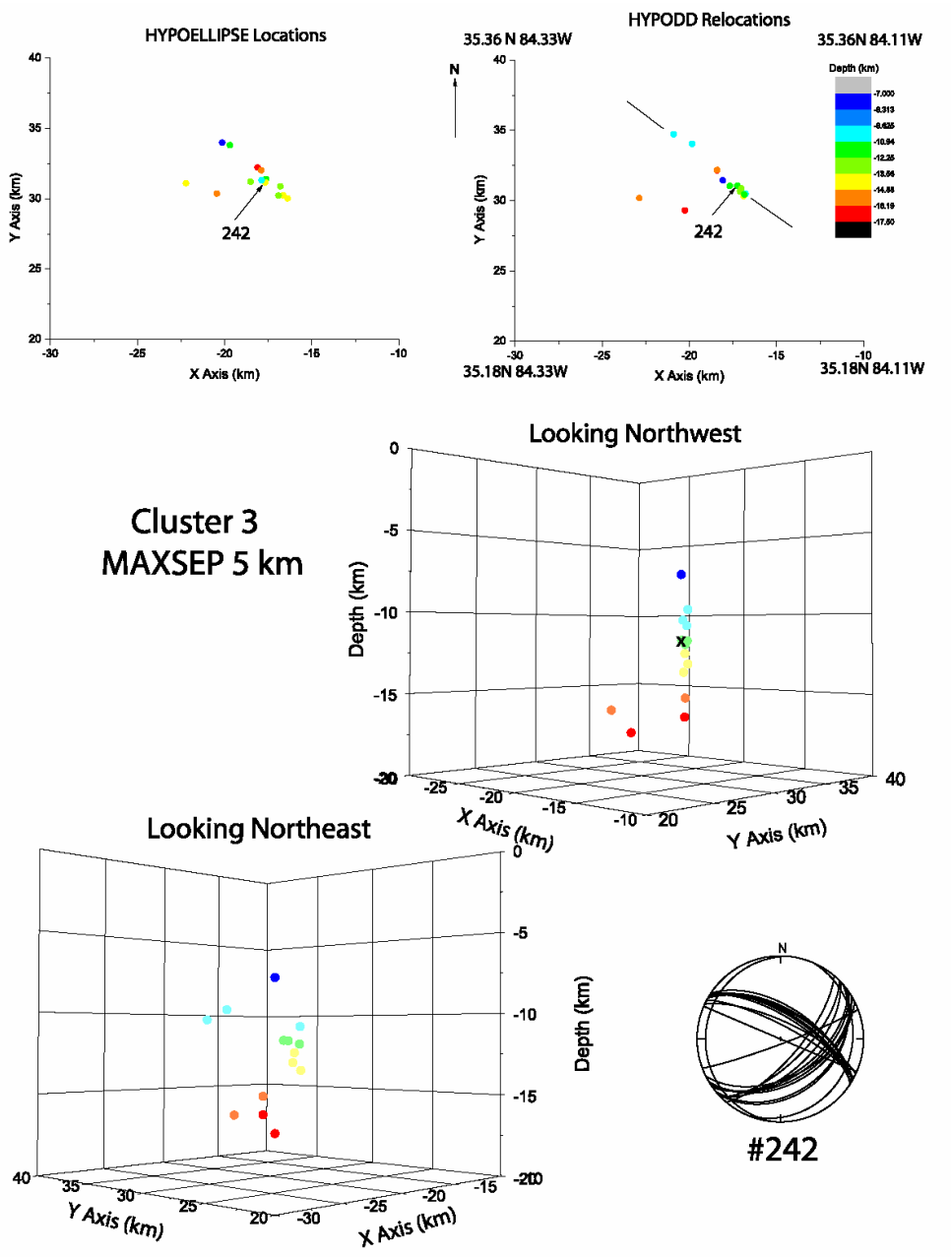

Figure 4.12. Hypocenter relocations of cluster 3 MAXSEP 5 km. Top Left: map view of HYPODD relocations (corresponding latitude and longitude of corner points of cluster 3 are shown). Top Right: HYPOELLIPSE single event locations. Lower Bottom: three-dimensional perspective view oriented northeast. Middle Right: Perspective oriented northwest. Also shown: focal mechanism for one event in cluster 1 (from Chapman et al., 1997). In the map view the numbers associated with arrows indicate events with focal mechanisms. The individual focal mechanisms are illustrated with an X in the three-dimensional plots. See APPENDIX 3 for listing of relocated hypocenters.

Combined Subset of Clusters 1 and 2, MAXSEP 5 km:

Clusters 1 and 2 represent adjacent areas of the densest seismic activity within the eastern Tennessee seismic zone. The area of densest activity is represented by two clusters, rather than one, because a small gap exceeding 5 km broke the chain that would have linked the two into one cluster. Therefore, I will examine both clusters simultaneously. There were two focal mechanisms calculated for each cluster (Chapman et al., 1997). The two focal mechanisms in cluster 1, #153 and #162, are located in the western portion of the cluster. The two focal mechanisms for cluster 2, #26 and #366, are located near the eastern edge of that cluster. In order to examine the spatial distribution of hypocenters in the vicinity of the events with focal mechanisms, I combine a subset of events from both clusters. The events included those in the western section of cluster 1 and those in the eastern section of cluster 2. Figure 4.13 shows the HYPODD relocations of these events in map-view and in three-dimensions.

Within the subset are the four focal mechanisms associated with the two clusters. The four focal mechanisms discussed in each cluster contained nodal planes trending to the north and west. The dips of the north-south trending nodal planes range from shallow dip to the east (event #366), to steep dip to the west (event #153). The east-west trending nodal planes of the four focal mechanisms show better agreement in terms of consistent dip to the north. Therefore, I favor the east-west trending nodal plane as a potential fault plane for all four mechanisms. This interpretation is strengthened by the overall east-west trend of the epicenters, as shown in map view at the top of figure 4.13. This interpretation appears consistent with the perspective plots shown at the bottom of figure 4.13. The view looking north shows no obvious planar features. However, the view looking west does suggest a west striking, north dipping, planar concentration of hypocenters. The dip, inferred from figure 4.13, is approximately 50 degrees. This

orientation matches the west striking nodal plane of event #26. If this feature is indeed a fault plane it would extend from approximately 8 km to at least 20 km in depth.

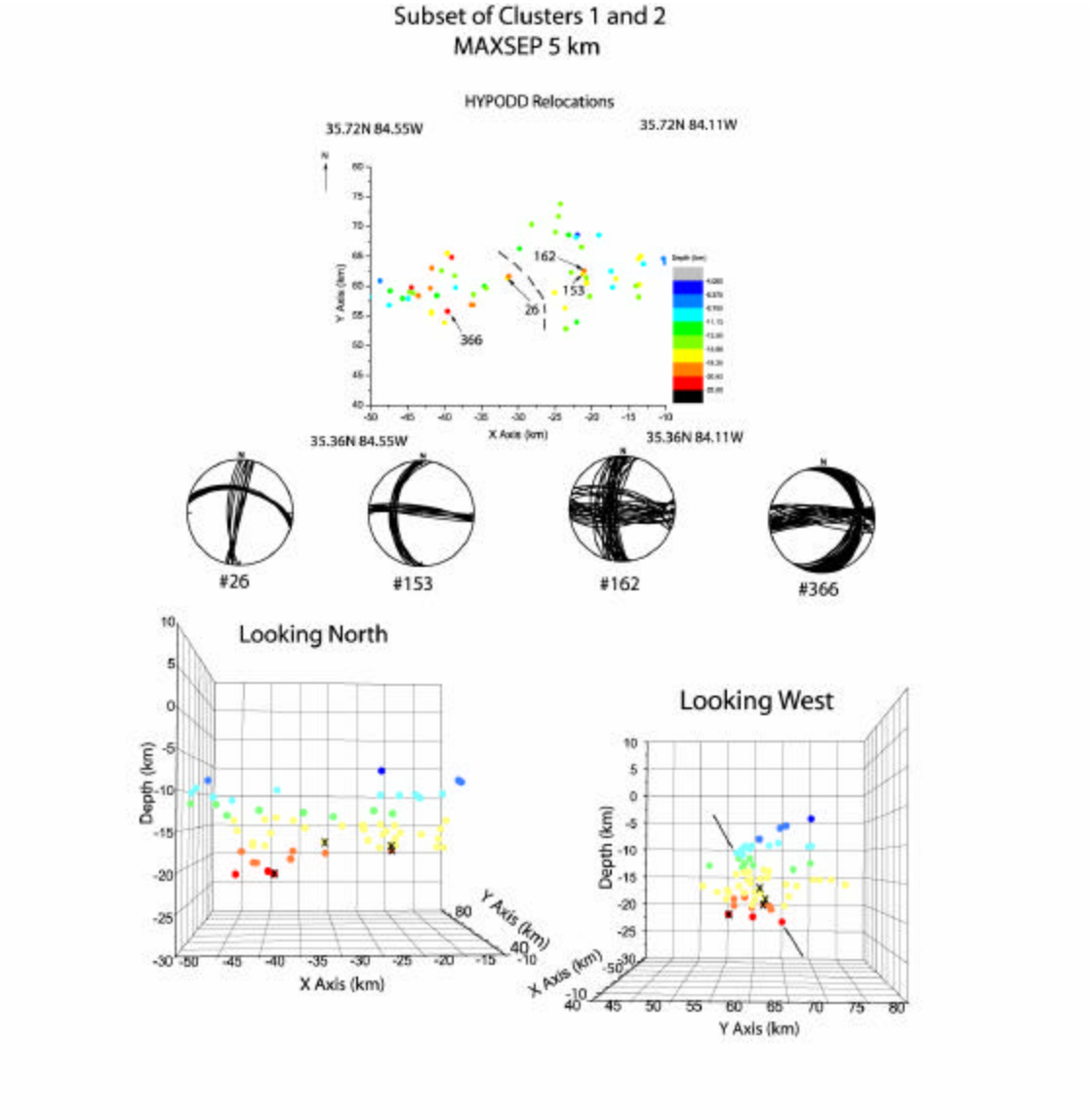

Figure 4.13: HYPODD Relocations of a sub-set of clusters 1 and 2. All events east of x-coordinate -31 are located in cluster 1, all epicenters located to the west are located in cluster 2. Top: Map View of epicenters, the two clusters are separated by a dotted line (corresponding latitude and longitude of corner points of the sub-set cluster are shown). Bottom Left: Perspective looking to north. Bottom Right: Perspective looking to west. Also shown: focal mechanism for four events in clusters 1 (from Chapman et al., 1997). In the map view the numbers associated with arrows indicate events with focal mechanisms. The individual focal mechanisms are illustrated with an X in the three-dimensional plots. See APPENDIX 3 for listing of relocated hypocenters.

A seismic reflection profile passes through the area shown at the top of figure 4.14. A section of seismic reflection profile ARAL1, processed and interpreted by Hopkins (1995), is shown in figure 4.14 (below). The seismicity in clusters 1 and 2 is between depths of 5 and 25 km. The limit of the depth in the ARAL1 profile is approximately 20 km. Therefore, the seismic record section shown in figure 4.14 images the crustal volume containing earthquakes in clusters 1 and 2. This crustal volume is below the horizontal reflector at 1.5 seconds, which marks the base of the Paleozoic sedimentary section. The upper to mid-crust containing the earthquake hypocenters is characterized by dipping reflectors. The apparent dip is approximately 35 degrees to the north. On the basis of the HYPODD relocations, it appears possible that the reflectors may mark the fault zones that are being reactivated, and are currently producing earthquakes, in the case of clusters 1 and 2.

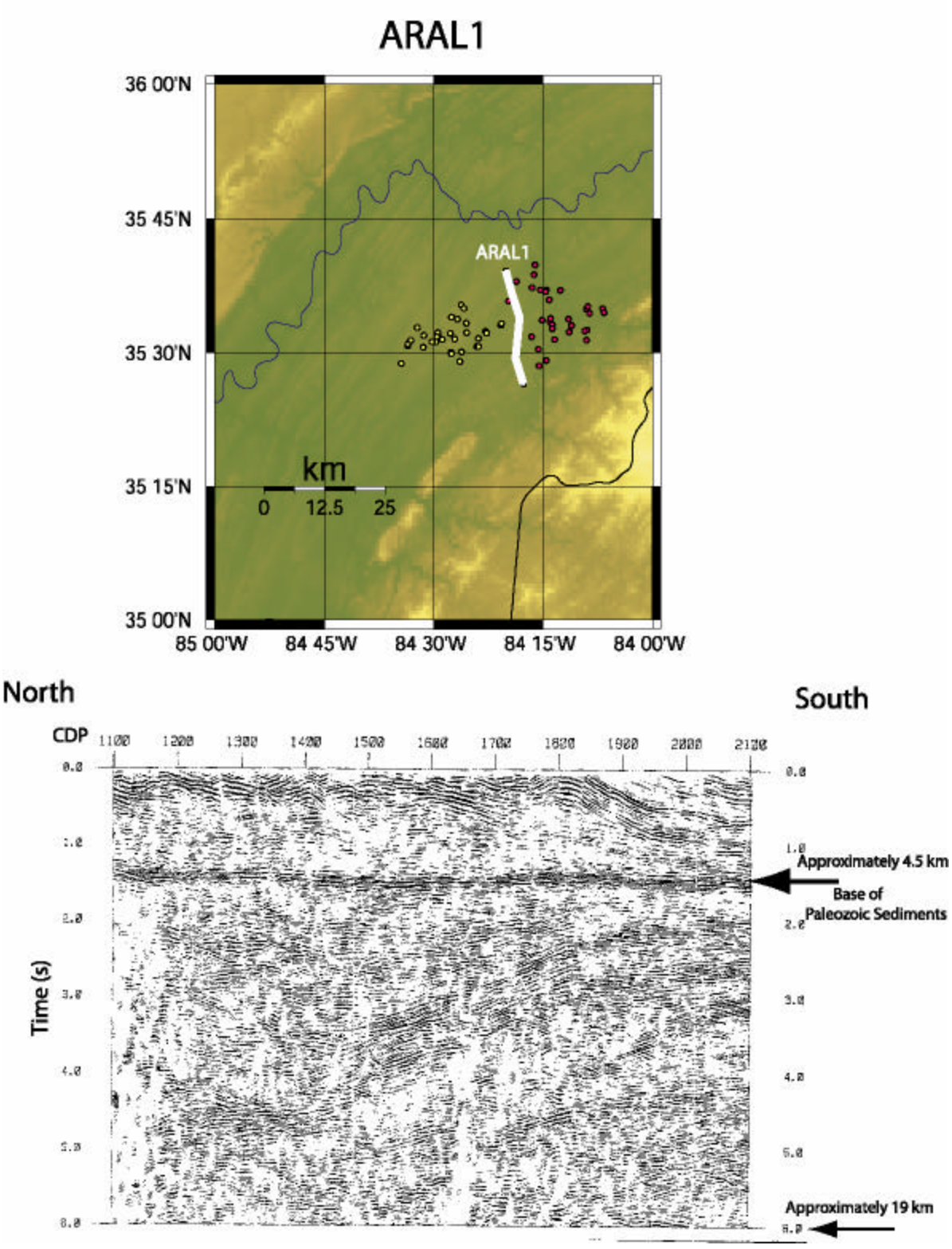

Figure 4.14. Top: Map view of epicenters of clusters 1 and 2 shown as small circles. The white line indicates seismic profile ARAL1 (from Hopkins, 1995). Epicenters to the east of ARAL1 are epicenters located in cluster 1 (yellow), epicenters to the west are located in cluster 2 (red) Bottom: Seismic profile ARAL1 (from Hopkins, 1995).

Sensitivity Testing of hypoDD:

There were two tests done on HYPODD to test for its sensitivity to different input velocity models.

In the first test, I compared the HYPODD relocations described above, with those developed using a different velocity model for single event location. The individual events were located using a velocity model developed for Giles County, Virginia instead of the velocity model developed by Vlahovic et al, (1998). The Giles County velocity model contains four layers, as opposed to the six layers used by Vlahovic et al. (1998). These single-event locations were then relocated with HYPODD, using MAXSEP 5 km. The Vlahovic one-dimensional P wave velocity model was used in all the HYPODD relocations described above. This test is done to simulate a situation in which many decades of single-event locations exist, in which a number of different velocity models may have been used, and test to see if HYPODD will accurately relocate the events, regardless of the initial velocity model.

The two sets of hypocenter locations for cluster 1, using MAXSEP 5 km, were compared to access any differences. The average difference in hypocenter locations was 0.18 km. The average horizontal difference was 0.1 km and the average difference in focal depth was 0.05 km. The average changes were all less than 1 km, supporting the assumption that the double difference algorithm is insensitive to the initial velocity model.

The second test applied examined the program's sensitivity to the one-dimensional velocity model used in the double difference algorithm. The HYPOELLIPSE single-event locations, all located with the Vlahovic et al. (1998) velocity model, were relocated by HYPODD using the Giles County 1-D velocity model in one run and the Vlahovic et al. velocity

model in another, for MAXSEP 5 km. The Giles County velocity model relocations of cluster 1 were compared to the cluster 1 relocations using the Vlahovic et al. velocity model. The average difference between the cluster 1 hypocenters was 1.6 km. The average epicenter difference was 0.3 km and the average difference in focal depths was 1.5 km. Both three-dimensional location changes, as well as changes in focal depths were greater than expected. This indicates that HYPODD is sensitive to the one-dimensional velocity model used for relocation. The test discussed above provides a minimum estimate of the errors involved in the relocation results. These errors apply only to this particular data set, located using the stations distribution illustrated above in eastern Tennessee.

The strength of HYPODD is its ability to obtain accurate relative hypocenter locations. The tests above that indicate sensitivity to the velocity model and suggest that the absolute locations are not necessarily improved by the double-difference algorithm. Accurate absolute locations require accurate velocity models and dense seismic network coverage. In the future, as more earthquakes are recorded in the ETSZ and more stations are installed, the relocations will become less sensitive to the velocity model. Despite these problems, I am confident that the relocations discussed above improved upon the original earthquake locations, primarily when considering the relative locations of events in the most active areas of the seismic zone.

Conclusions

The double difference algorithm of Waldhauser and Ellsworth (2000) was used to relocate earthquakes in the eastern Tennessee seismic zone. The data set was not ideal for this application. Station spacing is relatively sparse and approximately 800 earthquakes were recorded within an area approximately 300 km long by 50 km wide. Also, arrival time data contain considerable error, being based primarily on phase picks from analog records; as analog recording prevents the use of waveform cross correlations to reduce arrival time reading errors. Despite these limitations, HYPODD was very successful in developing improved hypocenter locations in several relatively small areas of the seismic zone. The relocations are interpreted as an improvement based on the increased agreement with specific nodal planes of available focal mechanisms, the tightening of clusters, and the increased presence of linear trends within some clusters. Within earthquake clusters, the analysis made it possible, for the first time, to meaningfully compare hypocenter spatial distributions with the available focal mechanism solutions for several small magnitude earthquakes.

HYPODD relocated two significant clusters using a maximum event separation of 10 km. In northwestern Georgia, HYPODD appears to have resolved a west-striking, northerly dipping planar structure that may correspond to a seismogenic fault (cluster 2, figure 4.5). Results for another cluster of earthquakes at the opposite end of the seismic zone, in northeastern Tennessee were more equivocal, but suggest the possibility that faulting may occur on northwest trending planes in that area (cluster 3, figure 4.6). Focal depths are systematically different in these two widely separated clusters. Earthquakes in the cluster in northwestern Georgia occur largely at depths less than 10 km. Events in clusters to the northeast occur at depths extending to 25 km.

Figure 15 shows the locations and orientations of potential seismogenic features associated with the various clusters involved in the study.

Analysis using MAXSEP 5 km provided the most encouraging results. Spatial tightening of the seismicity was demonstrated dramatically in a small cluster of earthquakes near the Tennessee-North Carolina border (cluster 3, figure 4.12). The hypocenters form a well defined, northwest-trending plane with near vertical dip. This spatial organization agrees perfectly with the one focal mechanism solution available for the cluster.

Analysis of the most seismically active area of the seismic zone, using MAXSEP 5 km, suggests that seismicity in two clusters at latitude 35.5 degrees north is occurring on west-striking, northerly-dipping faults (figure 4.13). These new results are important because a seismic reflection profile in this area indicates that the mid-to-upper crust is characterized by north-dipping reflectors. It appears possible that these reflectors may correspond to seismogenic faults in that part of the eastern Tennessee seismic zone.

The HYPODD relocations did show a vertical "tightening" along the northwest boundary of the eastern Tennessee seismic zone (figure 4.4). This boundary coincides with the steep magnetic gradient associated with the New York-Alabama lineament (King and Zietz, 1978). The presence of a vertical northwest boundary is consistent with previous arguments (Johnston et al. 1985, Teague et al. 1986, Powell et al. 1994, Vlahovic et al. 1998) concerning the association of seismicity with the NY-AL lineament. However, my results do not resolve any planar features dipping vertically along the northwest boundary. The data do not support the concept that the NY-AL lineament represents a major active strike slip fault as proposed by King and Zietz (1978).

Analysis of the most seismically active area indicates a west- trending, north- dipping zone of seismicity (figure 4.13). This orientation is completely different from the trend of the

ETSZ and the trend of the NY-AL lineament. However, this orientation is consistent with seismic reflection data that images the upper and mid-crust in the area (figure 4.14). The zone of relocated seismicity dips approximately 50 degrees to the north. Four focal mechanisms in the zone indicate dips in the range of 50 to 80 degrees on north trending planes. Apparent dips on mid-crustal reflectors are approximately 35 degrees (Hopkins, 1995). It is possible that the reflectors represent seismogenic faults in some cases. However, the difference in dips may indicate that the seismogenic features are imbedded within a larger scale tectonic fabric that is imaged by the reflection data.

The results of other areas within the seismic zone, such as cluster 3, MAXSEP 5 km (figure 4.12) and cluster 2, MAXSEP 10 km (figure 4.5), strongly suggest the presence of northwest trending seismogenic faults. This trend is perpendicular to the overall northeasterly trend of the ETSZ. The results of the HYPODD relocations indicate the possibility of several different faulting orientations within the eastern Tennessee seismic zone. All possible fault planes resolved by this study are consistent with an east-northeast oriented, sub-horizontal maximum regional compressional stress, consistent with findings by previous studies (Johnston et al., 1985, Teague et al., 1986, Davison, 1988, Chapman et al., 1997).

The analysis approach used in this study is promising, but the data set used here was derived from 20 years of monitoring and is capable of resolving major geological structures associated with the seismicity in only a few areas of the seismic zone. Future success in applying this approach in the study area will require substantial increases in the density of stations and the length of time those stations operate.

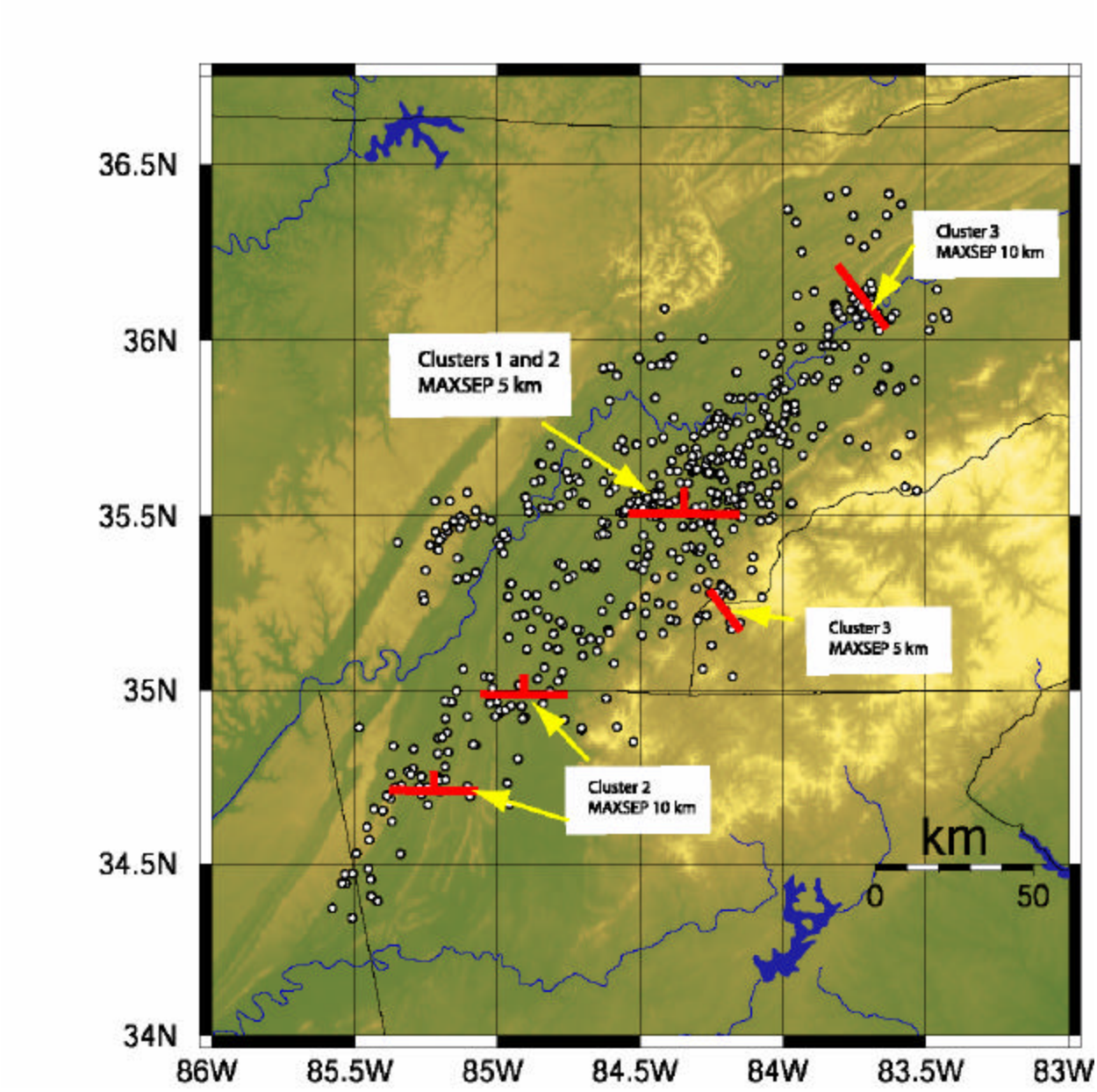

Figure 4.15 Strike and Dip symbols indicate interpreted orientation of potential seismogenic features.

References

Bollinger, G.A., A.C. Johnston, P. Talwani, L.T. Long, K.M. Shedlock, M.S. Sibol, and M.C. Chapman (1991). Seismicity of the southeastern United States; in Neotectonics of North America, Decade Map Col. 1, D.B. Slemmons, E.R. Engdahl, M.D. Zoback, and D.D. Blackwell (Editors), Geological Society of America, Boulder, Colorado.

Chapman, M.C. and G.A. Bollinger (1985). Crustal thickness variation in Virginia, derived from earthquake travel times, *Earthquake Notes* 56, no. 3, 71.

Chapman, M.C., C.A. Powell, G.C. Vlahovic, and M.S. Sibol (1997). A statistical analysis of earthquake focal mechanisms and epicenter locations in the Easter Tennessee Seismic Zone, Bulletin of the Seismological Society of America 87, no. 6, 1522-1536.

Cook, F.A., D.S. Albaugh, L.D. Brown, S.Kaufman, J.E. Oliver, and R.D. Hatcher Jr. (1979). Thin-skinned tectonics in the crystalline southern Appalachians; COCORP seismic-reflection profiling of the Blue Ridge and Piedmont, *Geology* 7, 563-567.

Davison, F.C. (1988). Stress tensor estimates derived from focal mechanism solutions of sparse data sets: Applications to the seismic zones in Virginia and eastern Tennessee, Ph.D. thesis, Virginia Polytechnic Institute and State University, Blacksburg.

Hopkins, D.L. (1995). The New York-Alabama magnetic lineament: its reflection character and relationship to the Grenville Front, Ph.D. thesis, Virginia Polytechnic Institute and State University, Blacksburg.

Johnston, A.C., D.J. Reinbold, and S.I. Brewer (1985). Seismotectonics of the southern Appalachians, Bulletin of the Seismological Society of America 75, 291-312.

Kaufmann, R.D. and L.T. Long (1996). Velocity structure and seismicity of southeastern Tennessee, Journal of Geophysical Research 101, 8531-8542.

King, E.R. and I. Zietz (1978). The New York-Alabama lineament: geophysical evidence for a major crustal break beneath the Appalachian basin, *Geology* 6, 312-318.

Lahr, J.C. (1980). HYPOELLIPSE/MULTICS, A computer program for determining local earthquake hypocentral parameters, magnitude, and first motion pattern, U.S. Geologic Survey Open-File Report.

Long, L.T. and K.H. Zelt (1991). A local weakening of the brittle-ductile transition can explain some intraplate seismic zones, *Tectonophysics*, 186, 175-192.

Marshak, S.(2001). *Earth: Portrait of a Planet*, W.W. Norton and Company, pp. 402-410.

Nava, S.J., J.W. Munsey, and A.C. Johnston (1989). First fault plane identification in the southeastern Appalachians: the m_{bLg} 4.2 Vonore, Tennessee earthquake of March 27, 1987, Seismological Research Letters 60, no. 3 119-129.

Nuttli, O.W., (1973), Seismic wave attenuation and magnitude relations for eastern North America, Journal of Geophysical Research, v. 78, pp. 876-885.

Paige, C.C. and M.A. Saunders (1982). LSQR:Sparse linear equations and least squares problems, *ACM Transactions on Mathematical Software* 8/2, 195-209.

Prejean, S.G., W.L. Ellsworth, M.D. Zoback, and F. Waldhauser (2002). Fault structure and kinematics of the Long Valley Caldera region, California, revealed by high-accuracy earthquake hypocenters and focal mechanism stress inversions, *Journal* of Geophysical Research 107, 2355-2373.

Powell, C.A., G. A. Bollinger, M.C. Chapman, M.S. Sibol, A.C. Johnston, and R.L. Wheeler (1994). A seismotectonic model for the 300 kilometer long eastern Tennessee seismic zone, *Science* 264, 686-688.

Southeastern U.S. Seismic Network Operators (1977-2002). Southeastern U.S. Seismic Network Bulletins, vols. 1-37, compiled and edited by Seismological Observatory, Virginia Polytechnic Institute and State University, Blacksburg, VA.

Teague, A.G., G.A. Bollinger, and A.C. Johnston (1988). Focal mechanism analysis for eastern Tennessee earthquakes (1981-1983), *Bulletin of the Seismological Society of America*, 76, 95-109.

Vlahovic, G.C. C.A. Powell, M.C. Chapman, and M.S. Sibol (1998). Joint hypocenter-velocity inversion for the eastern Tennessee seismic zone, *Journal of Geophysical Research* 103, 4879-4896.

Waldhauser, F. (2001). HYPODD--A program to compute double-difference hypocenter locations, U.S. Geologic Survey Open-File Report.

Waldhauser, F. and W.L. Ellsworth (2000). A double-difference earthquake location algorithm: Method and application to the Hayward fault, *Bulletin of the* Seismological Society of America 90, 1353-1368.

Wheeler, R.L. (1995). Earthquakes and the cratonwide limit of Iapetan faulting in eastern North America, *Geology* 23, 105-108.

Wheeler, R.L. (1996). Earthquakes and the southeastern boundary of the intact Iapetan margin in eastern North America, *Seismological Research Letters* 67, 77-83.

Wolfe, C.J. (2002). On the mathematics of using difference operators to relocate earthquakes, *Bulletin of the Seismological Society of America* 92, no. 8, 2879-2892.

Zoback, M.L. and M.D. Zoback (1980). State of stress in the conterminous United States, Journal of Geophysical Research, 85, 6113-6156.

Zoback, M.L. and M.D. Zoback (1985). Uniform NE to ENE maximum horizontal compressive stress throughout mid-plate North America, *EOS Trans. Am.* Geophys. U.,66,1056.

Zoback, M.L., M.D. Zoback, and R. Dart (1985). Reassessment of the state of stress in the Atlantic Coast region, Geological Society of America abstracts with *Programs,* 17. 759.

Zoback, M.D. and M.L. Zoback (1991). Tectonic stress field of North America and relative plate motions, in Slemmons, D.B., Engdahl, E.R., Zoback, M.D. and Blackwell, D.D., eds., *Neotectonics of North America. Geol. Soc. Amer., Decade Map Volume 1*, Boulder, Co.

Appendix 1: Input Parameters

The following tables specify the parameters used in the ph2dt program and the HYPODD program. For a detailed explanation of what the parameters are and what their effects are on the hypocenter relocations, see chapter 2. Several parameters were not held constant throughout the varies executions of the programs, the value of these parameters are specified in tables throughout the discussion.

Ph2dt Input Parameters:

Parameter	Input Value
MAXDIST	200
MAXSEP	Varies (see table 4.1 and 4.3)
MAXNGH	100
MINLNK	8
MINOBS	1
MAXOBS	100

HypoDD Input Parameters:

Parameter	Input Value
Data Type	Catalog only
Phase Type	P and S
DIST	200
OBSCC	N/A
OBSCT	8
Inversion Used	LSQR
Sets of Iterations	2
Number of Iterations (first set)	15,10
Weighting of P wave	1.0
Weighting of S wave	1.0
Threshold for Residuals (sec.)	0.6
WDCT	Varies (see table 4.1 and 4.3)
Damping Value	Varies (see table 4.1 and 4.3)
Number of Iterations (second set)	10
Weighting of P wave	1.0
Weighting of S wave	1.0
Threshold for Residuals (sec.)	0.4
WDCT	Varies (see table 4.1 and 4.3)
Damping Value	Varies (see table 4.1 and 4.3)
Velocity Model Used	Vlahovic et al. (unless otherwise stated)
Cluster to be Relocated	Varies (see text)

Appendix 2: Velocity Models

Two velocity models were used as input into HYPOELLIPSE (Lahr, 1980) or HYPODD (Waldhauser, 2002). Unless otherwise specifically stated within the discussion, the Vlahovic et al. (1998) velocity model was used. Below are both the Vlahovic et al. and Giles County velocity models used as input.

Giles County Velocity Model:

Layer	P Wave Velocity (km/s)	Depth to the Top of Layer	Vp/Vs ratio (km/s)
1	5.63	0.0	1.64
2	6.05	5.7	1.72
3	6.53	14.7	1.70
4	8.18	50.7	1.71

**** when used in HYPODD, the Vp/Vs ratio is held constant at 1.72 km/s

Vlahovic et al. Velocity Model:

Layer	P Wave Velocity (km/s)	Depth to the Top of Layer	Vp/Vs ratio (km/s)
1	6.05	0.0	1.74
2	6.24	5.7	1.73
3	6.34	10.0	1.73
4	6.43	14.7	1.72
5	6.52	20.0	1.72
6	8.00	45.0	1.72

****when used in HYPODD, the Vp/Vs ratio is held constant at 1.73 km/s

APPENDIX 3: Earthquakes Relocated by HypoDD

HYPODD Event ID	Latitude (Deg)	Longitude (Deg)	Depth (km)	Year	Month	Day	Hour	Minute	Seconds
1	35.59574	-84.35920	4.365	1984	1	5	5	49	27.1
2	35.64588	-84.09104	9.168	1984	2	2	6	33	56.79
3	35.65063	-84.68719	21.579	1984	2	7	6	32	19.83
4	36.12541	-83.71619	14.601	1984	2	14	20	51	46.39
5	36.11163	-83.70969	3.135	1984	2	14	20	54	31.13
6	35.50524	-84.18104	10.426	1984	2	22	22	15	30.57
7	34.65341	-85.40009	13.122	1984	2	27	17	8	10.98
9	35.85265	-84.02316	5.017	1984	3	17	23	26	11.25
11	35.17284	-84.70943	17.904	1984	3	27	1	20	34.77
12	34.72323	-85.10572	18.422	1984	4	16	7	40	12.2
14	34.87887	-85.17639	19.827	1984	4	23	6	8	0.53
16	35.59936	-84.62709	24.965	1984	5	25	10	15	38.69
17	35.53974	-84.14530	16.316	1984	6	7	16	57	50.39
18	35.77914	-83.99148	14.097	1984	6	23	14	3	57.35
20	35.40074	-84.30191	13.692	1984	7	18	19	57	12.57
21	35.17611	-84.17822	21.528	1984	7	22	16	30	18.94
22	35.54389	-84.51668	4.625	1984	8	4	12	49	57.78
26	35.55795	-84.34151	16.667	1984	8	30	16	26	28.45
27	35.55967	-84.35058	18.115	1984	8	30	16	41	52.21
28	35.75716	-83.86327	17.036	1984	9	6	23	42	1.38
30	34.78007	-85.18325	20.147	1984	10	9	11	54	27.94
31	34.74265	-85.20468	10.435	1984	10	9	12	12	45.8
32	34.75262	-85.20991	6.946	1984	10	15	16	56	52.87
33	34.80282	-84.92744	9.59	1984	10	29	9	39	48.83
34	35.80227	-84.06642	12.248	1984	11	4	15	38	19.5
35	35.58729	-84.59011	9.721	1984	11	7	9	31	19.52
36	35.47021	-84.42535	13.798	1984	11	12	18	42	28.52
37	35.62189	-84.26199	8.628	1984	11	26	11	42	59.07
39	36.14780	-83.70548	7.652	1984	12	16	4	2	11.19
40	35.41327	-84.32424	17.716	1984	12	17	18	48	28.04
41	35.62592	-84.26700	15.634	1984	12	19	12	28	53.08
42	36.41034	-83.83581	24.072	1984	12	20	8	24	48.87
43	35.49804	-85.12835	11.912	1984	12	23	7	22	44.8
44	35.69857	-84.57644	17.858	1985	1	15	0	25	18.82
45	35.69064	-84.22063	8.847	1985	1	19	1	9	0.11
46	35.42911	-84.99867	4.332	1985	1	25	2	13	34.54
47	35.98432	-83.78205	9.972	1985	2	7	8	4	46.84
48	35.54309	-84.19130	11.085	1985	2	13	19	50	56.02
50	36.29806	-83.51597	7.147	1985	2	26	23	52	23.5
51	35.00684	-85.01513	5.464	1985	3	9	14	29	57.92
52	35.26828	-84.47845	6.762	1985	3	12	8	57	43.53
53	35.86742	-83.58683	21.602	1985	3	12	13	4	47.75
54	35.74697	-84.04885	17.356	1985	4	9	20	51	12.42
55	35.73881	-84.03485	14.363	1985	4	9	21	41	0.94
56	35.73791	-84.05328	16.08	1985	4	10	10	53	59.24
57	35.47782	-84.56285	12.613	1985	4	20	4	21	3.36
58	35.62443	-84.21798	9.111	1985	4	29	7	4	23.29
59	35.11853	-84.78855	19.128	1985	5	7	14	10	4.06
60	35.58522	-84.14318	18.303	1985	6	17	0	30	47.95
61	35.58564	-84.13979	16.729	1985	6	17	0	39	17.13
62	35.05291	-84.77171	13.365	1985	6	20	12	9	22.22
64	35.67398	-83.92917	14.604	1985	8	15	17	31	52.85
65	35.07749	-84.59131	17.365	1985	8	22	17	54	13.78
66	35.18897	-84.76987	16.953	1985	8	23	7	56	33.99
67	36.07310	-83.68570	1.518	1985	8	25	1	52	47.32
68	35.49887	-84.03715	13.527	1985	9	17	16	25	8.19
69	35.71327	-84.00692	17.132	1985	9	24	0	1	12.33
70	36.35676	-83.63601	16.891	1985	11	5	0	59	29.13
71	35.49958	-84.43678	16.582	1985	11	20	3	10	2.58
72	36.10305	-83.81673	11.692	1985	11	22	13	19	26.61
73	35.41781	-85.23595	19.847	1985	11	23	14	36	16.2
74	35.52313	-84.50049	12.292	1985	11	26	2	28	52.09
75	35.30910	-84.26186	16.176	1985	11	28	22	49	9.08

76	35.78300	-84.04877	16.382	1985	12	8	4	45	58.28
78	35.82852	-84.60779	23.925	1985	12	18	12	23	29.68
79	34.91545	-84.76367	7.128	1985	12	20	15	15	6.62
80	35.69846	-83.70513	12.305	1985	12	22	0	56	5.04
81	35.60588	-84.74959	20.604	1986	1	7	1	26	43.71
82	35.35529	-84.50147	18.71	1986	1	8	7	10	39.89
83	35.32297	-84.44419	13.644	1986	1	8	8	54	18.9
84	35.62479	-84.75791	25.936	1986	1	8	15	39	59
86	35.20079	-84.37337	16.73	1986	1	17	0	46	0.47
87	35.92795	-83.63259	19.789	1986	1	27	6	44	27.08
88	35.92401	-83.63237	17.527	1986	1	27	6	46	0.52
89	36.08640	-83.75489	5.816	1986	1	30	11	45	33.26
90	35.10045	-84.70168	16.157	1986	2	2	22	19	36.88
91	35.92612	-83.63964	18.406	1986	2	3	0	53	7.22
92	35.34523	-85.25191	22.066	1986	2	8	3	9	19.31
93	34.83142	-85.29361	8.468	1986	2	19	2	43	37.28
94	35.83850	-84.10561	9.51	1986	2	19	7	57	11.66
95	35.68416	-84.15864	4.605	1986	2	22	10	20	15.91
97	35.22245	-84.47896	8.584	1986	3	25	4	45	34.31
98	34.65736	-85.43309	13.9	1986	4	11	6	5	26.01
100	34.77608	-85.29495	13.852	1986	4	23	7	18	57.66
101	35.91689	-83.73693	18.17	1986	4	27	22	30	26.91
102	35.14890	-84.67417	17.433	1986	5	1	1	21	20.82
103	35.51170	-84.19093	16.522	1986	5	4	19	25	40.53
104	35.54847	-84.18379	14.664	1986	5	13	14	30	36.44
106	35.51881	-84.52718	8.333	1986	5	19	23	46	47.52
107	35.67047	-84.18973	13.55	1986	5	30	17	44	25.12
108	35.44601	-84.48855	18.746	1986	6	2	7	46	12.57
109	35.21288	-84.29117	15.085	1986	6	6	8	49	55.48
110	35.76849	-84.20456	7.107	1986	6	11	9	3	52.63
111	35.37949	-85.13981	15.235	1986	6	21	0	40	2.76
112	35.97753	-83.93634	21.852	1986	6	24	19	22	42.45
113	35.98135	-83.93085	23.461	1986	6	24	22	54	46.95
114	36.05710	-83.65019	17.931	1986	7	4	21	55	10.08
115	35.88746	-83.88859	2.947	1986	7	5	21	16	12.92
116	34.93571	-84.99051	12.187	1986	7	11	14	26	15.04
118	36.03212	-83.66311	9.47	1986	7	12	17	25	7.38
119	34.94286	-84.98951	10.058	1986	7	19	12	31	53.95
120	35.64759	-84.26723	13.255	1986	7	25	12	43	55.53
121	35.51108	-84.56750	14.475	1986	8	7	12	36	46.45
122	36.37272	-83.98198	21.669	1986	8	17	6	4	10.49
123	34.37049	-85.57962	5.57	1986	8	29	7	49	3.16
124	35.52245	-84.50950	13.509	1986	9	1	23	47	7.71
125	34.72193	-85.27297	8.614	1986	9	17	8	32	10.16
126	35.89845	-83.92203	17.143	1986	10	26	8	19	33.83
127	36.29657	-83.51364	11.746	1986	11	2	3	44	40.67
128	35.76714	-84.19032	9.534	1986	11	2	17	4	47.6
129	35.88350	-83.81965	12.985	1986	11	15	12	7	56.74
130	35.93554	-84.41918	20.738	1986	11	16	19	8	36.49
131	35.55222	-84.08324	4.991	1986	11	21	13	49	55.05
132	35.73304	-83.55277	13.285	1986	11	21	18	50	34.6
133	35.37955	-84.24715	5.807	1986	11	24	18	39	35.46
134	35.51858	-84.53040	16.32	1986	12	4	3	8	21.67
135	35.90066	-83.87585	17.098	1986	12	21	13	32	44.13
136	35.53117	-84.52299	13.618	1986	12	26	8	59	38.42
137	35.60384	-84.84683	18.835	1987	1	2	4	10	27.77
138	35.50753	-84.24882	15.836	1987	1	12	18	56	3.28
140	35.82985	-84.78040	23.083	1987	1	16	14	41	54.93
141	35.49889	-84.44701	8.355	1987	2	3	14	31	28.55
142	34.96589	-85.00157	5.218	1987	2	10	9	2	46.44
143	35.24609	-84.38433	20.89	1987	2	11	8	20	0.95
144	35.58748	-84.42983	15.51	1987	2	21	10	14	3.06
145	35.20324	-84.39452	15.124	1987	2	21	22	21	40.58
146	35.72710	-84.31068	18.586	1987	2	23	8	12	43.38
147	34.72651	-85.33677	3.046	1987	2	24	9	58	11.05
149	35.66181	-84.21664	5.065	1987	3	13	19	55	22.79
150	35.77842	-84.11160	17.2	1987	3	14	20	41	58.48
151	35.27352	-85.2607	20.624	1987	3	16	5	0	24.42
152	35.52999	-84.27841	14.642	1987	3	24	20	13	43.13
153	35.56302	-84.23159	17.38	1987	3	27	7	29	30.83
154	35.56001	-84.23344	13.83	1987	3	27	7	35	39.43

155	35.55283	-84.23155	16.118	1987	3	27	16	23	5.29
156	35.65732	-84.38812	7.159	1987	3	28	15	30	17.05
157	35.54421	-84.23473	16.699	1987	4	1	8	17	21.26
158	35.58076	-84.58787	5.503	1987	4	3	21	35	35.34
162	35.56292	-84.22826	17.648	1987	4	9	1	31	23.67
164	34.89458	-84.57979	8.013	1987	4	23	23	31	30.22
165	35.51028	-84.55578	8.76	1987	4	28	3	2	39.12
166	35.51716	-84.55152	9.274	1987	4	28	3	39	38.81
167	35.64042	-84.79685	10.272	1987	4	30	6	49	25.84
169	35.62503	-84.25161	5.225	1987	5	5	19	41	22.83
170	34.72108	-85.24399	11.125	1987	5	9	9	10	8.94
171	35.99091	-84.00399	14.864	1987	5	12	12	17	59.96
172	36.28708	-83.76611	18.017	1987	5	16	0	55	7.82
173	35.03946	-85.04503	16.256	1987	5	22	7	36	22.57
174	35.52624	-84.48379	10.321	1987	5	25	11	17	44.71
175	35.70238	-84.81300	24.5	1987	5	29	7	24	20.46
176	35.56977	-84.25161	14.181	1987	6	1	2	50	22.92
177	34.52807	-85.33847	7.429	1987	6	9	20	20	55.15
178	35.27326	-84.21699	12.895	1987	6	14	6	17	30.19
179	35.53537	-84.45564	19.112	1987	7	4	10	47	25.13
180	35.56569	-84.19049	10.163	1987	7	7	15	3	34.46
181	36.10101	-83.81299	24.811	1987	7	11	0	4	29.87
182	36.10358	-83.81734	23.06	1987	7	11	0	22	18.93
183	36.10062	-83.81476	24.11	1987	7	11	2	48	6.22
184	35.87400	-83.65353	15.493	1987	7	11	22	24	10.93
185	35.79154	-83.99065	16.091	1987	7	14	23	2	12.38
186	35.98527	-83.85832	13.355	1987	7	17	8	19	11.52
187	36.08580	-83.81423	21.812	1987	7	17	15	30	25.73
188	34.84226	-85.07711	22.326	1987	7	19	23	32	37.73
189	35.78225	-84.20809	14.98	1987	7	25	2	15	53.01
190	35.54067	-84.42676	13.395	1987	8	1	7	40	13.38
191	35.06539	-84.83399	17.187	1987	8	8	0	41	48.15
192	34.99972	-85.14280	13.639	1987	8	13	7	4	19.63
193	35.62642	-84.31728	13.767	1987	8	13	13	37	1.23
194	35.44464	-84.64273	5.823	1987	8	14	2	21	27.49
195	35.41722	-84.98839	16.293	1987	8	14	19	48	20.17
197	35.65361	-84.17113	25.304	1987	8	22	20	3	36.82
198	35.63168	-84.02899	10.681	1987	8	25	10	53	9
199	35.51690	-84.39818	20.15	1987	9	1	23	2	49.73
200	35.51706	-84.39788	19.401	1987	9	1	23	15	42.73
201	34.74731	-85.20456	6.029	1987	9	2	7	57	21.78
202	35.55393	-84.90181	15.749	1987	9	5	20	13	17.03
203	35.01576	-84.92388	4.06	1987	9	6	8	46	40.89
204	34.97668	-84.61845	13.267	1987	9	7	6	6	54.47
205	36.07437	-83.71050	19.339	1987	9	16	21	32	32.64
206	35.53763	-84.70173	19.193	1987	9	19	3	22	50.24
207	35.62767	-84.31130	18.544	1987	9	22	17	23	50.43
209	35.38386	-84.10390	14.792	1987	10	5	20	9	50.9
210	35.71638	-84.56249	19.36	1987	10	10	11	39	11.66
211	35.83710	-84.44552	9.604	1987	10	20	22	49	56.62
212	35.83427	-84.17087	8.35	1987	10	23	9	40	7.82
213	34.85222	-84.52135	8.95	1987	10	23	10	52	51.8
214	34.70044	-85.26623	8.238	1987	11	4	20	30	46.18
215	35.53612	-83.97079	14.502	1987	11	4	22	17	39.73
216	35.53648	-83.96849	13.147	1987	11	4	22	19	8.68
217	34.75857	-85.37377	5.622	1987	11	8	5	15	7.67
218	36.32010	-83.48312	14.435	1987	11	8	8	46	51.46
219	35.46555	-85.13022	21.561	1987	11	10	8	38	23.24
220	35.21779	-84.55076	12.217	1987	11	10	23	56	36.55
221	35.69455	-84.15166	18.133	1987	11	11	7	2	40.68
225	35.58866	-84.02127	21.702	1987	11	29	15	20	35.33
226	36.09502	-83.80780	22.378	1987	11	30	7	2	44.22
227	35.39739	-84.29068	10.358	1987	12	1	8	15	0.44
228	34.75407	-85.26582	3.841	1987	12	6	14	53	6.24
229	36.01124	-84.42896	21.794	1987	12	7	4	4	48.75
230	34.74784	-85.21449	4.719	1987	12	8	9	28	7.55
231	35.53384	-84.68891	19.115	1987	12	11	6	30	45.59
232	35.36467	-84.48330	21.582	1987	12	13	0	39	30.26
233	35.76360	-84.21165	19.008	1987	12	14	7	13	20.46
234	35.78101	-84.38141	18.813	1987	12	15	10	20	21.37
235	35.66748	-84.15084	17.767	1987	12	16	11	22	41.97

236	35.27981	-84.25443	15.621	1987	12	23	6	4	29.54
237	35.02684	-84.78511	10.732	1987	12	26	7	27	43.84
238	35.86091	-83.99265	21.618	1987	12	29	13	39	11.13
239	35.27411	-84.18005	9.692	1988	1	8	23	27	51.96
240	35.28017	-84.1912	10.615	1988	1	8	23	47	10.4
241	35.27411	-84.17994	7.779	1988	1	9	0	3	29.33
242	35.27968	-84.18684	10.363	1988	1	9	0	16	55.86
243	35.27914	-84.18244	9.614	1988	1	9	0	24	37.44
244	35.28261	-84.19002	9.023	1988	1	9	1	7	41.15
245	35.27824	-84.18332	7.875	1988	1	9	1	15	5.74
246	35.28929	-84.19555	12.576	1988	1	9	19	21	5.06
247	35.27316	-84.18022	9.088	1988	1	9	22	11	25.09
248	35.29115	-84.19749	12.111	1988	1	10	13	22	58.41
249	35.42637	-84.22419	16.737	1988	1	11	12	21	59.6
252	35.17397	-84.72108	12.808	1988	1	18	5	47	51.87
253	36.32114	-83.50777	13.322	1988	2	7	8	39	29.86
254	35.39285	-84.97721	5.184	1988	2	7	10	54	11.52
255	35.62807	-84.39523	13.959	1988	2	11	20	13	9.75
256	35.47114	-84.31416	18.614	1988	2	11	22	13	12.24
257	35.72969	-83.99822	14.618	1988	2	12	14	47	39.13
258	35.35249	-84.66223	11.365	1988	2	13	5	53	1.89
259	35.59427	-84.33068	8.512	1988	2	14	4	4	52.83
261	36.31329	-83.47576	13.411	1988	2	17	11	30	24.11
263	35.45609	-85.21601	16.132	1988	2	18	16	47	57
264	35.8602	-83.59960	21.078	1988	2	20	20	31	2.68
265	36.30879	-83.48589	10.022	1988	3	2	18	28	11.11
267	35.81695	-83.98680	15.296	1988	3	11	16	39	32.9
268	34.96709	-85.16007	8.58	1988	3	24	4	22	40.63
269	35.19465	-84.18172	4.905	1988	3	31	2	45	29.86
270	35.56823	-84.04821	19.018	1988	4	2	0	10	11.4
271	35.53329	-84.04493	3.972	1988	4	2	17	18	35.64
272	35.78055	-84.21292	19.016	1988	4	23	1	1	16.93
273	36.11334	-83.74442	17.411	1988	4	24	0	8	47.93
274	35.14137	-84.70358	12.272	1988	5	1	0	34	52.72
275	36.10973	-83.74242	16.623	1988	5	2	11	13	32.3
276	34.92458	-85.10384	5.887	1988	5	5	8	19	27.09
278	35.83635	-84.14400	7.013	1988	5	19	11	21	57.39
280	34.91944	-85.18072	11.691	1988	5	21	3	51	22.14
281	35.34823	-84.28958	13.277	1988	5	23	9	32	52.3
282	35.88469	-83.93075	9.105	1988	5	26	9	53	41.14
283	35.70711	-83.97843	14.69	1988	5	27	15	6	26.35
284	35.25858	-85.25831	17.427	1988	6	3	15	47	53.51
285	35.41499	-84.46560	11.314	1988	6	14	1	54	59.91
286	35.35770	-84.69383	15.744	1988	6	14	12	10	40.84
287	36.14543	-83.68543	17.98	1988	6	14	13	37	52.01
288	34.47129	-85.50746	9.642	1988	6	16	9	0	44.22
289	35.57336	-84.14141	8.994	1988	6	18	10	36	28.68
290	35.83764	-84.18804	4.394	1988	6	20	7	50	18.99
291	35.65967	-84.15129	11.94	1988	6	22	16	48	3.51
292	36.14523	-83.45967	18.498	1988	6	30	12	57	31.7
293	35.69333	-84.30286	17.761	1988	7	3	11	28	8.55
294	35.66803	-84.14453	13.319	1988	7	15	13	15	29.35
295	35.21302	-84.93140	18.768	1988	7	26	19	27	26.65
296	35.43611	-84.9661	17.386	1988	7	27	4	37	18.21
297	34.81806	-85.20933	13.653	1988	7	29	2	33	1.31
298	35.26849	-84.96160	16.874	1988	8	7	6	54	41.43
299	35.74364	-84.01597	9.86	1988	8	14	6	38	38.48
300	35.16009	-84.49326	15.258	1988	8	14	17	6	45.49
301	36.38669	-83.58373	16.415	1988	8	23	22	0	28.75
302	35.23107	-84.20036	9.534	1988	9	10	5	35	20.24
304	35.30413	-84.21493	7.744	1988	9	15	23	40	59.44
305	35.29921	-84.20993	3.349	1988	9	15	23	42	53.18
306	36.13943	-83.88923	3.143	1988	10	1	7	49	44
308	35.27465	-84.89718	15.512	1988	10	8	22	1	48.43
309	34.34275	-85.50821	9.085	1988	10	13	9	17	26.04
310	34.69592	-85.09533	6.386	1988	10	14	22	17	13.17
311	35.53487	-84.15662	16.016	1988	10	15	9	28	5.49
312	35.50654	-84.16191	10.873	1988	10	19	8	56	47.08
313	35.52414	-84.89065	19.916	1988	10	25	0	23	52.99
314	35.61665	-84.21864	15.725	1988	10	27	15	37	54.24
315	35.73670	-84.08942	10.605	1988	11	1	13	7	41.04

316	36.26534	-83.71580	21.988	1988	11	1	16	34	16.61
317	35.52218	-84.81494	15.657	1988	11	8	18	44	18.96
318	35.55845	-84.46466	8.005	1988	11	17	7	21	46.57
319	36.04441	-83.66537	6.458	1988	11	24	22	37	50.86
320	35.76708	-84.15849	8.379	1988	12	1	9	18	28.99
321	35.54470	-84.37698	14.099	1988	12	4	3	0	1.39
322	35.44076	-85.19311	13.578	1988	12	17	4	22	11.77
323	35.81244	-84.06345	7.213	1989	1	6	4	30	8.08
324	35.79122	-84.22374	19.869	1989	1	17	11	30	24.99
325	36.00633	-84.27747	17.807	1989	1	18	4	25	36.68
326	35.67514	-83.60341	3.589	1989	1	19	11	38	26.05
327	35.19767	-84.77876	16.723	1989	1	23	10	28	12.4
329	35.48851	-85.02217	14.885	1989	2	15	4	46	20.21
330	35.79638	-83.95613	14.232	1989	2	27	5	5	5.76
331	35.40515	-84.51151	17.124	1989	3	4	9	28	3.67
332	35.17459	-84.61118	13.599	1989	3	10	10	52	23.13
333	35.56503	-84.44921	19.774	1989	3	13	1	24	48.94
334	35.33005	-84.73537	18.828	1989	3	16	0	43	58.63
335	36.26850	-83.51857	9.494	1989	3	16	9	5	52.98
336	34.96987	-85.18356	9.816	1989	4	1	22	15	23.93
337	36.07832	-83.60685	12.782	1989	4	3	10	13	7.74
339	35.27383	-84.86135	17.463	1989	4	20	15	25	47.92
340	35.36139	-84.52911	14.702	1989	4	30	17	34	49.95
341	35.62077	-84.25228	9.102	1989	5	3	14	47	15.48
342	35.70576	-84.51154	20.099	1989	5	4	6	33	30.13
343	34.39132	-85.41963	6.778	1989	5	8	2	8	54.31
344	35.47837	-84.25310	15.182	1989	5	25	13	27	54.62
345	35.71887	-83.76967	13.58	1989	5	26	17	21	45.76
346	35.11861	-84.89635	15.768	1989	5	31	6	44	24.89
347	36.06084	-83.62189	9.744	1989	6	9	9	44	22.76
348	36.35506	-83.75244	17.35	1989	6	15	6	9	2.89
349	35.03880	-84.17593	11.458	1989	6	23	5	47	29.25
350	34.48424	-85.45253	13.068	1989	7	1	4	41	14.9
351	35.52876	-84.45670	14.258	1989	7	9	11	51	58.11
352	35.5359	-84.47610	21.75	1989	7	11	14	53	28.84
353	35.52571	-84.30462	21.507	1989	7	17	6	39	44.51
355	35.59738	-84.86969	22.229	1989	7	25	5	5	45.98
356	36.03970	-83.94315	26.269	1989	7	30	20	38	59.86
357	35.96205	-84.06581	20.188	1989	8	8	9	42	11.68
358	35.32864	-84.38442	8.961	1989	8	9	9	26	0.93
360	35.91161	-84.16145	10.354	1989	8	20	22	54	25.86
361	35.47915	-84.61770	9.547	1989	8	25	5	38	36.78
362	36.09176	-84.41336	13.636	1989	8	27	23	51	55.44
364	35.53028	-84.49116	16.555	1989	9	3	9	57	33.97
365	35.54176	-84.50340	15.973	1989	9	3	9	57	36.83
366	35.50676	-84.43332	21.799	1989	9	7	5	18	6.54
368	35.53892	-84.23083	16.828	1989	10	4	18	16	17.93
369	35.36057	-84.65604	13.091	1989	10	5	9	4	30.5
370	35.75563	-84.04571	11.655	1989	12	2	0	59	41.71
371	35.98857	-83.84354	11.937	1989	12	2	13	31	46.09
372	36.26789	-83.71534	21.879	1989	12	29	12	51	12.94
373	34.9545	-84.91484	13.824	1990	1	19	17	36	53.07
375	35.66216	-84.26186	13.568	1990	2	2	11	14	36.22
376	35.26821	-84.07300	12.617	1990	2	10	23	42	8.3
377	35.57271	-83.53027	4.117	1990	2	14	10	43	38.86
378	35.75184	-84.25284	4.718	1990	2	17	16	30	32.22
379	35.51164	-84.45064	15.895	1990	2	23	17	10	45.16
380	35.50930	-84.44659	16.379	1990	2	23	17	12	54.04
381	36.09637	-83.72364	10.885	1990	3	1	4	41	5.18
382	35.67504	-84.29747	12.348	1990	3	18	3	41	35.33
383	36.03060	-83.48699	26.749	1990	3	20	16	10	56.02
384	34.84419	-85.08455	15.212	1990	3	21	9	44	39.32
385	35.14434	-84.64066	17.055	1990	3	24	6	51	48.02
386	35.19418	-84.14996	15.911	1990	3	25	13	47	16.34
387	35.94785	-84.50323	19.007	1990	3	31	16	27	44.62
388	35.95083	-84.00743	23.551	1990	4	19	20	36	48.49
389	34.44196	-85.53106	10.189	1990	5	4	21	40	37.19
390	34.83932	-85.36371	10.795	1990	6	13	11	1	58
391	35.43247	-85.20364	18.685	1990	6	16	23	0	0.56
393	35.53445	-84.13903	14.441	1990	6	22	9	26	4.81
394	35.81004	-83.98720	15.088	1990	7	11	18	41	10.91

396	35.68867	-84.36141	17.607	1990	7	14	23	48	29.63
398	34.92486	-85.00657	8.522	1990	7	28	11	9	39.56
399	35.20957	-84.82267	8.668	1990	7	29	14	19	42.93
400	36.41639	-83.62727	9.949	1990	8	4	11	16	48.8
402	35.49035	-84.04701	12.966	1990	8	19	21	10	33.49
404	35.11418	-84.64996	13.503	1990	8	28	4	55	11.03
405	35.54947	-84.15833	16.336	1990	9	1	5	4	12.73
406	35.62924	-84.60112	17.905	1990	9	10	14	5	57.34
407	34.52958	-85.49479	3.936	1990	9	19	21	56	45.19
408	35.85816	-83.66451	18.702	1990	10	11	10	38	47.57
409	35.39532	-84.38769	3.855	1990	11	4	2	22	27.82
410	35.62911	-84.36830	8.436	1990	11	18	19	29	25.91
411	35.58853	-84.42916	21.137	1990	12	19	18	10	31.25
412	36.07964	-83.42864	9.088	1991	1	14	5	6	30.73
413	36.06482	-83.42429	8.96	1991	1	15	6	15	29.15
414	36.07308	-83.80443	7.159	1991	1	15	21	3	46.56
415	36.08144	-83.43043	8.124	1991	1	16	18	22	15.3
416	36.06483	-83.79039	4.085	1991	1	21	1	40	58.35
417	35.50950	-84.33266	17.743	1991	2	19	1	15	15.5
418	35.62396	-84.25827	12.103	1991	2	19	14	0	1.74
419	36.42575	-83.77821	11.927	1991	3	7	3	44	58.34
420	35.49493	-84.24913	13.93	1991	3	7	9	31	40.83
421	35.58414	-83.57003	17.573	1991	4	15	5	55	46.83
422	35.73177	-84.10364	8.863	1991	4	28	19	37	44.41
423	36.33569	-83.95288	22.017	1991	5	5	3	2	17.16
425	34.86180	-85.20755	8.017	1991	5	10	19	40	37.15
426	35.30069	-84.79784	20.419	1991	5	19	1	44	29.46
427	34.72366	-85.10407	5.03	1991	5	20	10	5	24.44
428	35.48336	-84.63161	16.748	1991	5	26	5	49	27.6
429	35.41036	-84.28585	19.513	1991	5	29	2	47	19.38
430	34.96156	-84.84073	15.057	1991	6	13	6	14	52.61
431	35.56640	-84.73566	14.118	1991	6	13	22	46	3.21
432	35.75587	-84.19766	20.125	1991	6	20	7	20	49.27
434	35.55717	-84.42509	12.018	1991	7	14	7	31	56.67
435	34.98560	-84.83413	5.29	1991	7	18	9	31	17.24
436	35.12542	-84.82423	12.55	1991	7	29	15	33	21.92
438	34.89415	-85.48435	20.119	1991	8	17	17	59	9.41
439	35.48675	-84.07760	17.528	1991	8	18	15	32	17.16
441	36.14951	-83.76317	6.454	1991	9	8	22	14	20.39
442	35.70723	-84.11749	14.166	1991	9	24	7	21	7.24
444	34.92303	-84.90328	1.346	1991	10	9	4	27	51.75
445	35.60421	-84.20566	11.585	1991	10	14	11	10	37.68
446	34.74093	-85.20102	12.87	1991	10	19	15	30	21.45
447	34.74333	-85.18192	10.932	1991	10	21	1	10	48.96
448	34.45493	-85.44378	11.154	1991	10	22	6	30	57.18
451	35.60945	-84.72292	10.044	1991	10	28	10	46	21.26
452	34.88588	-84.70439	10.597	1991	10	30	14	54	13
453	35.46709	-84.25444	14.278	1991	11	3	6	53	3.07
454	35.45044	-84.23983	9.544	1991	11	3	7	6	0.27
455	34.72021	-85.35791	1.338	1991	11	10	9	54	42.6
456	35.56368	-84.48113	4.056	1991	11	11	23	6	5.14
457	35.34556	-84.10844	13.464	1991	11	15	8	52	13.31
458	35.47032	-84.35031	9.72	1991	11	21	5	12	2.29
459	35.48121	-84.28686	5.513	1991	11	22	5	33	42.09
461	35.44823	-84.97813	4.23	1991	11	25	20	15	52.53
462	34.94352	-84.9702	20.114	1991	12	1	22	39	6.55
463	35.58552	-84.11258	8.043	1991	12	3	15	15	21.17
464	35.58029	-84.11237	8.849	1991	12	5	16	10	31.32
465	35.76246	-84.23995	13.689	1991	12	14	2	15	50.87
466	35.36453	-84.78243	12.015	1991	12	22	2	56	11.19
469	35.26330	-84.60608	16.088	1992	2	14	10	36	3.77
470	35.97727	-83.94659	6.623	1992	3	7	10	30	44.27
471	35.53485	-84.39743	15.361	1992	3	13	22	49	41.36
472	35.2302	-84.85861	18.035	1992	3	17	8	47	23.04
473	35.86665	-83.65157	16.334	1992	3	18	1	45	41.08
474	35.81302	-84.26276	8.451	1992	3	21	7	23	31.84
475	35.93394	-84.02249	12.986	1992	3	23	8	47	36.76
476	35.51667	-85.07528	18.487	1992	3	30	9	20	30.62
477	35.36196	-84.65580	21.22	1992	4	2	11	17	10.57
478	34.89194	-84.70452	5.662	1992	4	25	20	1	59.54
480	35.24047	-84.53156	17.477	1992	5	5	1	29	56.29

481	36.12847	-83.94933	11.405	1992	6	14	11	27	40.41
482	36.16321	-83.69031	17.034	1992	7	4	16	23	19.14
483	35.95157	-84.50360	22.466	1992	7	19	5	2	42.93
484	34.82231	-85.17194	13.533	1992	8	3	11	34	28.68
485	34.56806	-85.44947	11.645	1992	8	8	3	51	42.07
486	35.29315	-84.30407	22.413	1992	8	12	4	16	53.91
487	35.95050	-84.39352	4.585	1992	9	26	19	16	50.15
489	35.51470	-84.46230	18.479	1992	10	21	17	44	45.75
490	34.73292	-84.96416	6.394	1992	10	24	12	27	58.61
491	35.16410	-84.41841	3.58	1992	10	25	14	48	44.98
492	35.57737	-84.51677	15.905	1992	11	10	12	3	49.09
493	35.65012	-84.14218	11.89	1992	11	10	17	16	47.32
494	36.08732	-83.76094	5.286	1992	11	18	9	37	7.29
496	35.16701	-84.60670	14.481	1993	1	8	21	19	26.02
497	35.03738	-85.0245	8.106	1993	1	15	2	2	51.26
498	35.13006	-84.24951	3.873	1993	1	28	1	51	40.44
499	35.34621	-84.48885	17.316	1993	2	13	11	35	55.14
500	36.30039	-83.6735	13.603	1993	2	20	1	10	13.73
501	35.71304	-84.45722	4.621	1993	3	12	9	56	38.54
502	35.50144	-84.46457	14.29	1993	3	22	14	10	25.27
504	34.75019	-85.26736	13.187	1993	5	5	4	57	16.26
505	35.51242	-84.88911	18.147	1993	5	19	10	31	18.8
506	35.53244	-84.89078	15.224	1993	5	19	10	37	58.03
507	34.96194	-85.02712	9.948	1993	5	25	1	11	0.92
509	35.93303	-84.42790	22.816	1993	7	28	3	58	25.35
510	35.25017	-84.43358	16.231	1993	7	28	4	15	51.91
511	36.06492	-83.47366	21.546	1993	8	1	8	49	44.07
512	35.67673	-84.16054	12.825	1993	9	6	11	48	20.65
513	34.66980	-85.24290	17.026	1993	9	8	7	41	12.58
515	34.76534	-85.31401	9.584	1993	11	16	6	25	8.21
516	34.75860	-85.30304	9.306	1993	11	16	6	32	9.81
520	35.72392	-84.41768	10.34	1996	10	25	4	29	20.49
521	35.50342	-84.32090	13.207	1996	10	29	9	56	10.5
526	35.61621	-84.45376	11.655	1997	1	23	17	7	56.92
530	34.95601	-84.95043	3.426	1997	4	2	8	5	59.43
531	35.88811	-83.53562	13.39	1997	4	11	8	2	20.35
532	34.62272	-85.36961	5.478	1997	5	19	22	22	34.2
534	36.06951	-83.66823	15.175	1997	5	27	4	54	18.9
535	35.49105	-85.11325	31.09	1997	6	4	23	7	30.37
536	36.07809	-83.66555	6.713	1997	6	8	9	42	4.04
539	35.06127	-85.11857	19.121	1997	7	27	8	52	8.21
541	35.86707	-83.82074	15.057	1997	8	3	3	7	5.15
542	35.95125	-83.71241	14.367	1997	8	4	6	28	13.79
547	35.92852	-84.45910	9.211	1997	9	14	23	42	50.46
548	35.65975	-84.22911	17.295	1997	9	24	2	16	16.37
549	36.06639	-83.61811	16.139	1997	9	28	7	47	27.94
551	34.40464	-85.44256	6.442	1997	10	12	6	55	33.31
552	35.45919	-85.17173	11.374	1997	10	14	6	16	23.62
553	35.38702	-84.47338	10.692	1997	10	14	7	22	33.5
556	35.32035	-84.75230	33.385	1997	10	19	18	39	55.03
558	35.92546	-84.60132	14.303	1997	10	31	11	1	37.16
559	34.46987	-85.53459	12.855	1997	11	3	16	34	59.99
560	35.06154	-84.27970	1.822	1997	11	12	15	10	43.83
561	35.73833	-84.27439	16.071	1997	11	19	16	10	7.66
563	35.75565	-84.25770	22.321	1997	11	23	22	40	18.93
564	35.15206	-84.95984	3.545	1997	11	27	17	3	6.47
565	36.06478	-83.74429	5.926	1997	12	2	2	34	0.68
567	35.48542	-85.12230	17.369	1997	12	24	1	35	49.45
568	35.84143	-84.03629	24.482	1998	1	14	3	1	25.13
569	36.07961	-83.80457	14.32	1998	1	24	15	15	18.81
571	34.44301	-85.54477	6.295	1998	1	28	16	44	22.02
575	35.75644	-84.03651	8.584	1998	3	3	12	16	43.09
576	35.47028	-85.17950	32.414	1998	3	12	10	45	24.52
577	35.28249	-84.22960	18.315	1998	3	18	20	22	7.58
578	35.55153	-84.47416	14.533	1998	3	20	15	0	5.92
580	34.91839	-84.91146	4.717	1998	4	14	8	39	13.27
581	36.04106	-83.73285	6.532	1998	4	16	18	21	28.01
583	35.54291	-85.21780	5.259	1998	4	26	6	2	27.47
585	35.98612	-83.82036	10.084	1998	4	30	4	0	9.27
586	35.22731	-84.63231	10.128	1998	5	15	9	6	24.07
587	35.65160	-84.03241	18.316	1998	5	25	10	46	57.96

589	36.12068	-83.75390	17.592	1998	6	17	4	1	2.01
590	35.95457	-84.38572	13.464	1998	6	17	8	0	23.74
591	35.93228	-84.40333	9.088	1998	6	17	18	7	45.99
592	34.7084	-85.20179	1.889	1998	6	18	5	9	59.36
594	35.56763	-85.10495	22.829	1998	7	3	13	6	49.45
595	35.53721	-84.53459	7.642	1998	7	4	11	24	18.67
597	35.77852	-84.23755	9.813	1998	8	8	6	54	33.84
598	35.77816	-84.22938	4.266	1998	8	8	7	53	52.16
602	34.86520	-85.19493	4.027	1998	9	5	7	16	34.69
603	35.2158	-84.26791	12.879	1998	9	13	11	22	43.24
604	36.12149	-83.68126	9.238	1998	9	13	15	47	8.5
608	35.40911	-84.33997	6.778	1998	10	20	16	30	10.74
610	35.40369	-85.20666	15.776	1998	11	13	22	28	48.62
611	34.60581	-85.45823	1.567	1998	12	5	5	46	58.8
614	35.56806	-84.60655	9.368	1999	1	16	22	49	28.71
619	36.02876	-83.66320	8.111	1999	3	13	6	57	56.78
620	35.49695	-84.14817	13.191	1999	4	2	11	3	24.72
621	35.49605	-84.14326	14.529	1999	4	2	11	34	42.36
623	34.99689	-84.81431	11.388	1999	4	12	6	42	40.04
624	35.88823	-84.01088	18.516	1999	4	15	1	11	56.82
625	35.64172	-84.32854	15.741	1999	4	17	0	31	0.05
626	35.55819	-84.44640	11.137	1999	4	24	10	43	51.86
627	36.11687	-83.68983	7.046	1999	4	27	1	6	51.96
628	35.30636	-84.956	9.415	1999	5	17	17	29	32.94
629	35.30754	-84.95133	5.726	1999	5	18	2	34	15.69
630	35.30664	-84.94978	8.251	1999	5	18	2	45	20.85
631	35.59954	-84.71144	23.055	1999	5	22	8	55	36.57
632	35.72701	-83.89456	22.671	1999	5	22	15	20	54.11
633	35.75147	-83.95476	16.013	1999	5	27	11	21	0.3
636	36.10293	-83.68581	0.094	1999	5	30	3	41	56.67
639	35.33840	-85.07542	9.864	1999	6	28	1	53	4.01
640	35.63502	-84.30471	27.336	1999	7	6	6	21	4.57
642	36.06804	-83.66218	4.429	1999	7	16	1	54	22.45
647	35.36282	-84.23611	25.602	1999	9	17	12	24	14.35
649	35.61602	-84.22115	15.918	1999	10	19	9	38	14.99
652	35.44782	-84.61825	11.617	1999	11	17	3	31	22.81
654	35.61778	-84.09335	8.995	1999	11	28	9	30	31.17
656	35.03312	-84.85881	8.133	1999	12	8	21	18	41.86
658	35.35742	-84.76864	22.913	2000	1	3	21	24	59.9
662	35.65631	-84.31710	4.337	2000	3	4	19	8	24.96
663	35.32379	-85.10728	12.1	2000	3	12	6	20	23.72
664	34.68782	-85.37566	11.736	2000	3	20	10	0	50.62
665	34.69636	-85.38698	7.906	2000	3	20	19	36	50.4
666	35.42440	-85.34932	12.399	2000	3	24	19	45	26.81
667	35.47575	-85.08097	20.79	2000	4	3	23	39	34.26
668	35.46373	-84.17242	17.16	2000	4	10	12	48	15.39
669	35.67113	-84.31596	7.791	2000	4	12	3	54	5.77
670	36.25286	-83.93386	11.576	2000	4	16	2	38	44.72
671	35.53052	-84.77809	13.247	2000	4	25	3	0	19.43
672	35.90247	-84.57987	25.858	2000	5	3	12	48	31.21
674	35.17504	-84.88263	3.925	2000	5	15	15	5	34.31
676	35.55076	-84.16821	9.814	2000	6	4	5	6	47.57
678	35.20297	-84.29849	15.242	2000	7	2	14	20	21.99
680	35.80457	-83.95900	13.453	2000	7	8	21	41	2.08
681	35.88677	-83.80862	12.98	2000	7	11	14	59	47.61
682	35.48564	-85.15323	20.512	2000	7	11	17	44	26.83
683	35.54238	-85.16744	16.18	2000	7	12	6	27	5.32
684	35.31910	-85.14016	16.934	2000	7	21	15	35	12.03
685	35.66848	-84.25034	16.355	2000	7	28	20	16	39.4
689	35.92153	-84.62807	19.693	2000	8	23	8	12	43.06
696	35.62277	-84.06882	7.08	2000	10	19	6	39	27.01
697	35.72996	-84.21058	20.2	2000	10	21	18	36	0.48
698	35.56171	-84.75045	9.75	2000	10	23	7	57	30.51
700	35.49536	-85.04865	16.388	2000	11	9	15	13	55.51
701	35.53067	-84.48425	13.215	2000	11	18	16	22	9.71
702	35.51542	-84.47334	14.117	2000	11	18	17	8	1.99
704	35.45169	-84.62983	34.748	2000	12	10	17	51	50.53
714	35.76654	-83.99796	7.31	2001	2	18	19	17	4.26
715	35.16201	-84.80193	11.404	2001	2	20	7	8	36.28
718	35.69314	-84.34763	23.11	2001	2	27	16	46	26.88
719	35.52412	-84.83973	14.058	2001	3	7	17	12	24.05

723	35.52275	-84.49177	15.434	2001	3	30	22	1	12.58
724	35.63378	-84.30080	6.93	2001	4	5	23	20	33.22
733	36.03911	-83.83907	4.582	2001	5	17	6	43	48.5
734	35.82045	-83.95873	3.236	2001	5	21	2	36	6
748	35.21674	-84.90629	23.73	2001	10	29	21	40	41.82
755	35.69219	-84.06832	20.003	2001	12	5	13	7	39.44
760	35.68838	-84.55464	8.205	2002	2	17	7	0	43.57
762	36.01712	-83.84101	8.536	2002	2	25	1	53	16.06
766	34.67133	-84.95742	9.995	2002	4	6	20	49	51.79
769	35.53726	-84.07339	19.876	2002	5	15	6	34	50.34
770	35.62119	-84.21688	18.991	2002	5	16	7	5	30.18
773	35.94528	-83.83785	13.015	2002	7	24	11	31	21.69
774	35.88061	-84.02473	21.603	2002	8	4	1	56	54.05
775	35.65113	-84.85143	4.271	2002	8	16	13	40	12.35
777	35.64809	-84.84318	5.621	2002	8	27	14	7	35.57
780	35.37647	-84.36163	15.975	2002	10	2	21	55	19.66